Università degli Studi di Pisa
15 Febbraio 2010

PROBLEMI DI FRATTURA E DANNEGGIAMENTO IN MATERIALI E SISTEMI COMPOSITI

Parte 1:
MECCANICA DELLA FRATTURA LINEARE E NON LINEARE NELLO STUDIO DEI MATERIALI COMPOSITI

Roberta Massabò
Università degli Studi di Genova

INDICE DELLA PRESENTAZIONE

RICHIAMI DI MECCANICA DELLA FRATTURA ELASTICA LINEARE

FIBER-REINFORCED COMPOSITE LAMINATES

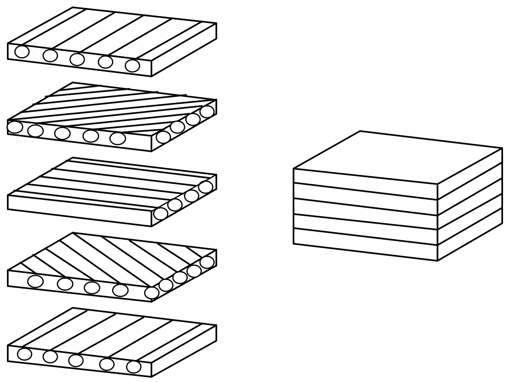

Lamina:
unidirectionally reinforced composite

Laminate:
stacking sequences: $[0]_n$, $[\pm\alpha]_n$, $[0/90]_n$, $[0/\pm 45/90]_n$, ….

Manufacturing procedures:
- lay-up
- resin impregnation (in PMC): RTM, RFI

CHARACTERISTICS:

- High degree of tailoring of elastic properties
- High strength to weight ratios
- High stiffness to weight ratios

(⇒ aeronautics/aerospace/defence)

DRAWBACKS:

- Lack of strength in through-thickness direction
- Low damage / impact tolerance and resistance
- High sensitivity to interlaminar flaws
- Catastrophic failures
  (inter-ply layers: low-toughness fracture paths)

REMEDIES:

- Tougher matrices
- Inter-ply films, addition of particles,…
- <u>Through-thickness reinforcement</u> (trans-laminar reinforcement)

SINGLE AND MULTIPLE DELAMINATION

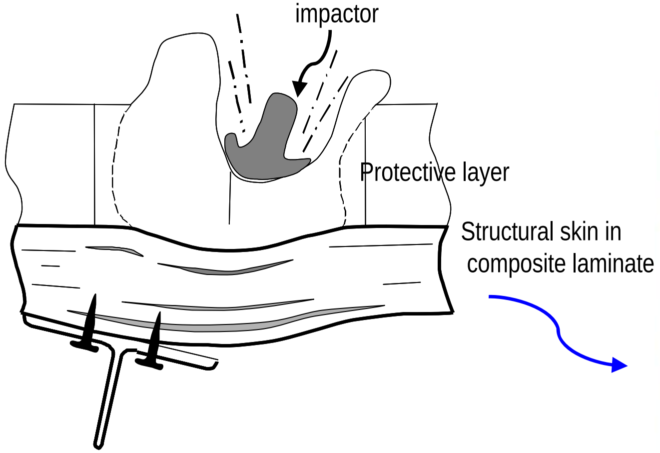

STRUCTURAL COMPOSITE

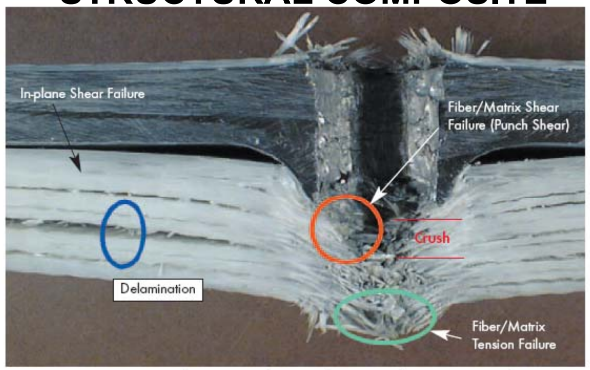

Cheeseman et al., *Amptiac*, (8), 2004.

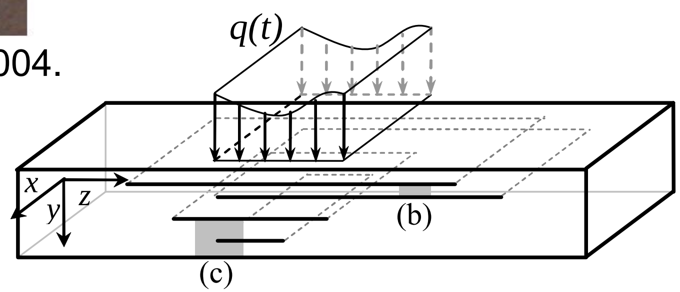

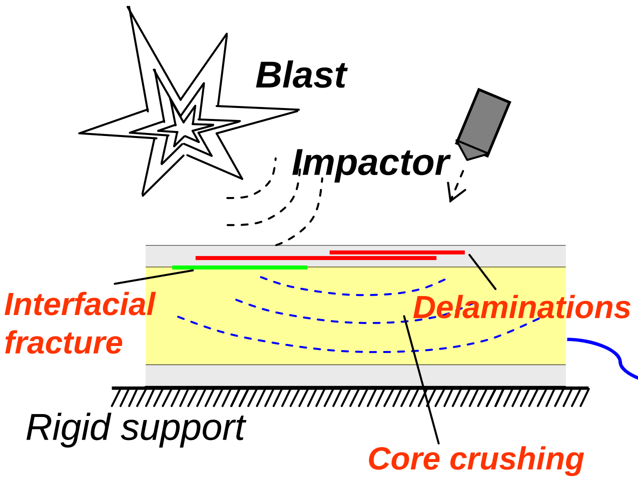

COMPOSITE SANDWICH

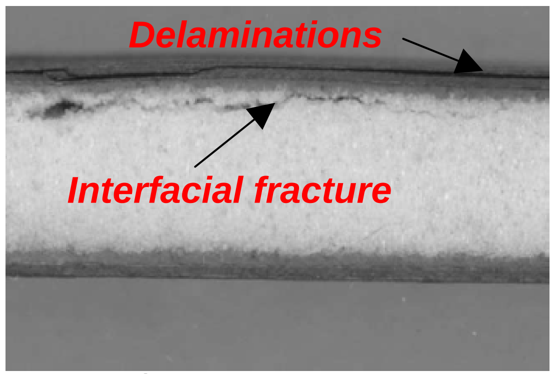

(Kim and Swanson, *Comp. Struct.*, 2001)

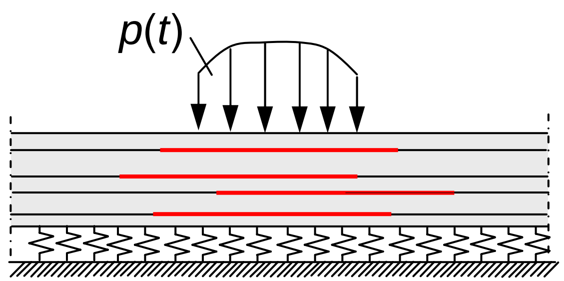

THE EFFECTS OF SHEAR AND NEAR TIP DEFORMATIONS ON ENERGY RELEASE RATE AND MODE MIXITY OF EDGE-CRACKED ORTHOTROPIC LAYERS

(M.G. Andrews & R. Massabò, 2007, *Engineering Fracture Mechanics*)

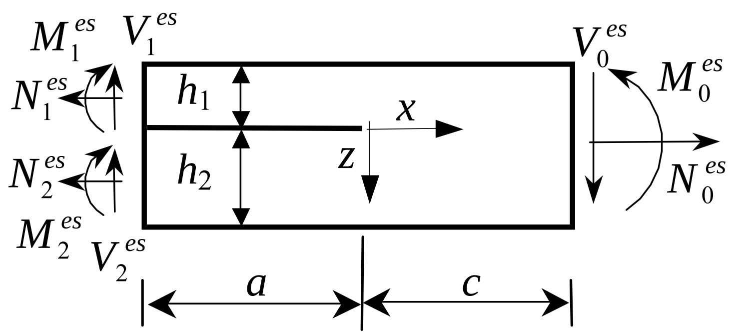

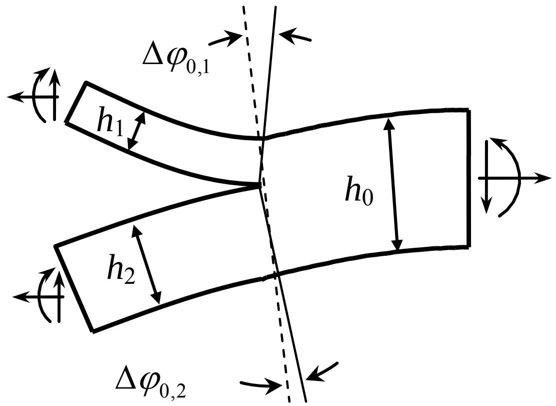

Edge cracked layer subject to generalized end forces

Reference solutions from the literature:

Suo, JAM, (1990):

- axial loading only (bending moments and normal forces)
- analytical expression for energy release rate, ≡ elementary beam theory
- analytical mode decomposition based on dimensional considerations, linearity, relationship between ERR and SIF (Irwin, Sih) (derivation is analytical except for a single parameter extracted from numerical solution of one loading case

Li, Wang and Thouless, JMPS, (2004):

- accounts for effects of shear in bimaterial isotropic beams
- numerical FE solution for the energy release rate
- expressions for SIFs depending on 5 numerically determined constants

THE EFFECTS OF SHEAR AND NEAR TIP DEFORMATIONS ON ENERGY RELEASE RATE AND MODE MIXITY OF EDGE-CRACKED ORTHOTROPIC LAYERS

(M.G. Andrews & R. Massabò, 2007, *Engineering Fracture Mechanics*)

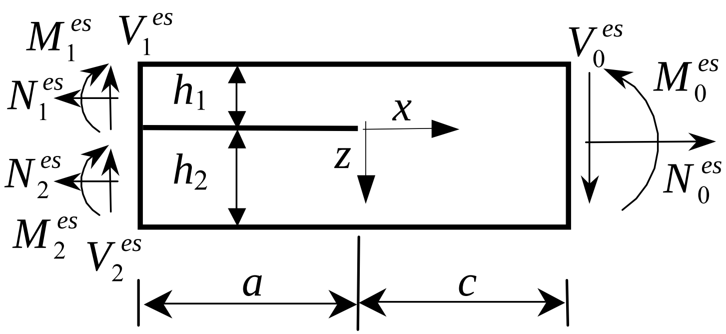

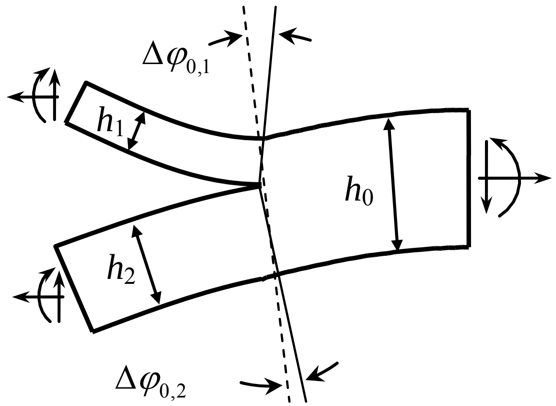

Edge cracked homogeneous and orthotropic linear elastic layer subject to generalized end forces

- **Plane problem**
- **x and z = principal material axes**

- **Non dimensional orthotropy ratios (plane stress):** $\lambda = \frac{E_z}{E_x}, \qquad \rho = \frac{\sqrt{E_x E_z}}{2G_{xz}} - \sqrt{\nu_{zx}\nu_{xz}}$

$0 < \rho < 5$ and $0 < \lambda < 1$ (typical values for composites)

- $a, c \geq c_{min} = h_i \lambda^{-1/4}$ $(i = 0,1,2)$:

so that crack tip fields independent of distance from load points

THE EFFECTS OF SHEAR AND NEAR TIP DEFORMATIONS ON ENERGY RELEASE RATE AND MODE MIXITY OF EDGE-CRACKED ORTHOTROPIC LAYERS

(M.G. Andrews & R. Massabò, 2007, *Engineering Fracture Mechanics*)

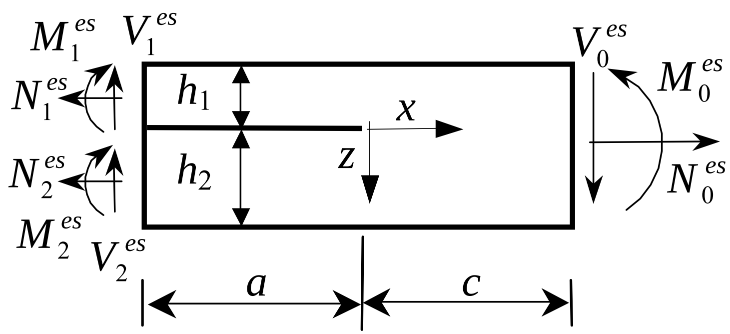

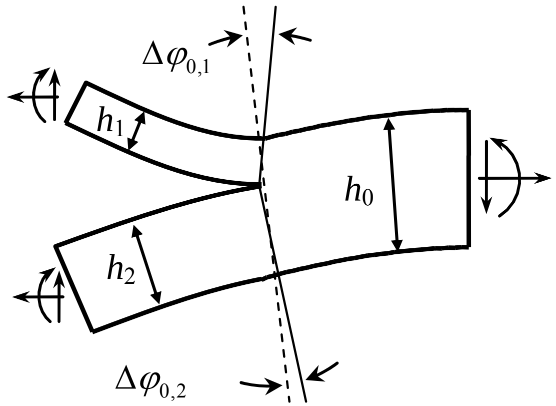

Edge cracked homogeneous and orthotropic linear elastic layer subject to generalized end forces

- Plane problem

- x and

- Non d

$0 < \rho < 5$

- a,c ≥

so that

Aim of our work:

-Derive semi-analytical expressions for the energy release rate and the stress intensity factors in homogeneous orthotropic layers that depend on the crack tip stress resultants;

- The expressions have physical significance and allow separation of the different contributions

ENERGY RELEASE RATE AND STRESS INTENSITY FACTORS

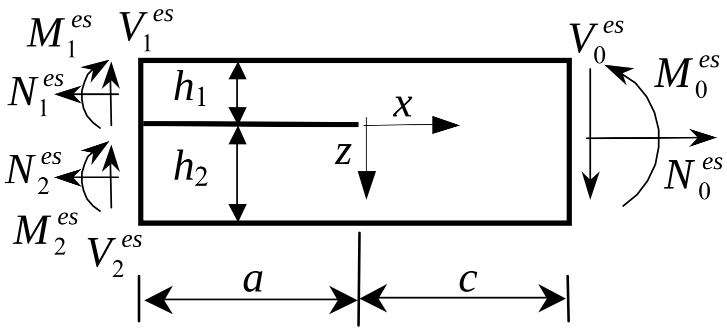

Self equilibrated crack tip loading systems:

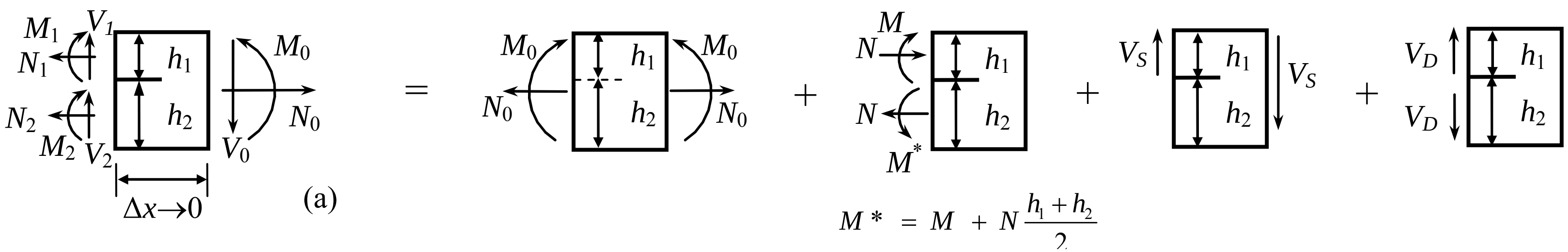

$$R = [M/E_x h_1^2; N/E_x h_1; V_S/E_x h_1; V_D/E_x h_1].$$

ENERGY RELEASE RATE AND STRESS INTENSITY FACTORS

Relationship between energy release rate and stress intensity factors in orthotropic body (Sih, 1965):

$$\mathcal{G} = \frac{1}{E_x}\sqrt{\frac{1+\rho}{2}}[\lambda^{-3/4}K_{\mathrm{I}}^2 + \lambda^{-1/4}K_{\mathrm{II}}^2],$$

Complex stress intensity factor:

$$K = \lambda^{-3/8}K_{\mathrm{I}} + \mathrm{i}\lambda^{-1/8}K_{\mathrm{II}},$$

$$|K| = \sqrt{\lambda^{-3/4}K_{\mathrm{I}}^2 + \lambda^{-1/4}K_{\mathrm{II}}^2},$$

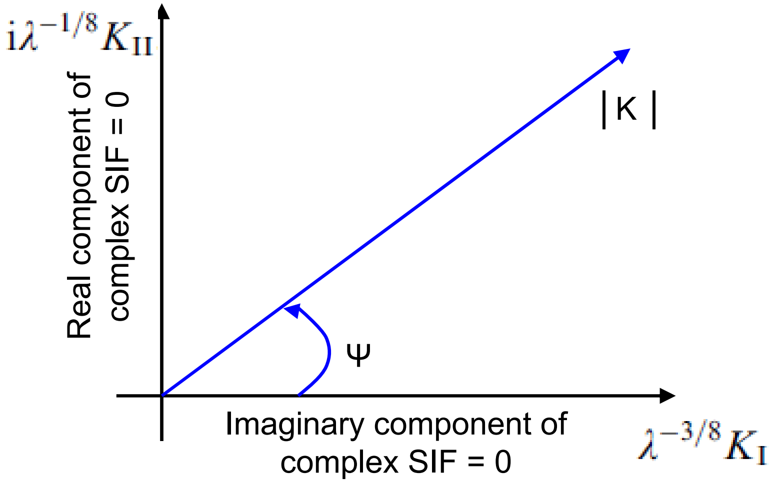

$$\Rightarrow \quad \sqrt{E_x\mathcal{G}} = \left(\frac{1+\rho}{2}\right)^{1/4}|K|. \qquad \text{(*)}$$

Dimensional considerations, linearity and Eq. (*) :

$$|K_R| = f_R(\eta,\lambda,\rho)RE_x\sqrt{h_1}\left(\frac{1+\rho}{2}\right)^{-1/4}, \qquad f_R^2 = \mathcal{G}_R/(R^2E_xh_1).$$

ENERGY RELEASE RATE AND STRESS INTENSITY FACTORS

Components of complex stress intensity factor:

$$K_{\mathrm{I}R} = \lambda^{3/8} |K_R| \cos(\Psi_R)$$

$$K_{\mathrm{II}R} = \lambda^{1/8} |K_R| \sin(\Psi_R)$$

$$\Psi = \tan^{-1}\left(\lambda^{1/4}\frac{K_{\mathrm{II}}}{K_{\mathrm{I}}}\right).$$

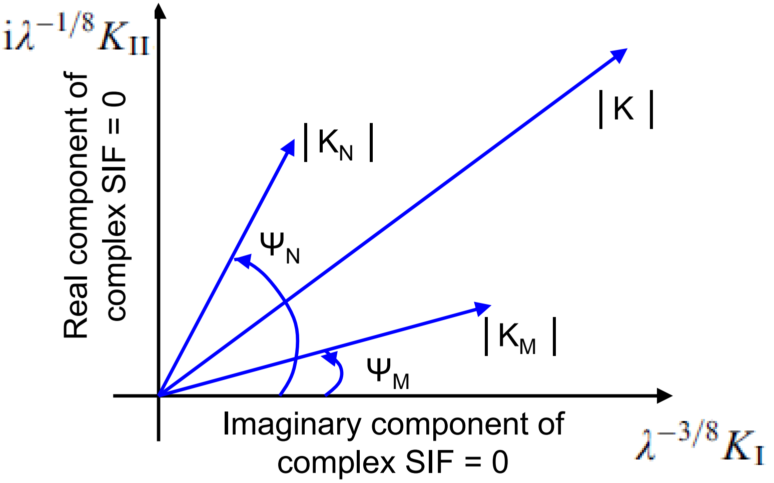

Assuming:

$$\Psi_N = \omega, \quad \Psi_M = \gamma_M + \omega - \frac{\pi}{2}, \quad \Psi_{V_D} = \gamma_{V_D} + \omega - \frac{\pi}{2}, \quad \Psi_{V_S} = \gamma_{V_S} + \omega - \frac{\pi}{2}.$$

Stress Intensity Factors:

$$K_{\mathrm{I}} = \frac{\lambda^{3/8}}{\left(\frac{1+\rho}{2}\right)^{1/4}}\left[\frac{f_M M \sin(\gamma_M + \omega)}{h_1^{3/2}} + \frac{f_N N \cos(\omega)}{\sqrt{h_1}} + \frac{f_{V_D} V_D \sin(\gamma_{V_D} + \omega)}{\sqrt{h_1}} + \frac{f_{V_S} V_S \sin(\gamma_{V_S} + \omega)}{\sqrt{h_1}}\right],$$

$$K_{\mathrm{II}} = \frac{\lambda^{1/8}}{\left(\frac{1+\rho}{2}\right)^{1/4}}\left[-\frac{f_M M \cos(\gamma_M + \omega)}{h_1^{3/2}} + \frac{f_N N \sin(\omega)}{\sqrt{h_1}} - \frac{f_{V_D} V_D \cos(\gamma_{V_D} + \omega)}{\sqrt{h_1}} - \frac{f_{V_S} V_S \cos(\gamma_{V_S} + \omega)}{\sqrt{h_1}}\right].$$

ROOT ROTATIONS

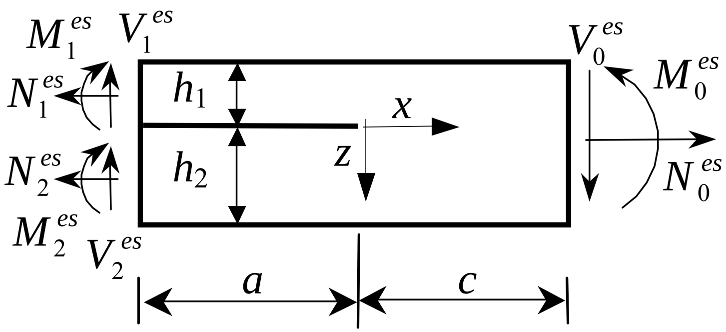

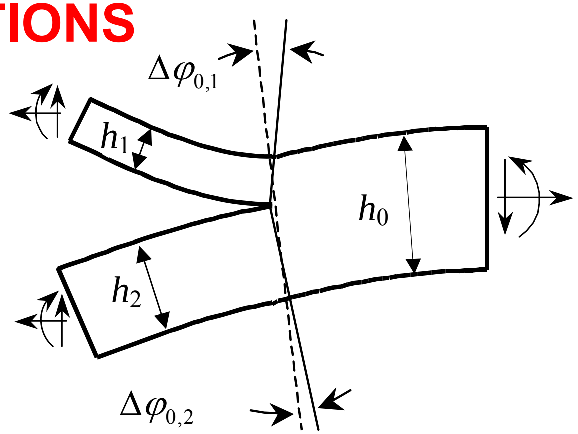

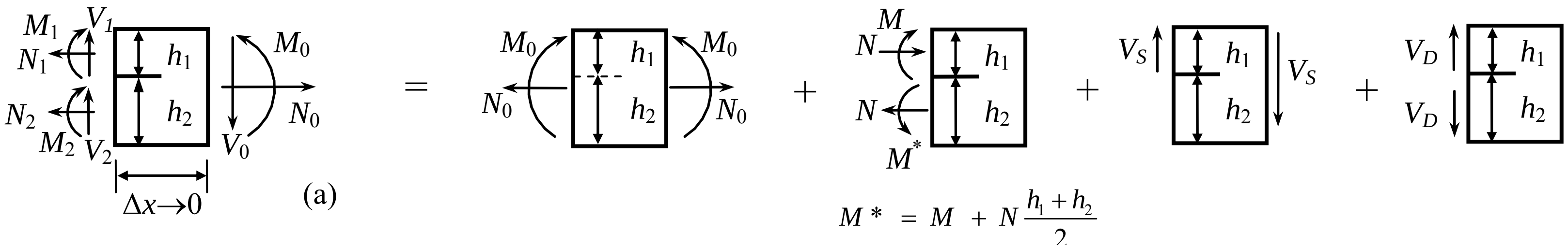

Root rotations:

$$\Delta\varphi_{0,1} = \frac{1}{E_x h_1}\left(\frac{a_1^M}{h_1}M + a_1^N N + a_1^{V_S}V_S + a_1^{V_D}V_D\right)$$

$$\Delta\varphi_{0,2} = \frac{1}{E_x h_1}\left(\frac{a_2^M}{h_1}M + a_2^N N + a_2^{V_S}V_S + a_2^{V_D}V_D\right)$$

where:

$$a_1^M, a_2^M, a_1^N, a_2^N = b\lambda^{-1/4}$$

$$a_1^{V_D} = b\lambda^{-1/2} - \nu_{xz}/\kappa_S$$

$$a_2^{V_D} = b\lambda^{-1/2} + \eta\,\nu_{xz}/\kappa_S$$

$$a_1^{V_S} = b\lambda^{-1/2} - 1/(1+\eta)\,\nu_{xz}/\kappa_S$$

$$a_2^{V_S} = b\lambda^{-1/2} + \eta/(1+\eta)\,\nu_{xz}/\kappa_S$$

and: $\eta = h_1/h_2 \quad \lambda = E_z/E_x \quad \rho = \frac{\sqrt{E_x E_z}}{2G_{xz}} - \sqrt{\nu_{zx}\nu_{xz}}$

ROOT ROTATIONS

Table 1
Root rotation compliance coefficients of an orthotropic edge cracked layer with arbitrary generalized end forces acting at a distance $\gg c_{\min} = h_i\lambda^{-1/4}$ $(i = 0, 1, 2)$ from the crack tip; results apply to any $a, c \geqslant c_{\min} = h_i\lambda^{-1/4}$ with uncertainties lower than ±2%

$$\Delta\varphi_{0,1} = \frac{1}{E_x h_1}\left(\frac{a_1^M}{h_1}M + a_1^N N + a_1^{V_S} V_S + a_1^{V_D} V_D\right) \quad \Delta\varphi_{0,2} = \frac{1}{E_x h_1}\left(\frac{a_2^M}{h_1}M + a_2^N N + a_2^{V_S} V_S + a_2^{V_D} V_D\right)$$

$a_1^M, a_2^M, a_1^N, a_2^N = b\lambda^{-1/4}$,

$a_1^{V_D} = b\lambda^{-1/2} - \nu_{xz}/\kappa_S$, $a_2^{V_D} = b\lambda^{-1/2} + \eta\nu_{xz}/\kappa_S$

$a_1^{V_S} = b\lambda^{-1/2} - \dfrac{1}{1+\eta}\dfrac{\nu_{xz}}{\kappa_S}$, $a_2^{V_S} = b\lambda^{-1/2} + \dfrac{\eta}{1+\eta}\dfrac{\nu_{xz}}{\kappa_S}$

with $\lambda = \dfrac{E_z}{E_x}$, $\rho = \dfrac{\sqrt{E_x E_z}}{2G_{xz}} - \sqrt{\nu_{zx}\nu_{xz}}$ and $\kappa_S = 5/6$

Modified crack tip stress resultants

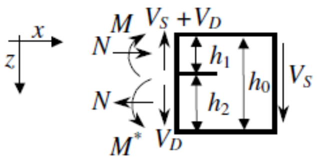

$M^* = M + N(h_1 + h_2)/2$

	Constant b							
for:	a_1^M	a_2^M	a_1^N	a_2^N	$a_1^{V_D}$	$a_2^{V_D}$	$a_1^{V_S}$	$a_2^{V_S}$
$\eta = h_1/h_2$	$\rho = 1$ and $0.025 \leqslant \lambda \leqslant 1$							
→0.0	7.439	0.000	1.732	0.000	2.606	0.000	2.606	0.000
0.2	7.529	−0.372	2.066	−0.331	2.188	−0.137	2.208	−0.146
0.4	7.672	−1.399	2.304	−1.077	1.945	−0.410	1.758	−0.350
0.6	7.817	−3.034	2.492	−2.163	1.769	−0.746	1.382	−0.506
0.8	7.952	−5.262	2.649	−3.567	1.631	−1.120	1.087	−0.604
1.0	8.077	−8.077	2.782	−5.280	1.518	−1.518	0.858	−0.656
η	$\rho = 3$ and $0.025 \leqslant \lambda \leqslant 1$							
→ 0.0	10.046	0.000	2.107	0.000	2.825	0.000	2.825	0.000
0.2	10.234	−0.480	2.604	−0.475	2.237	−0.126	2.684	−0.184
0.4	10.487	−1.860	2.935	−1.544	1.943	−0.384	2.200	−0.408
0.6	10.705	−4.094	3.183	−3.087	1.743	−0.709	1.716	−0.526
0.8	10.884	−7.156	3.379	−5.069	1.591	−1.074	1.306	−0.544
1.0	11.029	−11.029	3.541	−7.472	1.469	−1.469	0.977	−0.488
η	$\rho = 5$ and $0.025 \leqslant \lambda \leqslant 1$							
→ 0.0	12.029	0.000	2.408	0.000	2.931	0.000	2.931	0.000
0.2	12.313	−0.566	3.043	−0.586	2.226	−0.115	3.105	−0.221
0.4	12.663	−2.225	3.449	−1.902	1.904	−0.357	2.613	−0.463
0.6	12.946	−4.927	3.745	−3.796	1.692	−0.668	2.034	−0.542
0.8	13.163	−8.637	3.975	−6.221	1.533	−1.022	1.518	−0.475
1.0	13.331	−13.331	4.161	−9.153	1.406	−1.406	1.093	−0.308

Uncertainties estimated on root rotations from FE solution and interpolation affect the fourth decimal digit.

ROOT ROTATIONS

Table 1
Root rotation compliance coefficients of an orthotropic edge cracked layer with arbitrary generalized end forces acting at a distance $\gg c_{\min} = h_i\lambda^{-1/4}$ $(i = 0, 1, 2)$ from the crack tip; results apply to any $a, c \geqslant c_{\min} = h_i\lambda^{-1/4}$ with uncertainties lower than ±2%

$$\Delta\varphi_{0,1} = \frac{1}{E_x h_1}\left(\frac{a_1^M}{h_1}M + a_1^N N + a_1^{V_S}V_S + a_1^{V_D}V_D\right) \quad \Delta\varphi_{0,2} = \frac{1}{E_x h_1}\left(\frac{a_2^M}{h_1}M + a_2^N N + a_2^{V_S}V_S + a_2^{V_D}V_D\right)$$

$a_1^M, a_2^M, a_1^N, a_2^N = b\lambda^{-1/4}$,

$a_1^{V_D} = b\lambda^{-1/2} - \nu_{xz}/\kappa_S$, $a_2^{V_D} = b\lambda^{-1/2} + \eta\nu_{xz}/\kappa_S$

$a_1^{V_S} = b\lambda^{-1/2} - \frac{1}{1+\eta}\frac{\nu_{xz}}{\kappa_S}$, $a_2^{V_S} = b\lambda^{-1/2} + \frac{\eta}{1+\eta}\frac{\nu_{xz}}{\kappa_S}$

with $\lambda = \frac{E_z}{E_x}$, $\rho = \frac{\sqrt{E_x E_z}}{2G_{xz}} - \sqrt{\nu_{zx}\nu_{xz}}$ and $\kappa_S = 5/6$

Modified crack tip stress resultants

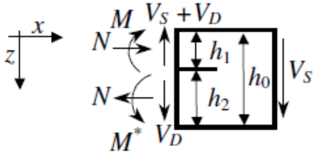

$M^* = M + N(h_1 + h_2)/2$

	Constant b							
for:	a_1^M	a_2^M	a_1^N	a_2^N	$a_1^{V_D}$	$a_2^{V_D}$	$a_1^{V_S}$	$a_2^{V_S}$
$\eta = h_1/h_2$	$\rho = 1$ and $0.025 \leqslant \lambda \leqslant 1$							
→0.0	7.439	0.000	1.732	0.000	2.606	0.000	2.606	0.000
0.2	7.529	−0.372	2.066	−0.331	2.188	−0.137	2.208	−0.146
0.4	7.672	−1.399	2.304	−1.077	1.945	−0.410	1.758	−0.350
0.6	7.817	−3.034	2.492	−2.163	1.769	−0.746	1.382	−0.506
0.8	7.952	−5.262	2.649	−3.567	1.631	−1.120	1.087	−0.604
1.0	8.077	−8.077	2.782	−5.280	1.518	−1.518	0.858	−0.656
η	$\rho = 3$ and $0.025 \leqslant \lambda \leqslant 1$							
→ 0.0	10.046	0.000	2.107	0.000	2.825	0.000	2.825	0.000
0.2	10.234	−0.480	2.604	−0.475	2.237	−0.126	2.684	−0.184
0.4	10.487	−1.860	2.935	−1.544	1.943	−0.384	2.200	−0.408
0.6	10.705	−4.094	3.183	−3.087	1.743	−0.709	1.716	−0.526
0.8	[illegible]	[illegible]	[illegible]	[illegible]	[illegible]	[illegible]	[illegible]	[illegible]
1.0	[illegible]	[illegible]	[illegible]	[illegible]	[illegible]	[illegible]	[illegible]	[illegible]
η	[illegible]							
→ 0.0	[illegible]	[illegible]	[illegible]	[illegible]	[illegible]	[illegible]	[illegible]	[illegible]
0.2	[illegible]	[illegible]	[illegible]	[illegible]	[illegible]	[illegible]	[illegible]	[illegible]
0.4	[illegible]	[illegible]	[illegible]	[illegible]	[illegible]	[illegible]	[illegible]	[illegible]
0.6	[illegible]	[illegible]	[illegible]	[illegible]	[illegible]	[illegible]	[illegible]	[illegible]
0.8	[illegible]	[illegible]	[illegible]	[illegible]	[illegible]	[illegible]	[illegible]	[illegible]
1.0	[illegible]	[illegible]	[illegible]	[illegible]	[illegible]	[illegible]	[illegible]	[illegible]

Uncertainties es

-Root rotations are generated by all crack tip stress resultants and strongly depend on the local two-dimensional fields.

- This result can explain limitations of models based on plate theory and an interface approach in accurately predicting fracture parameters for short and moderately long cracks

ENERGY RELEASE RATE AND STRESS INTENSITY FACTORS

Energy release rate from 2D elasticity:

$$\mathscr{G} = \frac{1}{E_x}\sqrt{\frac{1+\rho}{2}}[\lambda^{-3/4}K_{\mathrm{I}}^2 + \lambda^{-1/4}K_{\mathrm{II}}^2],$$

Energy release rate from first order shear deformation beam theory:

$$\mathscr{G} = J = \frac{1}{2}\left[\sum_{i=1}^{2}\left(\frac{M_i^2}{E_x h_i^3/12} + \frac{V_i^2}{\kappa_S G_{xz} h_i} + \frac{N_i^2}{E_x h_i} + 2V_i \Delta\varphi_{0,i}\right) - \frac{M_0^2}{E_x h_0^3/12} - \frac{V_0^2}{\kappa_S G_{xz} h_0} - \frac{N_0^2}{E_x h_0}\right],$$

$$\Downarrow$$

$$f_N(\eta) = \frac{1}{\sqrt{2}}\sqrt{1+4\eta+6\eta^2+3\eta^3}$$

$$f_M(\eta) = \frac{1}{\sqrt{2}}\sqrt{12(1+\eta^3)}$$

$$f_{V_D}(\eta,\lambda,\rho) = \sqrt{\left(a_1^{V_D} - a_2^{V_D} + \frac{1+\eta}{\kappa_S}\left(\frac{\rho}{\sqrt{\lambda}} + \nu_{xz}\right)\right)}$$

$$f_{V_S}(\eta,\lambda,\rho) = \sqrt{\left(a_1^{V_S} + \frac{1}{\kappa_S}\frac{1}{1+\eta}\left(\frac{\rho}{\sqrt{\lambda}} + \nu_{xz}\right)\right)}$$

$$\gamma_M(\eta) = \sin^{-1}\left(\frac{3(1+\eta)\eta^2}{f_M f_N}\right)$$

$$\gamma_{V_D}(\eta,\rho) = \sin^{-1}\left(\frac{a_1^N - a_2^N}{2 f_N f_{V_D}}\right)$$

$$\gamma_{V_S}(\eta,\rho) = \sin^{-1}\left(\frac{a_1^N}{2 f_N f_{V_S}}\right)$$

$$\omega = 52.1^\circ - 3^\circ\eta.$$

ENERGY RELEASE RATE AND STRESS INTENSITY FACTORS

Energy release rate from 2D elasticity:

$$\mathcal{G} = \frac{1}{E_x}\sqrt{\frac{1+\rho}{2}}\left[\lambda^{-3/4}K_{\mathrm{I}}^2 + \lambda^{-1/4}K_{\mathrm{II}}^2\right],$$

Energy release rate from first order shear deformation beam theory:

$$\mathcal{G} = J = \frac{1}{2}\left[\sum_{i=1}^{2}\left(\frac{M_i^2}{E_x h_i^3/12} + \frac{V_i^2}{\kappa_S G_{xz} h_i} + \frac{N_i^2}{E_x h_i} + 2V_i \Delta\varphi_{0,i}\right) - \frac{M_0^2}{E_x h_0^3/12} - \frac{V_0^2}{\kappa_S G_{xz} h_0} - \frac{N_0^2}{E_x h_0}\right],$$

$$f_N(\eta) = \frac{1}{\sqrt{2}}\sqrt{1+4\eta+6\eta^2+3\eta^3}$$

$$\gamma_M(\eta) = \sin^{-1}\left(\frac{3(1+\eta)\eta^2}{f_M f_N}\right)$$

$$f_M(\eta) = \frac{1}{\sqrt{2}}\sqrt{12\left(1+\eta^3\right)}$$

$$\gamma_{V_D}(\eta,\rho) = \sin^{-1}\left(\frac{a_1^N - a_2^N}{2 f_N f_{V_D}}\right)$$

$$f_{V_S}(\eta,\lambda,\rho) = \sqrt{\left(a_1^{V_S} + \frac{1}{\kappa_S}\frac{1}{1+\eta}\left(\frac{\rho}{\sqrt{\lambda}} + \nu_{xz}\right)\right)}$$

-Expression for the energy release rate fully resolve all crack problems where conditions are either mode I or mode II (e.g. laboratory specimens)

ENERGY RELEASE RATE AND STRESS INTENSITY FACTORS

Stress Intensity Factors:

$$K_{\mathrm{I}} = \frac{\lambda^{3/8}}{\left(\frac{1+\rho}{2}\right)^{1/4}} \left[\frac{f_M M \sin(\gamma_M + \omega)}{h_1^{3/2}} + \frac{f_N N \cos(\omega)}{\sqrt{h_1}} + \frac{f_{V_D} V_D \sin(\gamma_{V_D} + \omega)}{\sqrt{h_1}} + \frac{f_{V_S} V_S \sin(\gamma_{V_S} + \omega)}{\sqrt{h_1}} \right],$$

$$K_{\mathrm{II}} = \frac{\lambda^{1/8}}{\left(\frac{1+\rho}{2}\right)^{1/4}} \left[-\frac{f_M M \cos(\gamma_M + \omega)}{h_1^{3/2}} + \frac{f_N N \sin(\omega)}{\sqrt{h_1}} - \frac{f_{V_D} V_D \cos(\gamma_{V_D} + \omega)}{\sqrt{h_1}} - \frac{f_{V_S} V_S \cos(\gamma_{V_S} + \omega)}{\sqrt{h_1}} \right].$$

Semi-analytically derived constants:

$$f_N(\eta) = \frac{1}{\sqrt{2}} \sqrt{1 + 4\eta + 6\eta^2 + 3\eta^3}$$

$$f_M(\eta) = \frac{1}{\sqrt{2}} \sqrt{12\left(1+\eta^3\right)}$$

$$f_{V_D}(\eta, \lambda, \rho) = \sqrt{\left(a_1^{V_D} - a_2^{V_D} + \frac{1+\eta}{\kappa_S} \left(\frac{\rho}{\sqrt{\lambda}} + \nu_{xz} \right) \right)}$$

$$f_{V_S}(\eta, \lambda, \rho) = \sqrt{\left(a_1^{V_S} + \frac{1}{\kappa_S} \frac{1}{1+\eta} \left(\frac{\rho}{\sqrt{\lambda}} + \nu_{xz} \right) \right)}$$

$$\gamma_M(\eta) = \sin^{-1}\left(\frac{3(1+\eta)\eta^2}{f_M f_N} \right)$$

$$\gamma_{V_D}(\eta, \rho) = \sin^{-1}\left(\frac{a_1^N - a_2^N}{2 f_N f_{V_D}} \right)$$

$$\gamma_{V_S}(\eta, \rho) = \sin^{-1}\left(\frac{a_1^N}{2 f_N f_{V_S}} \right)$$

$$\omega = 52.1^\circ - 3^\circ \eta.$$

ENERGY RELEASE RATE AND STRESS INTENSITY FACTORS

Stress Intensity Factors:

$$K_{\mathrm{I}} = \frac{\lambda^{3/8}}{\left(\frac{1+\rho}{2}\right)^{1/4}}\left[\frac{f_M M \sin(\gamma_M+\omega)}{h_1^{3/2}} + \frac{f_N N \cos(\omega)}{\sqrt{h_1}} + \frac{f_{V_D} V_D \sin(\gamma_{V_D}+\omega)}{\sqrt{h_1}} + \frac{f_{V_S} V_S \sin(\gamma_{V_S}+\omega)}{\sqrt{h_1}}\right],$$

$$K_{\mathrm{II}} = \frac{\lambda^{1/8}}{\left(\frac{1+\rho}{2}\right)^{1/4}}\left[-\frac{f_M M \cos(\gamma_M+\omega)}{h_1^{3/2}} + \frac{f_N N \sin(\omega)}{\sqrt{h_1}} - \frac{f_{V_D} V_D \cos(\gamma_{V_D}+\omega)}{\sqrt{h_1}} - \frac{f_{V_S} V_S \cos(\gamma_{V_S}+\omega)}{\sqrt{h_1}}\right].$$

Semi-analytically derived constants:

$$f_N(\eta) = \frac{1}{\sqrt{2}}\sqrt{1+4\eta+6\eta^2+3\eta^3}$$

$$\gamma_M(\eta) = \sin^{-1}\left(\frac{3(1+\eta)\eta^2}{f_M f_N}\right)$$

$$f_M(\eta) = \frac{1}{\sqrt{2}} \ldots$$

$$f_{V_D}(\eta,\lambda,\rho) = \ldots$$

$$f_{V_S}(\eta,\lambda,\rho) = \ldots$$

-Expressions for the stress intensity factors fully resolve mixed mode fracture problems in statically determined systems. In statically undeterminate systems calculation of the crack tip stress resultants is first required (using 2D analyses or beam theory models accounting for the root rotations.

-Expressions are very accurate (uncertainties below 2%) for crack lengths

$a, c \geq c_{min} = h_i \lambda^{-1/4}$ $(i = 0,1,2)$

ENERGY RELEASE RATE AND STRESS INTENSITY FACTORS

Table 2
Energy release rates and stress intensity factors in an edge-cracked orthotropic layer subject to arbitrary generalized end forces acting at a distance $\geqslant c_{\min} = h_i\lambda^{-1/4}$ $(i = 0, 1, 2)$ from the crack tip

Energy release rate:

$$\mathcal{G} = J = \frac{1}{2}\left[\sum_{i=1}^{2}\left(\frac{M_i^2}{E_x h_i^3/12} + \frac{V_i^2}{\kappa_S G_{xz} h_i} + \frac{N_i^2}{E_x h_i} + 2V_i\Delta\varphi_{0,i}\right) - \frac{M_0^2}{E_x h_0^3/12} - \frac{V_0^2}{\kappa_S G_{xz} h_0} - \frac{N_0^2}{E_x h_0}\right]$$

where:
N_i, M_i, V_i $(i = 1, 2, 3)$ = crack tip stress resultants (see picture *a*),
$\Delta\varphi_{0,i} = \frac{1}{E_x h_1}\left(\frac{a_i^M}{h_1}M + a_i^N N + a_i^{V_S} V_S + a_i^{V_D} V_D\right)$ = root rotation sub-layer i $(i = 1, 2)$
N, M, V_S, V_D = modified crack tip stress resultants (see picture *b*),
$a_i^M, a_i^N, a_i^{V_S}, a_i^{V_D}$ = root rotation compliances $(i = 1, 2)$ (Table 1),
E_x, E_z, G_{xz}, ν_{xz} = Young's and shear moduli, Poisson ratio.
$\kappa_S = 5/6$

Crack tip stress resultants

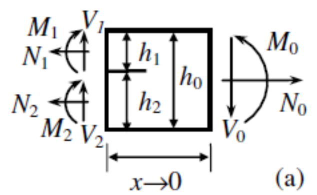

(a)

where:
$h_0 = h_1 + h_2$
$\eta = h_1/h$
$M_0 = M_1 + M_2 + \frac{1}{2}(h_1 N_2 - h_2 N_1)$,
$N_0 = N_1 + N_2$,
$V_0 = V_1 + V_2$.

Stress intensity factors:

$$K_{\mathrm{I}} = \frac{\lambda^{3/8}}{\left(\frac{1+\rho}{2}\right)^{1/4}}\left[\frac{f_M M \sin(\gamma_M + \omega)}{h_1^{3/2}} + \frac{f_N N \cos(\omega)}{\sqrt{h_1}} + \frac{f_{V_D} V_D \sin(\gamma_{V_D} + \omega)}{\sqrt{h_1}} + \frac{f_{V_S} V_S \sin(\gamma_{V_S} + \omega)}{\sqrt{h_1}}\right]$$

$$K_{\mathrm{II}} = \frac{\lambda^{1/8}}{\left(\frac{1+\rho}{2}\right)^{1/4}}\left[-\frac{f_M M \cos(\gamma_M + \omega)}{h_1^{3/2}} + \frac{f_N N \sin(\omega)}{\sqrt{h_1}} - \frac{f_{V_D} V_D \cos(\gamma_{V_D} + \omega)}{\sqrt{h_1}} - \frac{f_{V_S} V_S \cos(\gamma_{V_S} + \omega)}{\sqrt{h_1}}\right]$$

with:

$f_M(\eta) = \frac{1}{\sqrt{2}}\sqrt{12(1+\eta^3)}$, $f_N(\eta) = \frac{1}{\sqrt{2}}\sqrt{1 + 4\eta + 6\eta^2 + 3\eta^3}$,

$f_{V_S}(\eta, \lambda, \rho) = \sqrt{\left(a_1^{V_S} + \frac{1}{\kappa_S}\frac{1}{1+\eta}\left(\frac{\rho}{\sqrt{\lambda}} + \nu_{xz}\right)\right)}$,

$f_{V_D}(\eta, \lambda, \rho) = \sqrt{\left(a_1^{V_D} - a_2^{V_D} + \frac{1+\eta}{\kappa_S}\left(\frac{\rho}{\sqrt{\lambda}} + \nu_{xz}\right)\right)}$,

$\gamma_M(\eta) = \sin^{-1}\left(\frac{3(1+\eta)\eta^2}{f_M f_N}\right)$,

$\gamma_{V_S}(\eta, \rho) = \sin^{-1}\left(\frac{a_1^N}{2 f_N f_{V_S}}\right)$, $\gamma_{V_D}(\eta, \rho) = \sin^{-1}\left(\frac{a_1^N - a_2^N}{2 f_N f_{V_D}}\right)$,

$\omega = 52.1° - 3°\eta$

$\lambda = \frac{E_z}{E_x}$ and $\rho = \frac{\sqrt{E_z E_x}}{2G_{xz}} - \sqrt{\nu_{xz}\nu_{zx}}$

Modified crack tip stress resultants

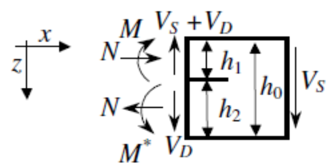

$M^* = M + N(h_1 + h_2)/2$ (b)

where:
$M = M_1 - \frac{1}{(1+1/\eta)^3}M_0$,
$N = -N_1 + \frac{1}{1+1/\eta}N_0 - \frac{6}{\eta}\frac{1}{(1+1/\eta)^3}\frac{M_0}{h_1}$,
$V_S = V_0$, $V_D = -V_2$

APPLICATION – The exemplary case of the DCB specimen

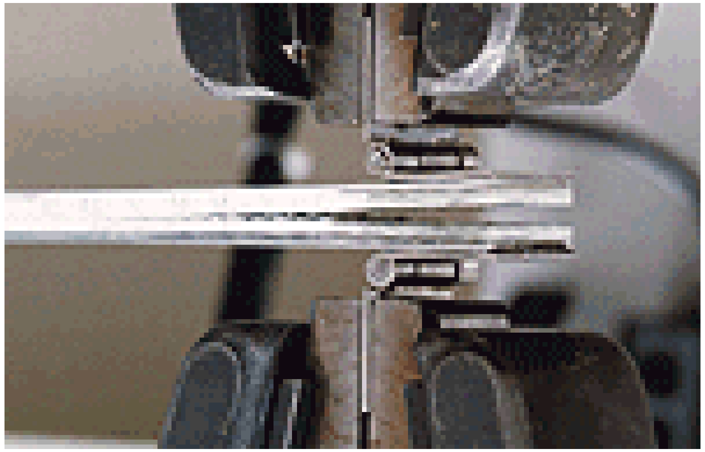

Near tip deformations due to shear

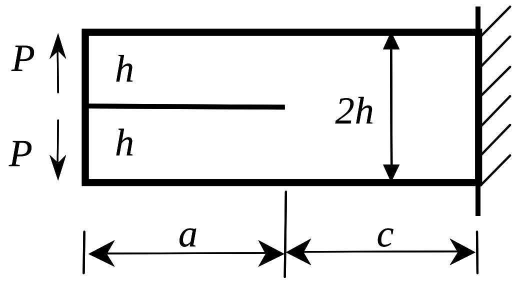

Dimensionless energy release rate:

$$\frac{\mathcal{G}_{\mathrm{DCB}} E_x h}{P^2} = 12\left(\frac{a}{h}\right)^2\left[1+\frac{1}{6}\left(\frac{1}{\kappa_S}\left(\frac{\rho}{\sqrt{\lambda}}+\nu_{xz}\right)+\frac{a_1^{V_D}-a_2^{V_D}}{2}\right)\left(\frac{h}{a}\right)^2+\frac{1}{12}\left(a_1^M-a_2^M\right)\left(\frac{h}{a}\right)\right],$$

- Elementary beam theory
- Shear deformations along the arms
- Near tip deformations due to shear
- Near tip deformations due to bending (and shear)

Dimensionless energy release rate for degenerate orthotropic beams:

$$\frac{\mathcal{G}_{\mathrm{DCB}} E_x h}{P^2} = 12\left(\frac{a}{h}\right)^2\left[1+0.673\lambda^{-1/4}\left(\frac{h}{a}\right)\right]^2.$$

BRIDGED- AND COHESIVE-CRACK MODELS

To describe fracture processes where nonlinear mechanisms arise in narrow, finite size bands, or process zones, ahead of traction free cracks

Cohesive crack

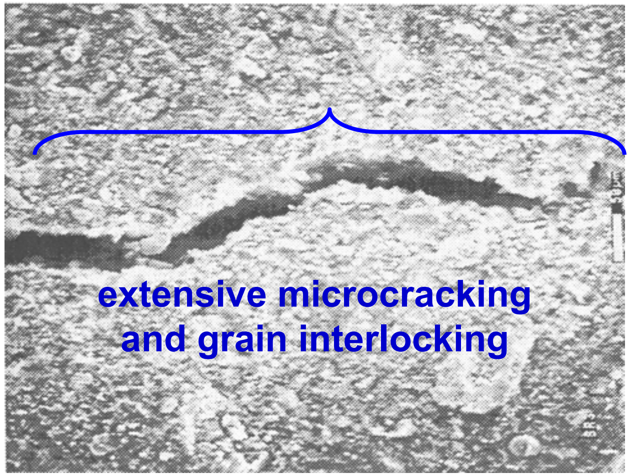

epoxy mortar
(Steiger, Sadouki & Wittmann)

Bridged crack

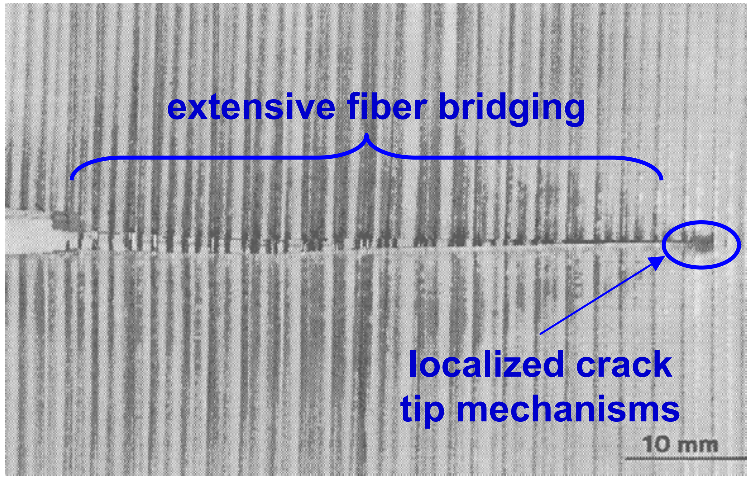

PMMA/Al composite
(Zok & Hom, 1990)

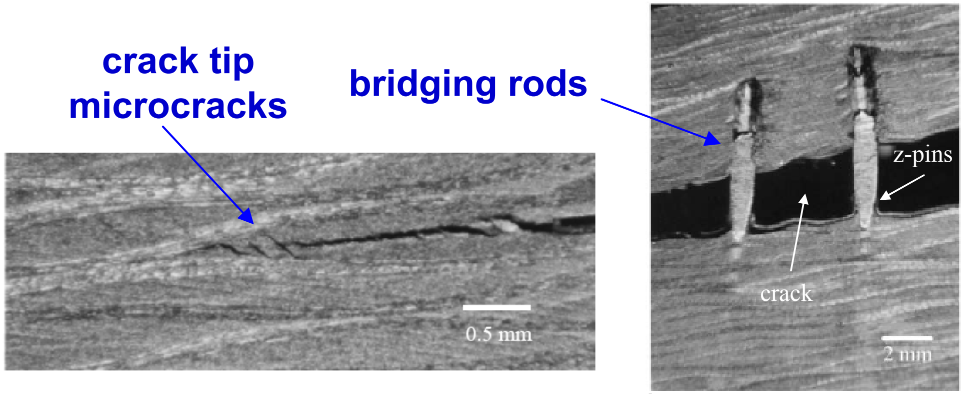

carbon-epoxy laminate/Ti z-pins
(Rugg, Cox & Massabò, 2002)

COHESIVE CRACK MODEL

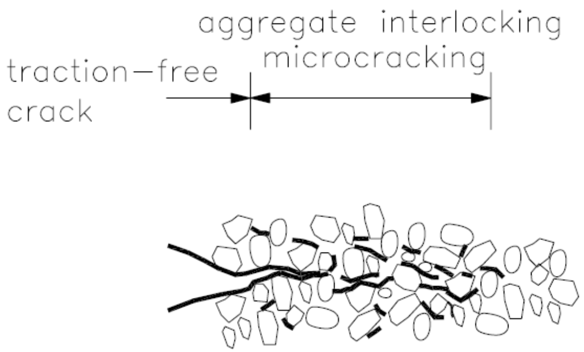

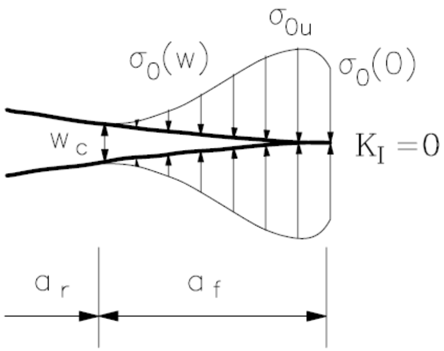

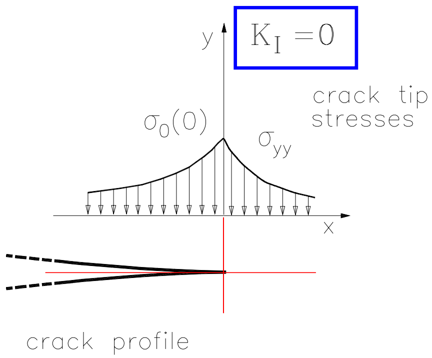

COHESIVE CRACK MODEL

BRIDGED CRACK MODEL

continuous model

discontinuous model

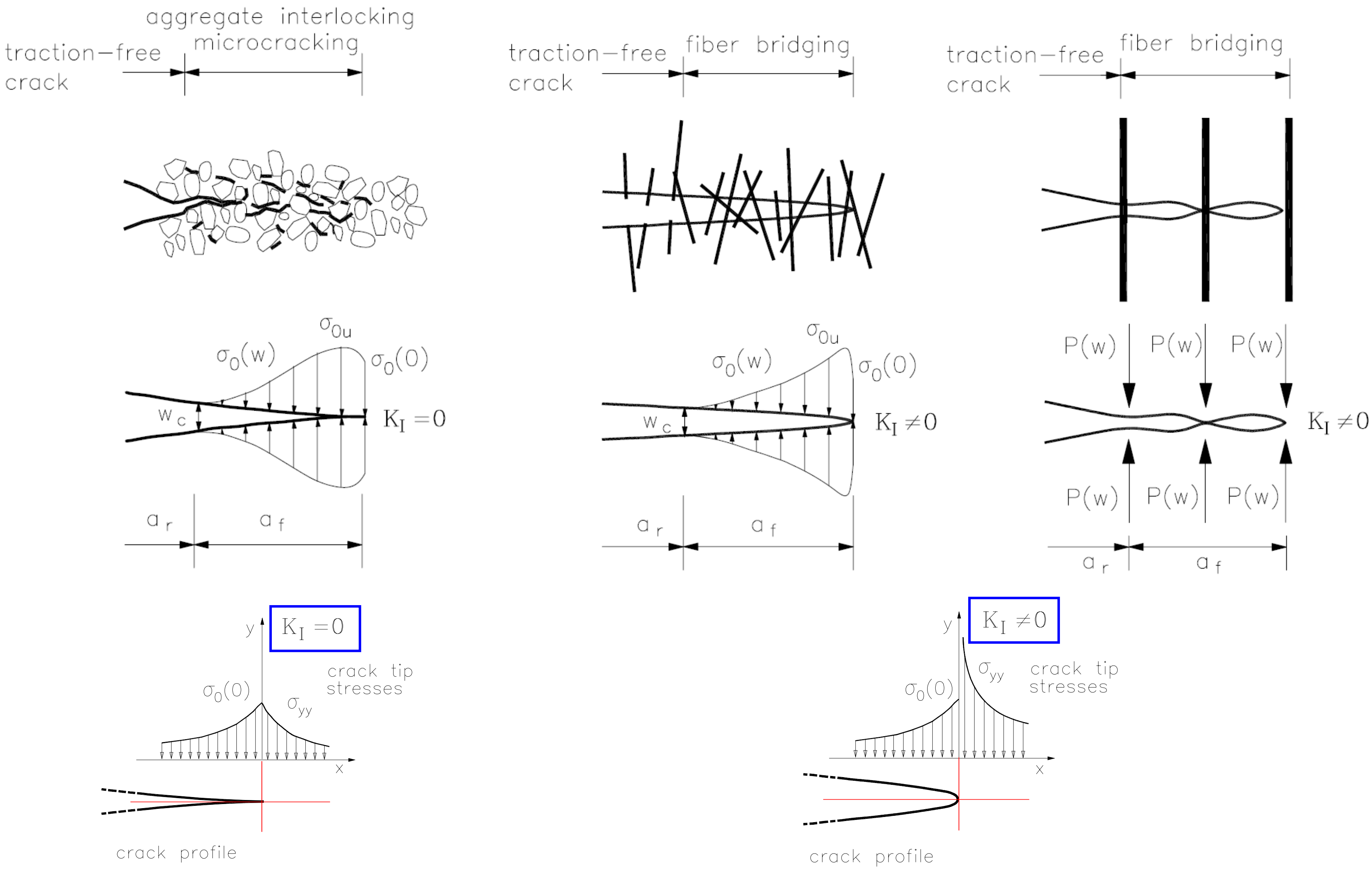

COHESIVE CRACK MODEL

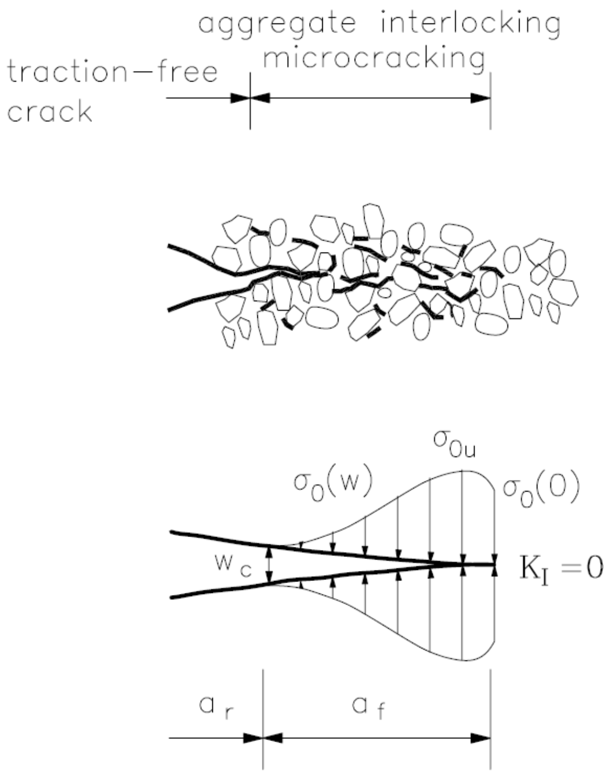

BRIDGED CRACK MODEL

continuous model

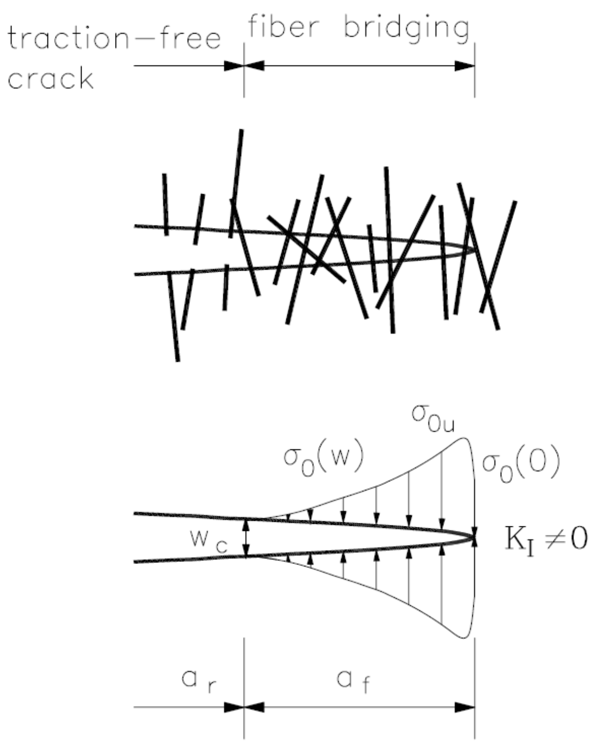

discontinuous model

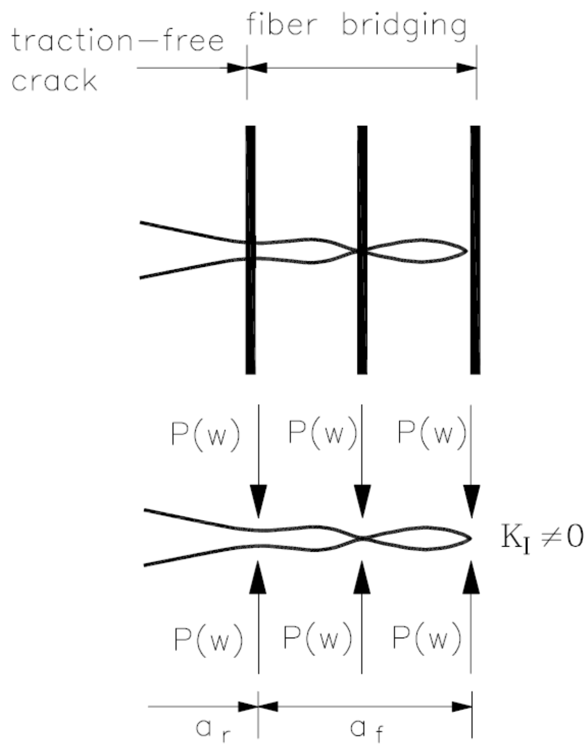

Model parameters:

cohesive/bridging traction laws

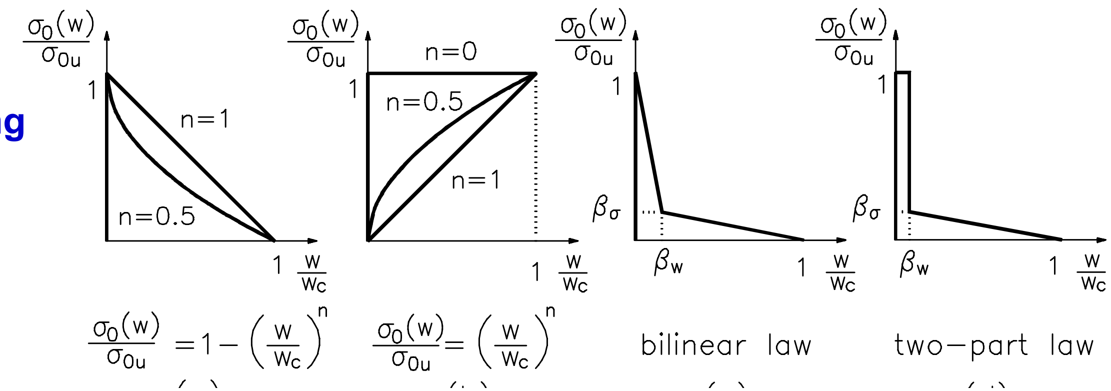

$+$ $\mathcal{G}_{IC}$ or K_{IC}

(in bridged crack model)

BRIDGED CRACK MODEL - SOLUTION

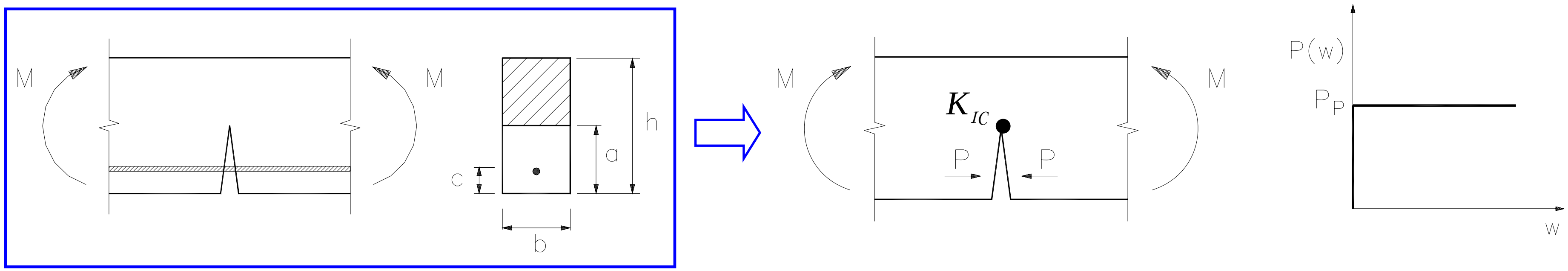

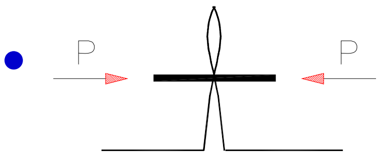

statically indeterminate problem

Kinematic compatibility condition → determination of forces P

$$w = w_{\mathrm{M}} + w_{\mathrm{P}} = \underbrace{\frac{2\mathrm{M}}{E}\int_{c}^{a}\frac{K_{\mathrm{IP}}K_{\mathrm{IM}}}{PM}\,b\mathrm{d}a}_{w_{\mathrm{M}}} + \underbrace{\frac{2\mathrm{P}}{E}\int_{c}^{a}\frac{K_{\mathrm{IP}}^{2}}{P^{2}}\,b\mathrm{d}a}_{w_{\mathrm{P}}} = 0$$

(Castigliano's theorem)

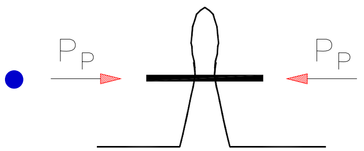

$$w = f(M, P_{\mathrm{P}}, \ldots)$$

- **Crack propagation:**

$$K_{\mathrm{I}} = K_{\mathrm{IM}} - K_{\mathrm{IP}} = K_{\mathrm{IC}}$$

(Carpinteri, 1981, 1984; Bosco & Carpinteri, 1992; Carpinteri & Massabò, 1996,1997)

Extension to other problems: weight function method

(e.g. weight functions for orthotropic double cantilever beams in Brandinelli, Massabò & Cox, 2003; Brandinelli & Massabò, 2006)

DEVELOPMENT OF BRIDGED-CRACK MODELS

	Material systems	
Barenblatt (1959)	crystals	
Dugdale (1960)	metals	($K_I = 0$)
Bilby, Cottrell & Swinden (1963)	metals	
…		
Romualdi & Batson (1963)	reinforced concrete	
Carpinteri (1981, 1984)	reinforced concrete	
Marshall, Cox & Evans (1985)	fiber reinforced ceramics	
Budiansky, Hutchinson & Evans (1986)	fiber reinforced ceramics	
Jenq & Shah (1985,1986)	fiber reinforced concrete	
Foote, Mai & Cotterell (1986)	fiber reinforced cementitious composites	
Rose (1987a,b)	crack reinforcement by springs and patches	
Swanson et al. (1987)	coarse grain ceramics	($K_I \neq 0$)
Erdogan & Joseph (1987)	particle reinforced ceramics	
Mc Meeking & Evans (1990)	metal matrix composites, fatigue	
Kendall, Clegg & Gregory (1991)	polymer crazing	
Bower & Ortiz (1991)	particle reinforced brittle matrix composites	
Suo, Ho & Gong (1993)	ceramic matrix composites, notch sensitivity	
Ballarini & Muju (1993)	brittle matrix composites	
Carpinteri & Massabò (1996)	fiber reinforced cementitious composites	
Massabò & Cox (1999)	through-thickness reinforced laminates	
…		

(For reviews: Bao & Suo, 1992; Cox & Marshall, 1994; Massabò, 1999)

ASYMPTOTIC SOLUTIONS FOR BRIDGED CRACKS
THE SMALL SCALE BRIDGING LIMIT

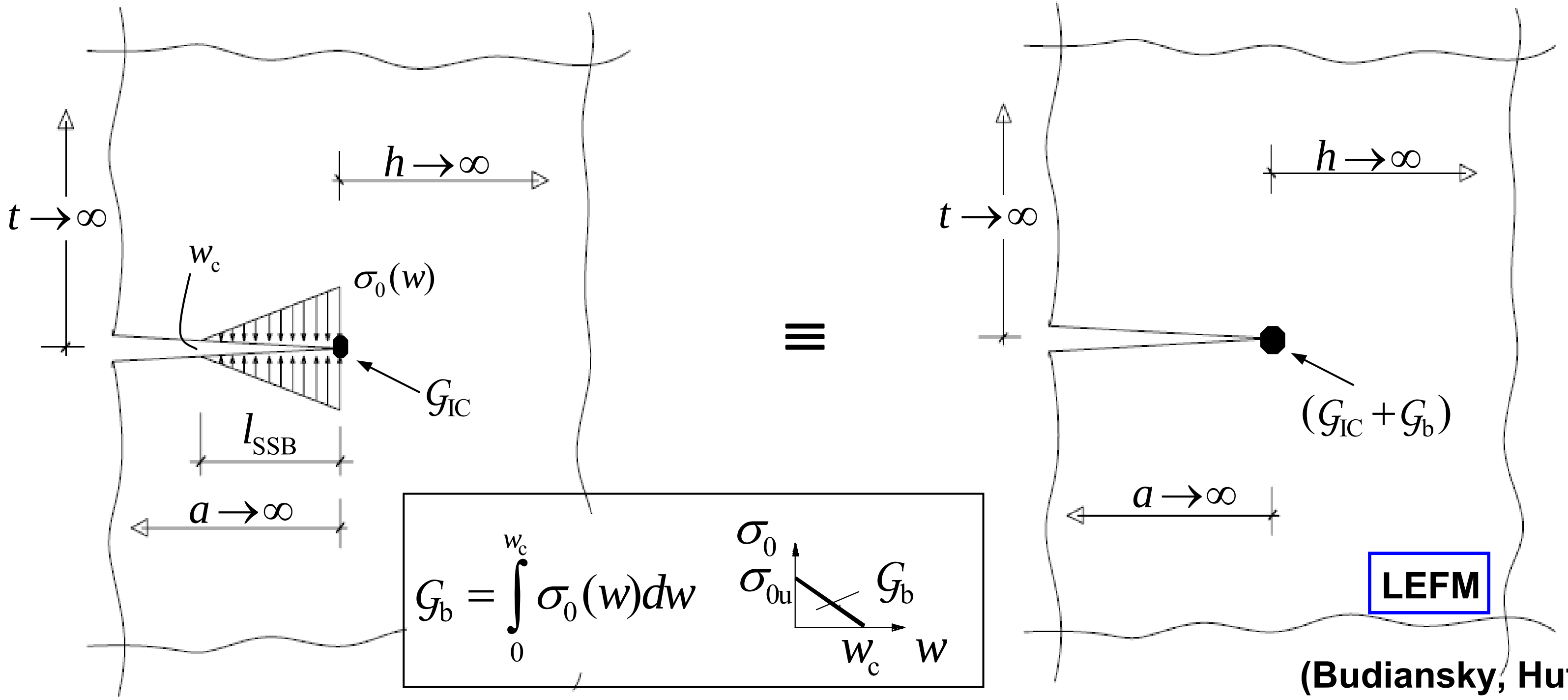

$$\mathcal{G}_b = \int_0^{w_c} \sigma_0(w)\,dw$$

(Budiansky, Hutchinson & Evans, 1986; Rose, 1987)

ASYMPTOTIC SOLUTIONS FOR BRIDGED CRACKS
THE SMALL SCALE BRIDGING LIMIT

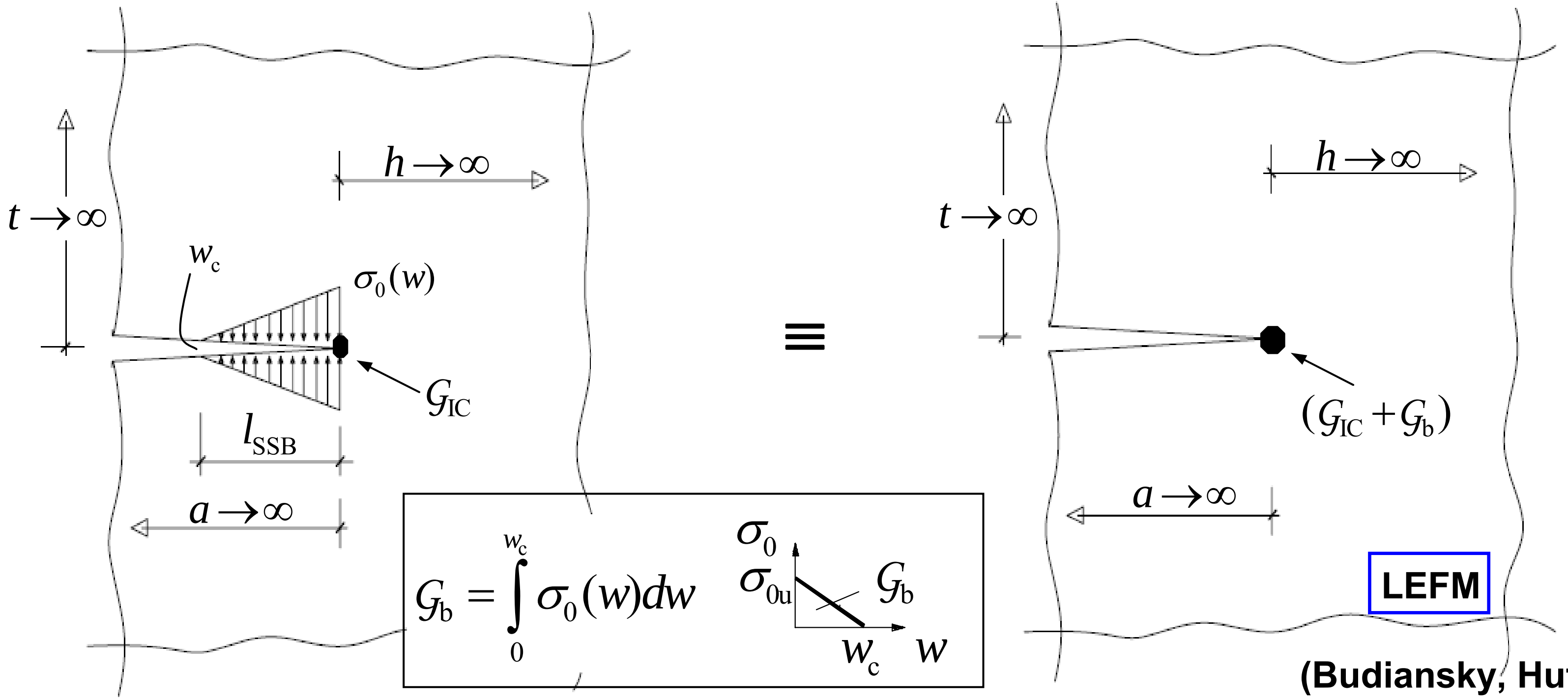

(Budiansky, Hutchinson & Evans, 1986; Rose, 1987)

Small scale bridging characteristic length scales:

Bridged crack $(\mathcal{G}_{IC} \neq 0)$

$$l_{SSB} = \frac{\pi}{8}\frac{w_c E}{\sigma_{0u}}\left(\sqrt{1+\frac{\mathcal{G}_{IC}}{\mathcal{G}_b}} - \sqrt{\frac{\mathcal{G}_{IC}}{\mathcal{G}_b}}\right)^2$$

(For rectangular bridging law)
(Bao & Suo, 1992; Cox & Marshall, 1994)

Cohesive crack $(\mathcal{G}_{IC} = 0)$

$$l_{SSB} = \frac{\pi}{8}\frac{w_c E}{\sigma_{0u}}$$

(Bilby, Cottrell, Swinden, 1963; Hillerborg, 1976)

ASYMPTOTIC SOLUTIONS FOR BRIDGED CRACKS
THE SMALL SCALE BRIDGING LIMIT

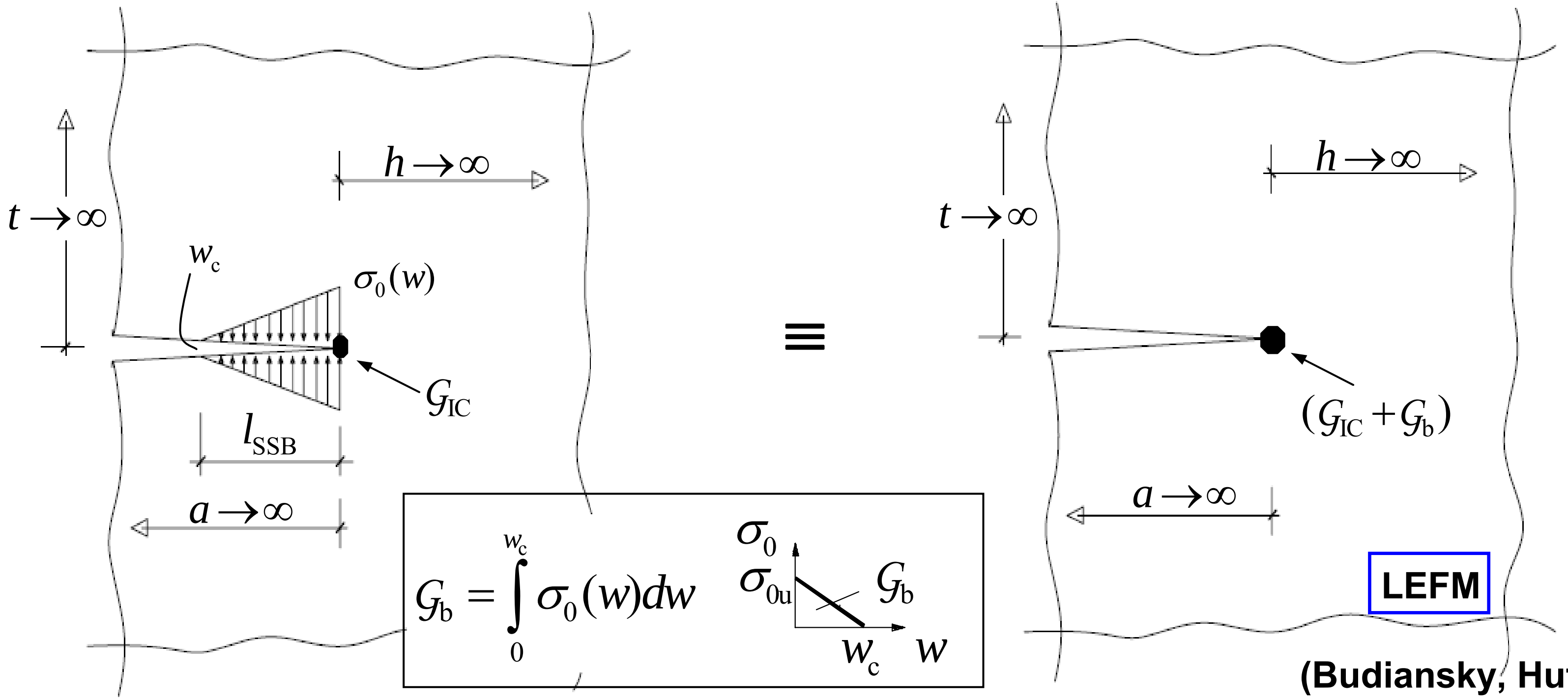

(Budiansky, Hutchinson & Evans, 1986; Rose, 1987)

Small scale bridging characteristic length scales:

Bridged crack $(\mathcal{G}_{IC} \neq 0)$

$$l_{SSB} = \ldots$$

...ging law) ...x & ...Marshall, 1994)

Small scale bridging characteristic length scale defines material brittleness and varies over many order of magnitude in different material systems

Cohesive crack $(\mathcal{G}_{IC} = 0)$

$$l_{SSB} = \frac{\pi}{8}\frac{w_c E}{\sigma_{0u}}$$

(Bilby, Cottrell, Swinden, 1963; Hillerborg, 1976)

ASYMPTOTIC SOLUTIONS FOR BRIDGED CRACKS
THE SMALL SCALE BRIDGING LIMIT IN SLENDER BODIES

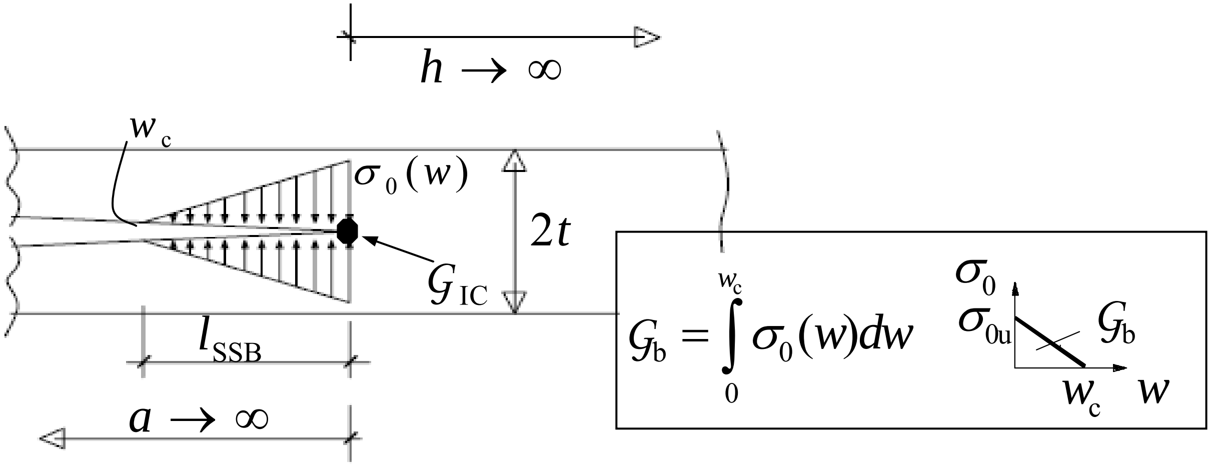

Mode I and mode II characteristic length scales:

$$l^{I}_{SSB} \approx (l_{SSB})^{1/4} t^{3/4}$$ (for mode I fracture)

$$l^{II}_{SSB} \approx (l_{SSB} t)^{1/2}$$ (for mode II fracture)

where l_{SSB} is the characteristic length scale in an infinite body

(Suo, Bao, Fan, 1992; Massabo & Cox, 1999)

ASYMPTOTIC SOLUTIONS FOR BRIDGED CRACKS
THE SMALL SCALE BRIDGING LIMIT IN SLENDER BODIES

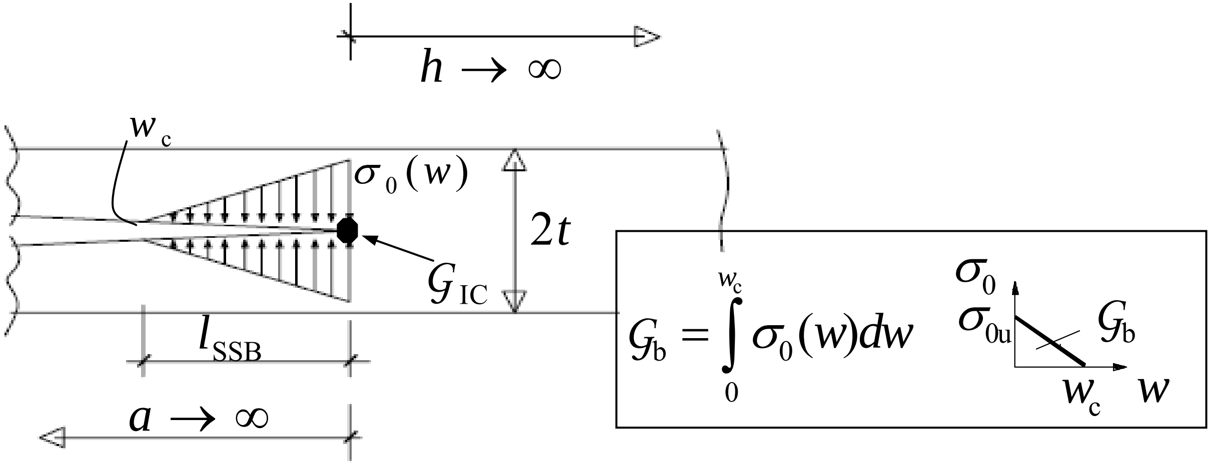

Mode I and mode II characteristic length scales:

l^{I} … $(l$ … $)^{1/4} t^{3/4}$

Characteristic length scales in slender bodies are smaller than those in infinite bodies

Important consequences when length scale is used to size the mesh in numerical descriptions of fracture processes

where l_{SSB} is the characteristic length scale in an infinite body

(Suo, Bao, Fan, 1992; Massabo & Cox, 1999)

ASYMPTOTIC SOLUTIONS FOR BRIDGED CRACKS
THE ACK LIMIT IN SLENDER AND NON SLENDER BODIES

(Avenston, Cooper & Kelly, 1971)

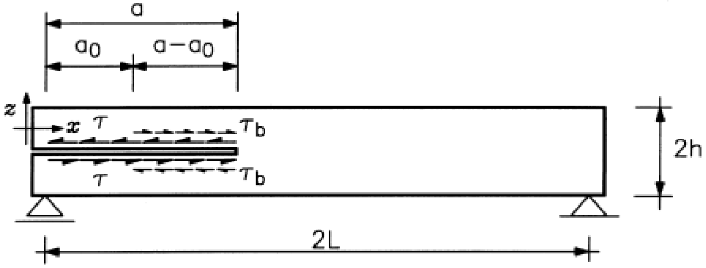

L >> h   a >> h

Slender body loaded in mode II

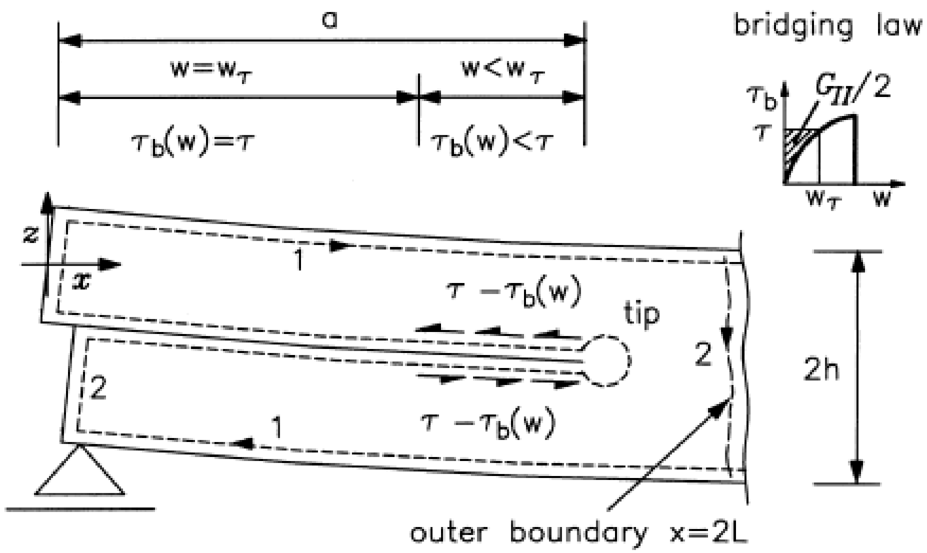

ACK limit

ACK characteristic length scales:

$$l_{\mathrm{ACK}} = \frac{\pi E}{4}\left(\frac{1+\alpha}{2\alpha}\mathcal{G}_{\mathrm{Ic}}\right)^{\frac{1-\alpha}{1+\alpha}} \beta^{\frac{-2}{1+\alpha}}$$

$$l_{\mathrm{ACK}}^{\mathrm{II}} \approx \left(l_{\mathrm{ACK}}\, t\right)^{1/2}$$

For power law bridging:

$$\sigma_0(w) = \beta(w/2)^{\alpha}$$

in an infinite body
(Cox & Marshall, 1994)

in a slender body (mode II)
(Massabò & Cox, 1999)

ASYMPTOTIC SOLUTIONS FOR BRIDGED CRACKS
THE ACK LIMIT IN SLENDER AND NON SLENDER BODIES

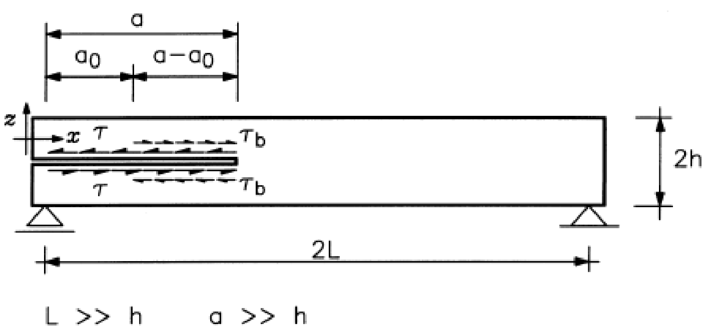

Slender body loaded in mode II

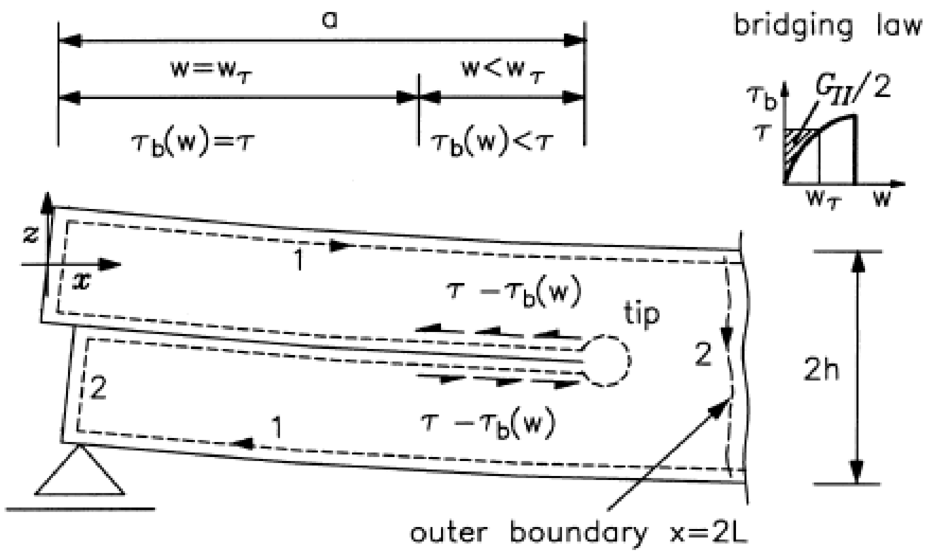

ACK limit

ACK charac

Comparing the characteristic length scales in long unnotched bodies determines whether crack will approach:

- ssb limit (if $l_{ssb} << l_{ACK}$) → catastrophic failure

- ACK limit (if $l_{ACK} << l_{ssb}$) → noncatastrophic failure

The presence of a notch favours catastrophic failure

If length scales are similar or body is finite, crack growth is in large scale bridging and detailed calculations are required

ridging:

$/\,2)^{\alpha}$

dy

994)

y (mode II)

999)

LARGE SCALE BRIDGING FRACTURE IN THROUGH-THICKNESS REINFORCED LAMINATES

CONTINUOUS TTR (stitching / weaving)

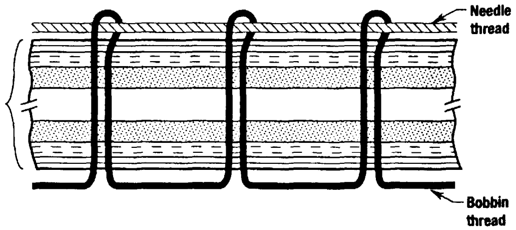

DISCONTINUOUS TTR (Fibrous/metallic Z-pins)

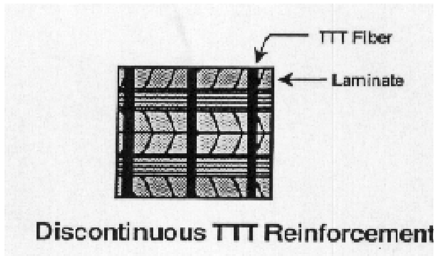

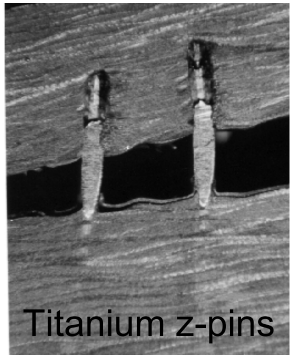

3D woven composites

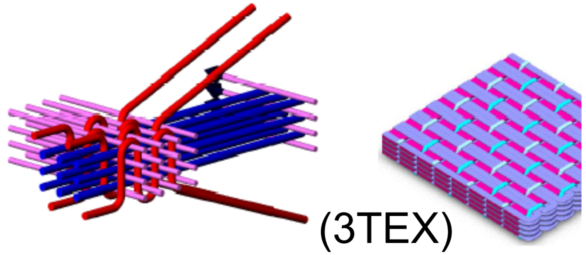

LARGE SCALE BRIDGING FRACTURE IN THROUGH-THICKNESS REINFORCED LAMINATES

CONTINUOUS TTR (stitching / weaving)

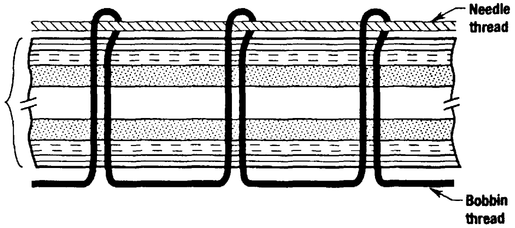

DISCONTINUOUS TTR (Fibrous/metallic Z-pins)

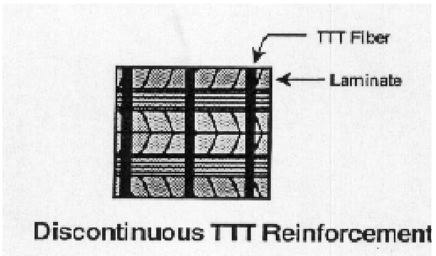

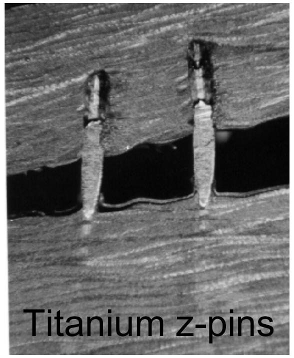

3D woven composites

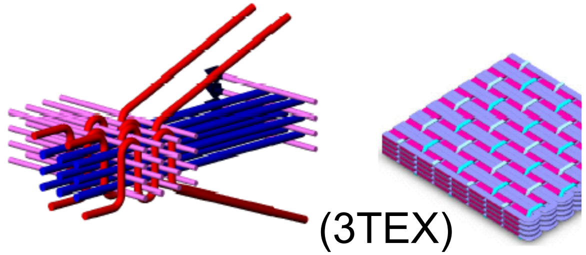

Load versus mid-span deflection curves in ENF specimens

unstitched

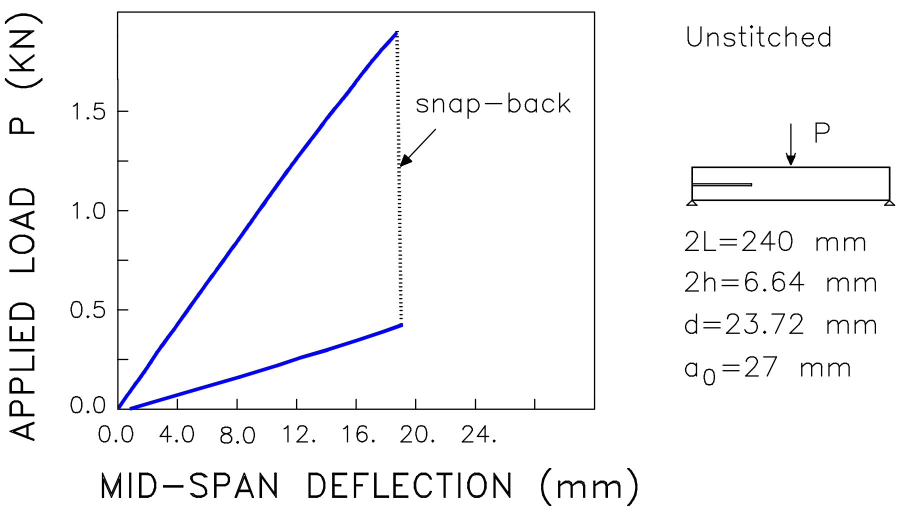

stitched

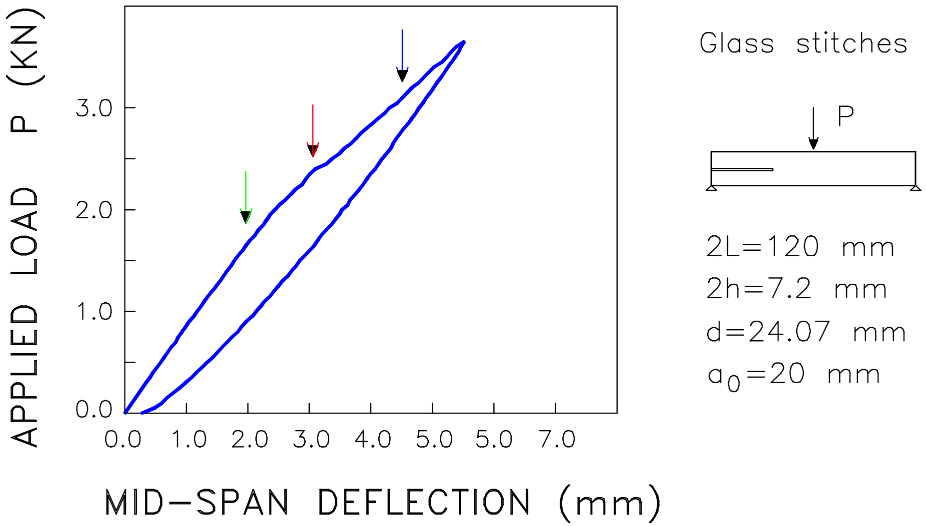

LARGE SCALE BRIDGING FRACTURE IN THROUGH-THICKNESS REINFORCED LAMINATES

CONTINUOUS TTR (stitching / weaving)

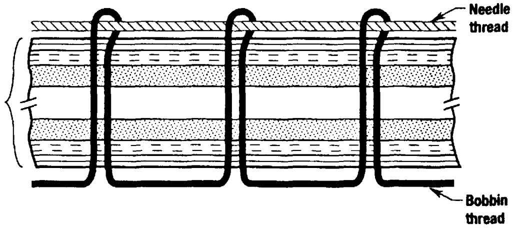

DISCONTINUOUS TTR (Fibrous/metallic Z-pins)

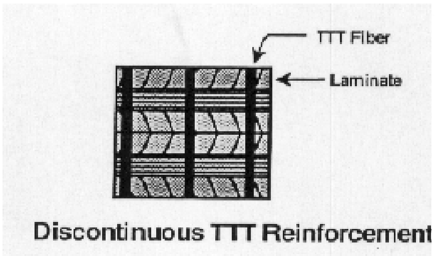

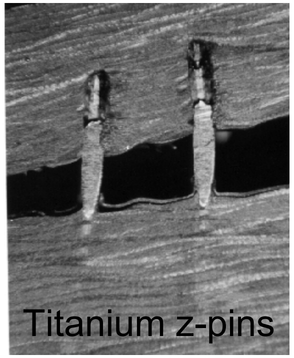

3D woven composites

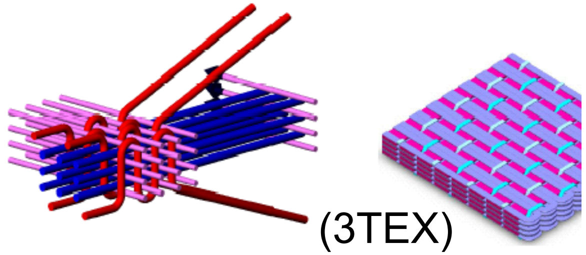

Load versus mid-span deflection curves in ENF specimens

unstitched

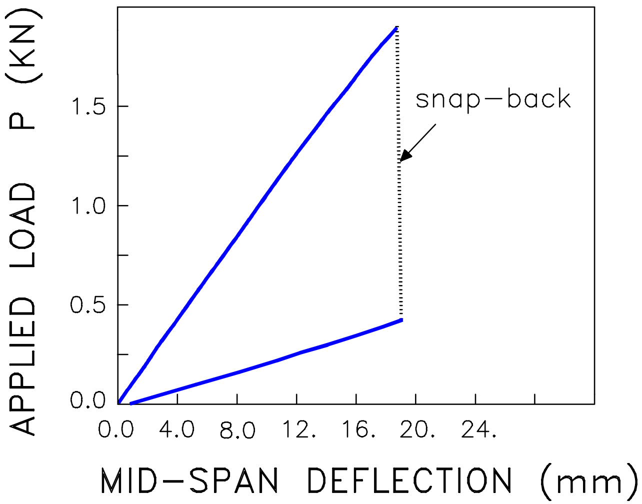

stitched

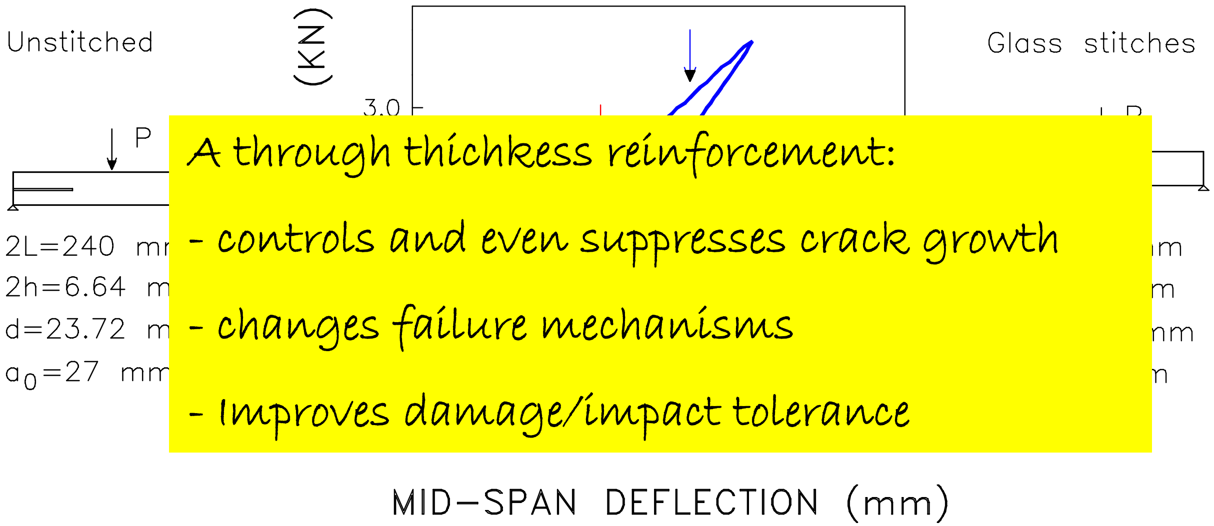

A through thickness reinforcement:

- controls and even suppresses crack growth
- changes failure mechanisms
- Improves damage/impact tolerance

TRANSITION FROM NON-CATASTROPHIC TO CATASTROPHIC FAILURE IN SLENDER BODIES

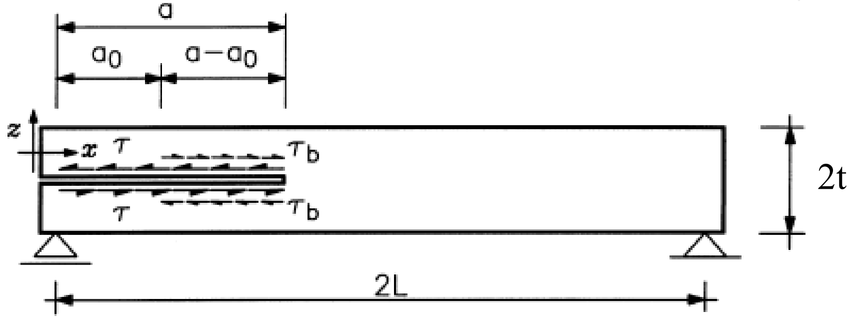

L >> h a>>h

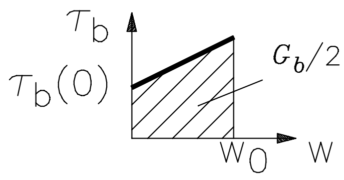

$$\tau_b(w) = \tau_b(0) + \beta w$$

$$\tau_b(0) = 2(\mathcal{G}_{IIC}\beta)^{1/2}$$

$$\mathcal{G}_b / \mathcal{G}_{IIC} = 80$$

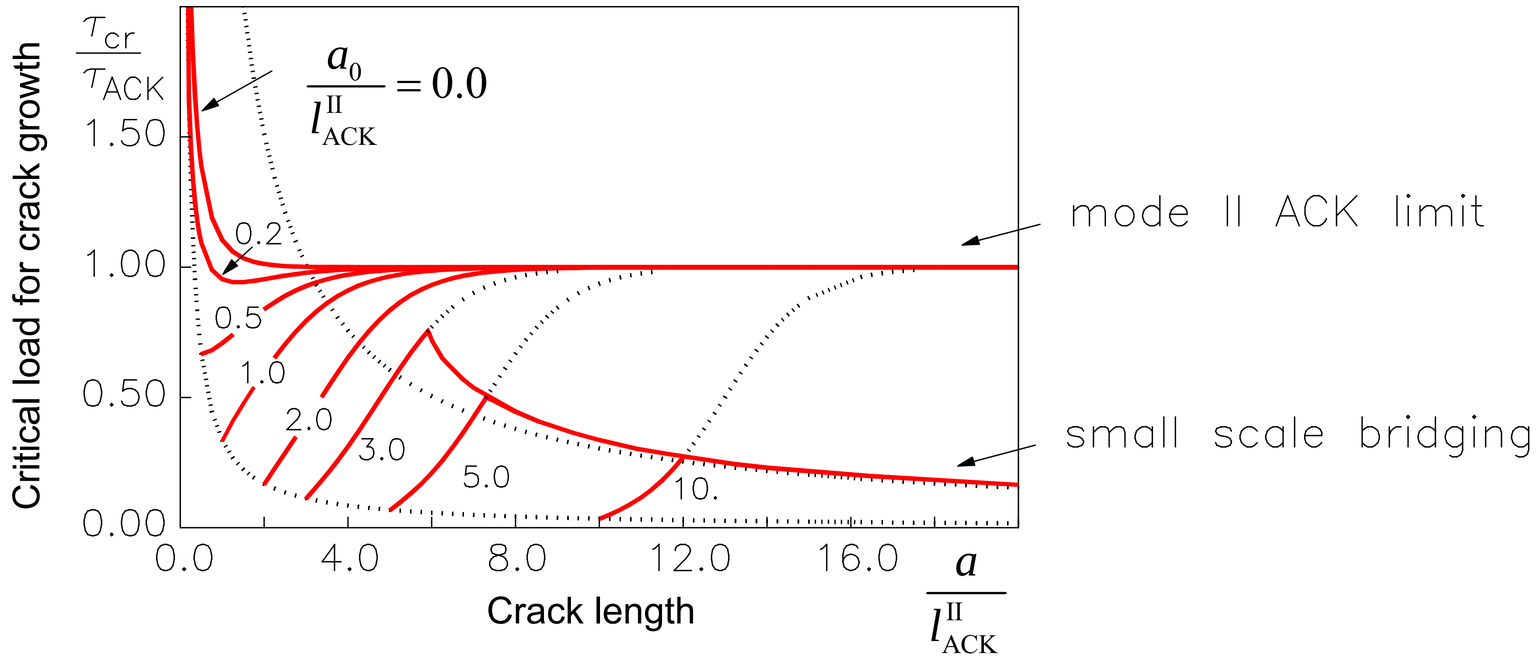

$$\tau_{ACK} = \tau_b(0) + (\mathcal{G}_{IIC}\beta)^{1/2}$$

$$l^{II}_{ACK} = \sqrt{(E/4\beta)t}$$

(Massabò & Cox, 1999)

TRANSITION FROM NON-CATASTROPHIC TO CATASTROPHIC FAILURE IN SLENDER BODIES

EXPERIMENTAL DERIVATION OF BRIDGING TRACTION LAW FOR A STITCHED COMPOSITE

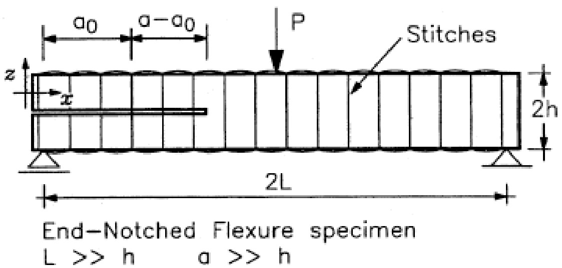

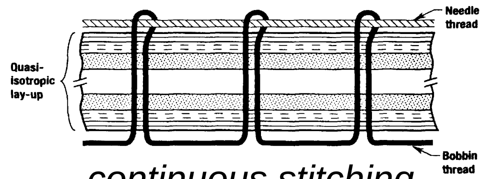

continuous stitching

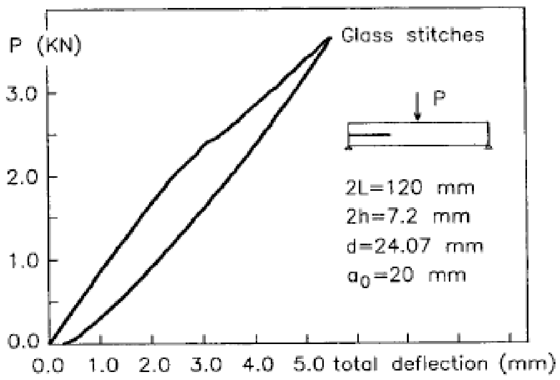

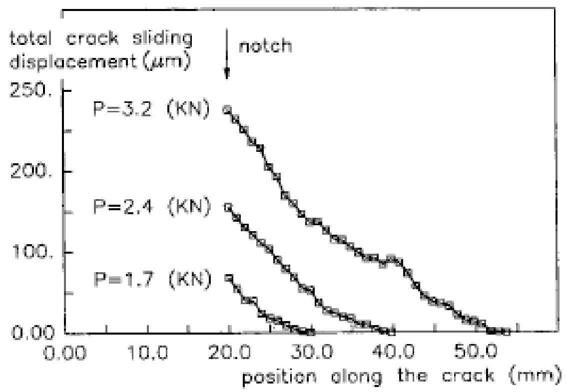

⇩

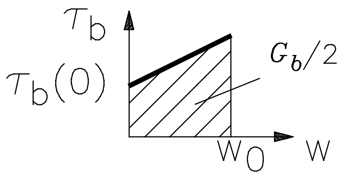

$$\tau_b(w) = 12.7 + 102w \text{ MPa}$$

$$\mathcal{G}_{IIC} = 0.37 \text{ kJ/m}^2$$

$$w_c = 0.5 \text{ mm}$$

(Massabò, Mumm & Cox, 1998)

$$\tau_b(w) = \tau_b(0) + \beta w$$

$$\tau_b(0) = 2(\mathcal{G}_{IIC}\beta)^{1/2}$$

$$\mathcal{G}_b / \mathcal{G}_{IIC} = 80$$

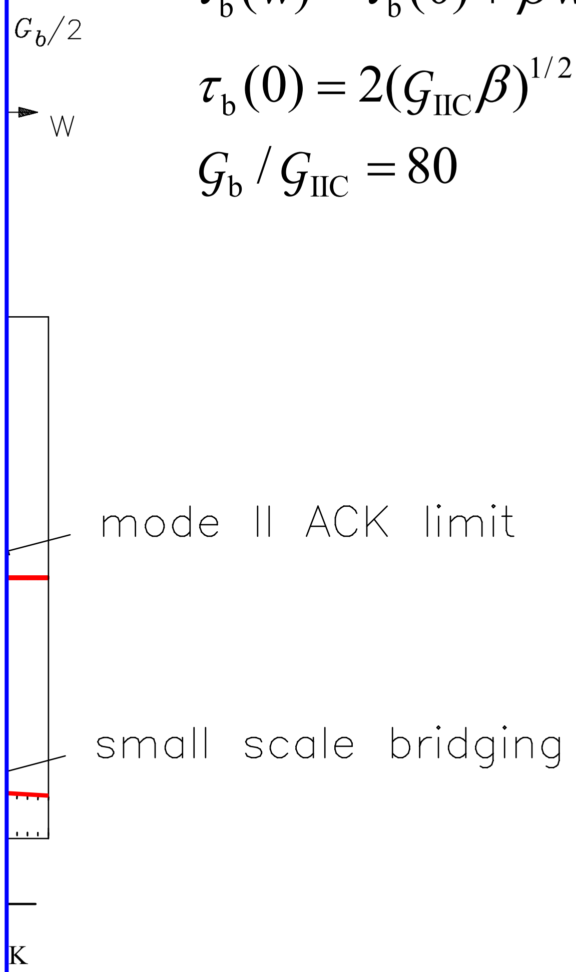

TRANSITION FROM NON-CATASTROPHIC TO CATASTROPHIC FAILURE IN SLENDER BODIES

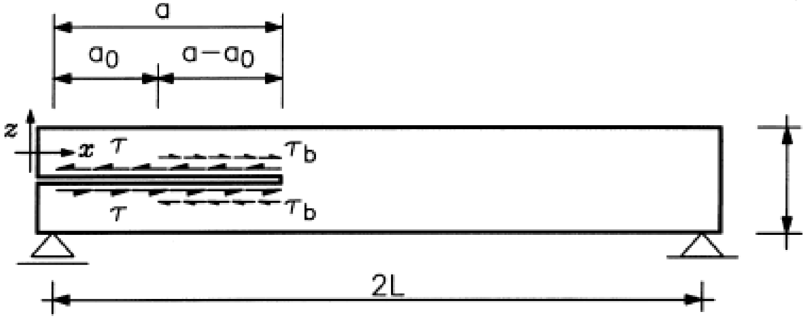

L >> h a>>h

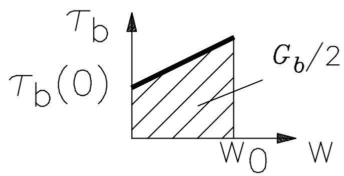

$$\tau_b(w) = \tau_b(0) + \beta w$$

$$\tau_b(0) = 2(\mathcal{G}_{IIC}\beta)^{1/2}$$

$$\mathcal{G}_b / \mathcal{G}_{IIC} = 80$$

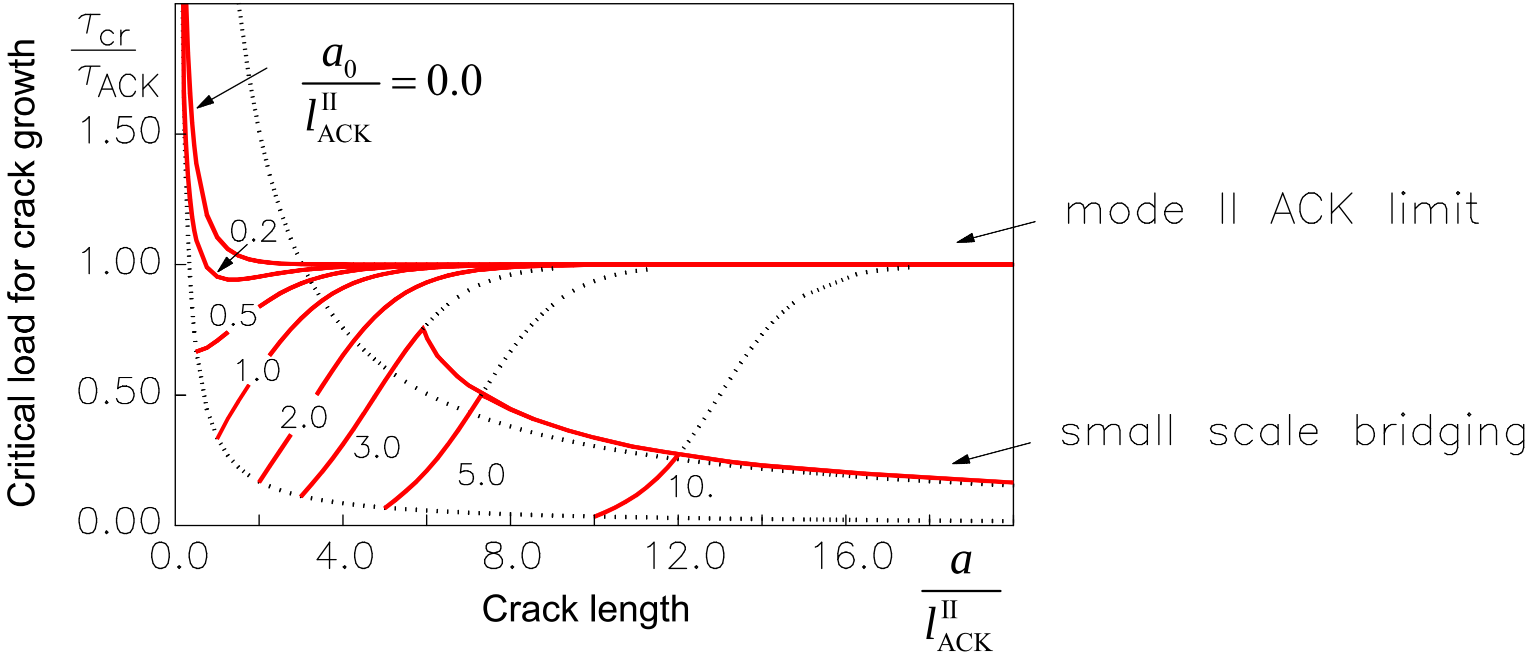

$$\tau_{ACK} = \tau_b(0) + (\mathcal{G}_{IIC}\beta)^{1/2}$$

$$l_{ACK}^{II} = \sqrt{(E/4\beta)t}$$

(Massabò & Cox, 1999)

TRANSITION FROM NON-CATASTROPHIC TO CATASTROPHIC FAILURE IN SLENDER BODIES

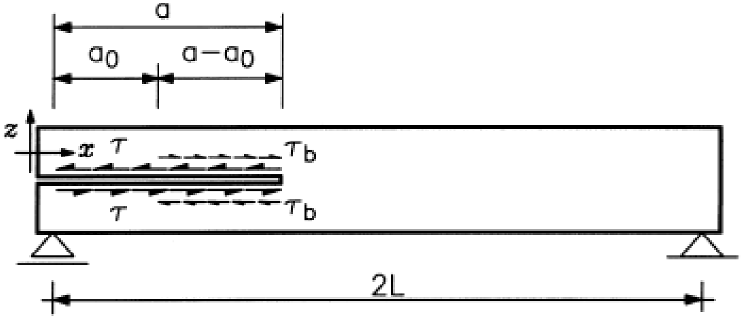

L >> h a>>h

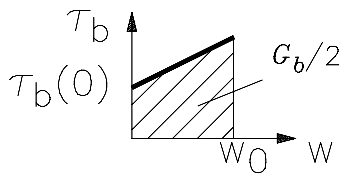

$$\tau_b(w) = \tau_b(0) + \beta w$$

$$\tau_b(0) = 2(\mathcal{G}_{IIC}\beta)^{1/2}$$

$$\mathcal{G}_b / \mathcal{G}_{IIC} = 80$$

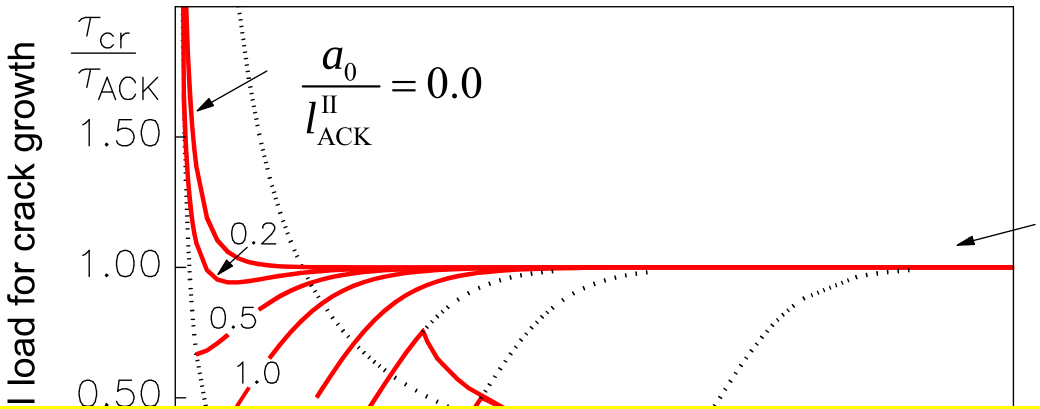

Design of and with advanced composites:

In through-thickness reinforced laminates overdesigning should be avoided since insertion process degrades inplane properties → bridging action must be understood and quantified using characteristic length scales and bridged-crack modeling

$$\tau_{ACK} = \tau_b(0) + (\mathcal{G}_{IIC}\beta)^{1/2}$$

$$l^{II}_{ACK} = \sqrt{(E/4\beta)t}$$

(Massabò & Cox, 1999)

OTHER CHARACTERISTIC LENGTH SCALES

Through thickness reinforced laminates

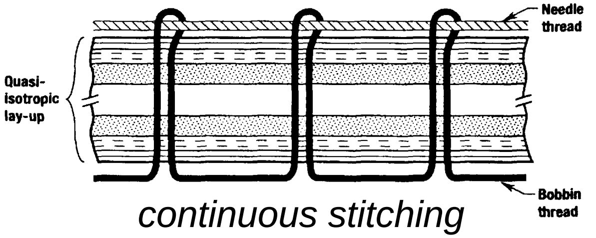

continuous stitching

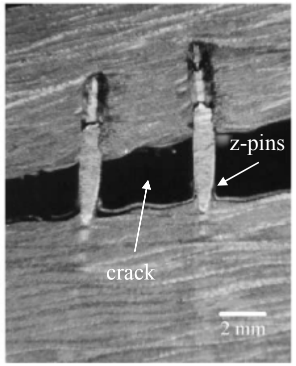

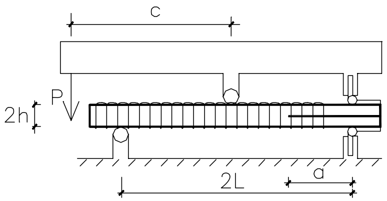

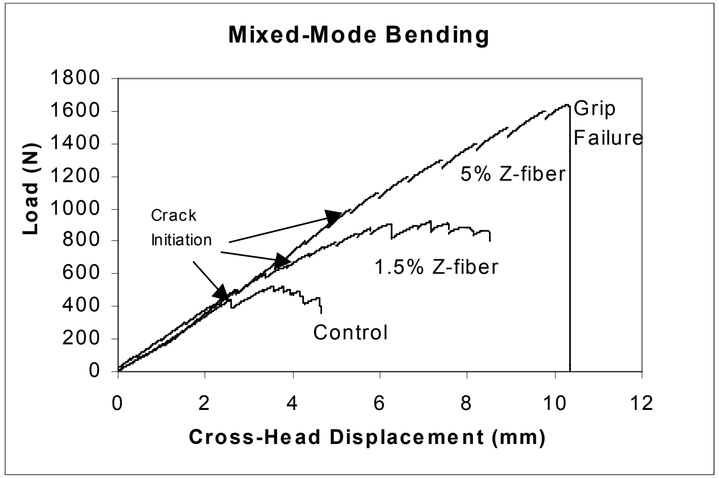

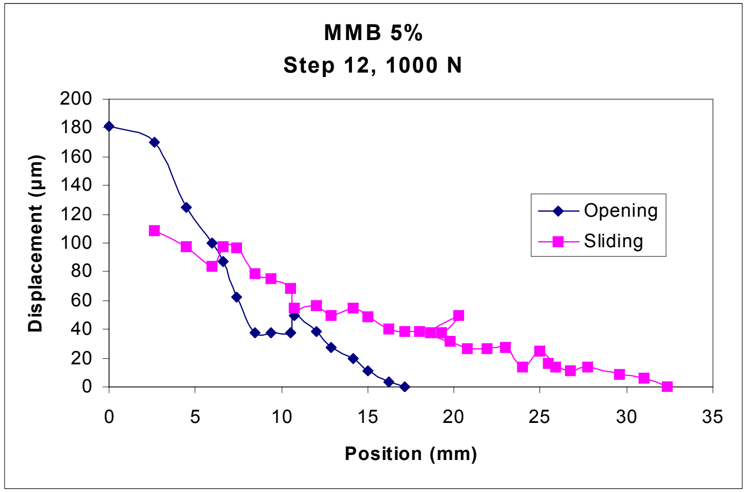

(Rugg, Cox & Massabo, 2002)

OTHER CHARACTERISTIC LENGTH SCALES

Through thickness reinforced laminates

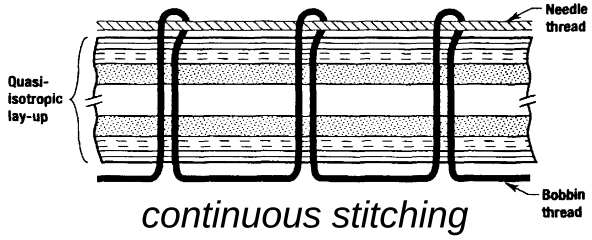

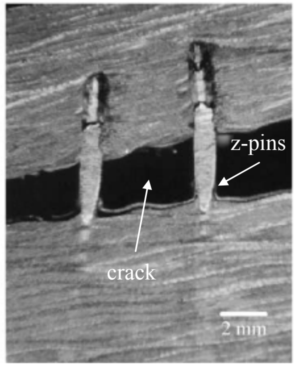

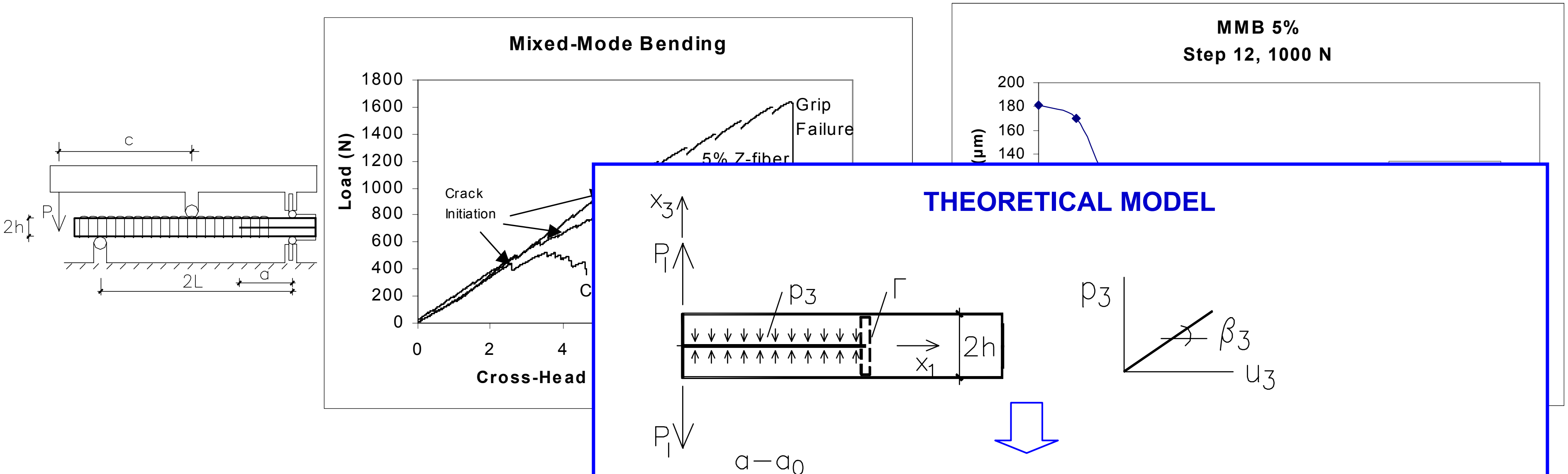

$$\lambda = 2\pi \sqrt[4]{\frac{4EI}{\beta_3}}$$

(Massabo & Cox, 2001)

FRACTURE IN FINITE SIZE BODIES
DIMENSIONLESS GROUPS GOVERNING MECHANICAL BEHAVIOR

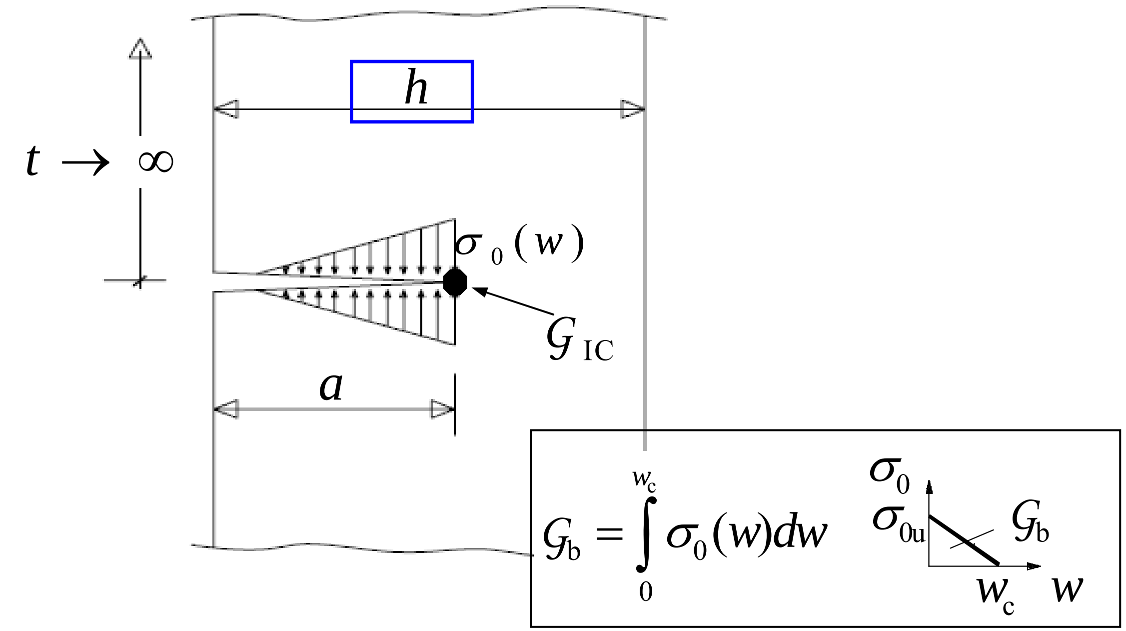

Cohesive crack: $(\mathcal{G}_{IC} = 0)$ $\quad \dfrac{l_{SSB}}{h}$ **(one group)**

Bridged crack: $(\mathcal{G}_{IC} \neq 0)$ $\quad \dfrac{l_{SSB}}{h}$ and $\dfrac{\mathcal{G}_{IC}}{\mathcal{G}_b}$ **(two groups)**

FLEXURAL RESPONSE OF BRITTLE MATRIX COMPOSITES WITH DISCRETE DUCTILE REINFORCEMENTS

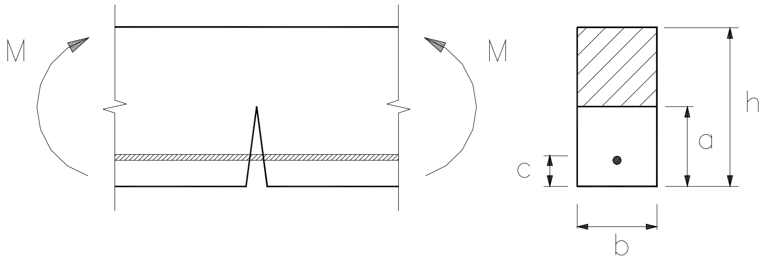

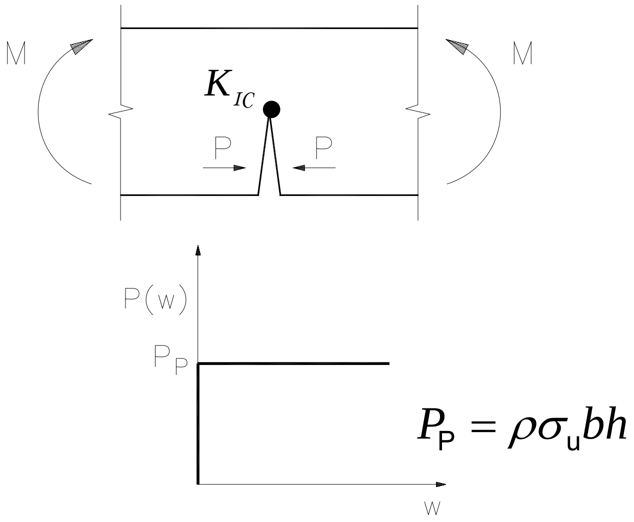

$$P_P = \rho \sigma_u b h$$

$$N_P = \frac{\rho \sigma_u h^{0.5}}{K_{IC}}$$

(Carpinteri 1981, 1984; Massabò, 1994)

FLEXURAL RESPONSE OF BRITTLE MATRIX COMPOSITES WITH DISCRETE DUCTILE REINFORCEMENTS

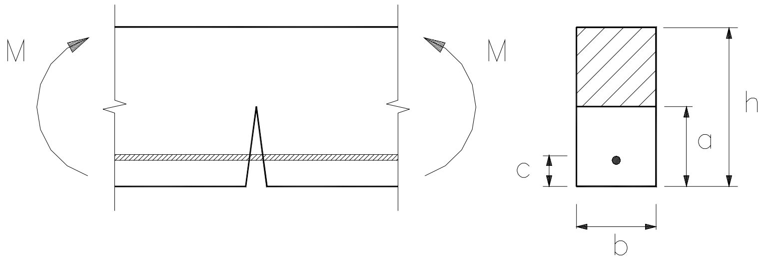

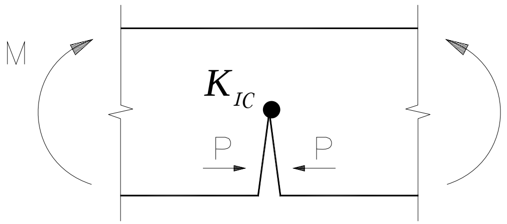

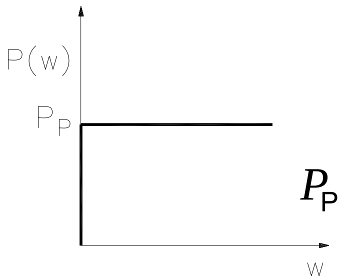

$$P_P = \rho \sigma_u b h$$

$$N_P = \frac{\rho \sigma_u h^{0.5}}{K_{IC}}$$

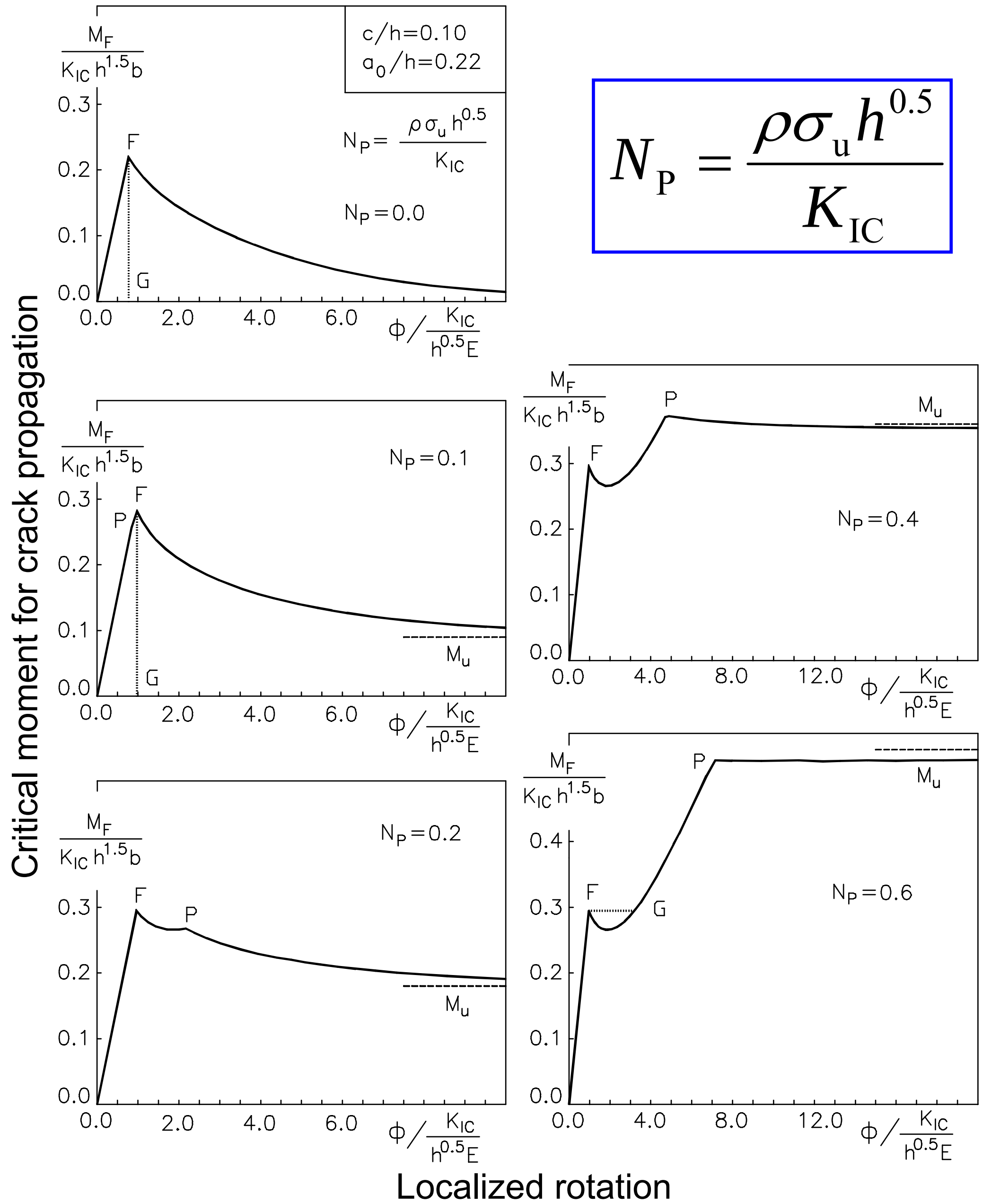

(Carpinteri 1981, 1984; Massabò, 1994)

FLEXURAL RESPONSE OF BRITTLE MATRIX COMPOSITES WITH DISCRETE DUCTILE REINFORCEMENTS

EXPERIMENTS

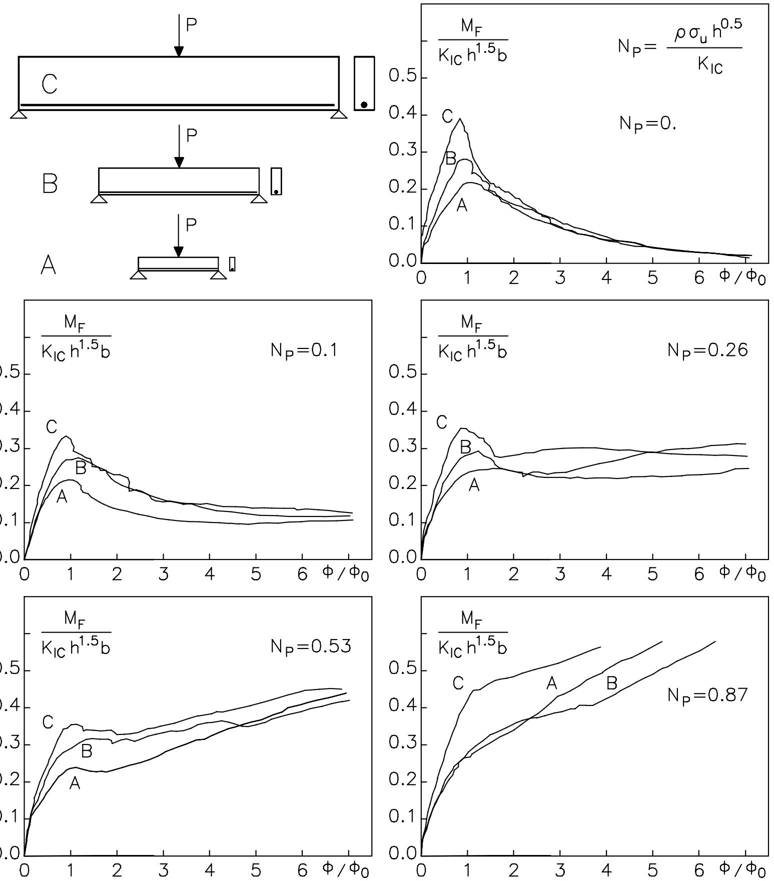

High-strength reinforced concrete

(Bosco, Carpinteri & Debernardi, 1990)

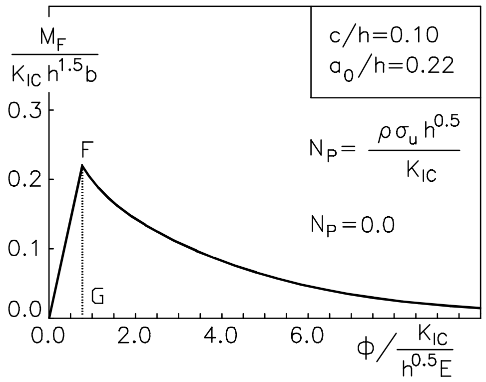

$$N_P = \frac{\rho \sigma_u h^{0.5}}{K_{IC}}$$

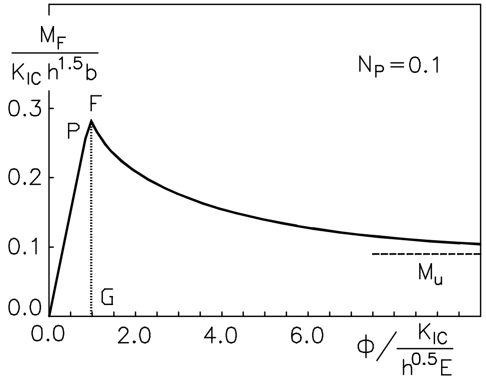

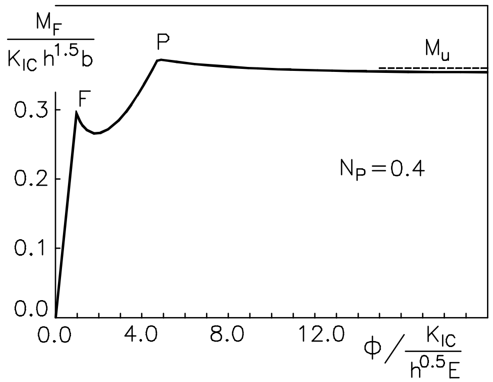

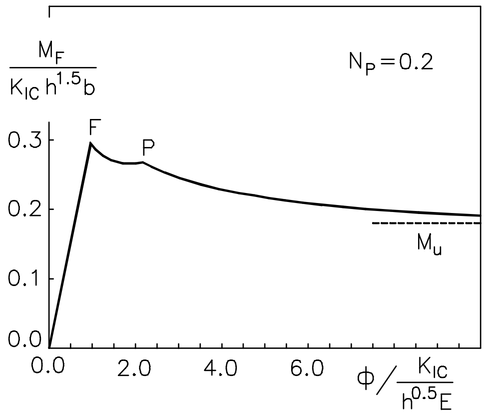

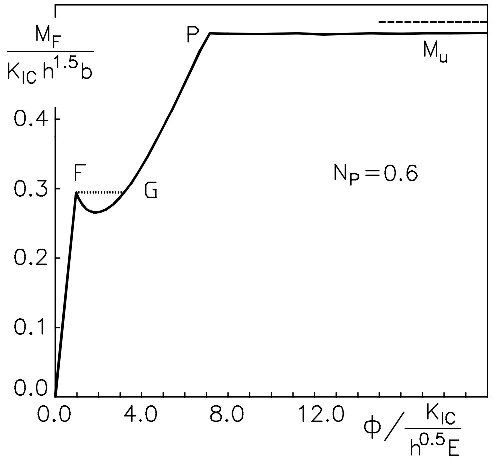

Localized rotation

FLEXURAL RESPONSE OF BRITTLE MATRIX COMPOSITES WITH DISCRETE DUCTILE REINFORCEMENTS

EXPERIMENTS

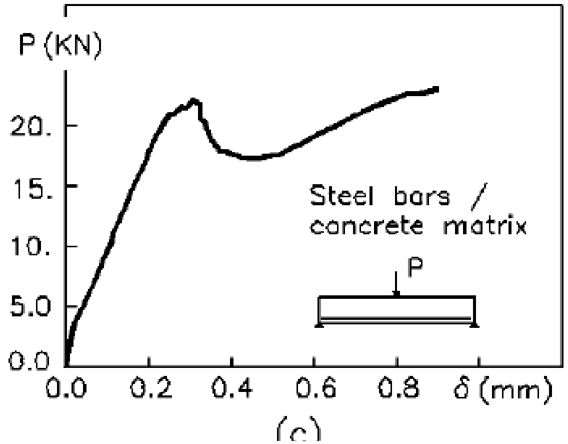

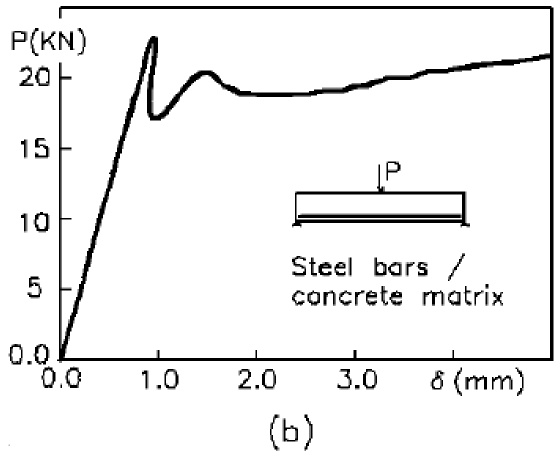

(Levi, Bosco & Debernardi, 1998
Bosco, Carpinteri & Debernardi, 1990)

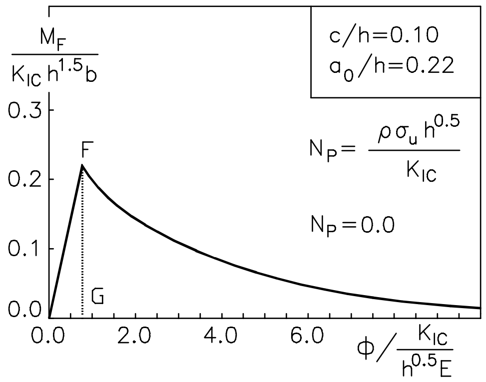

$$N_{\mathrm{P}} = \frac{\rho \sigma_{\mathrm{u}} h^{0.5}}{K_{\mathrm{IC}}}$$

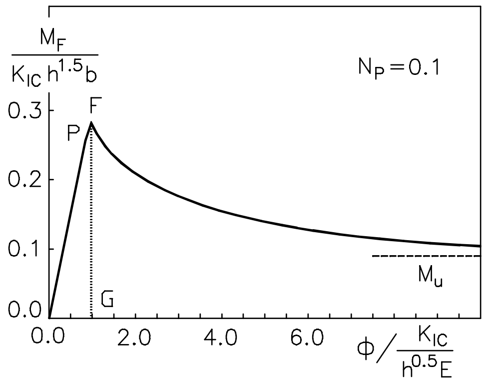

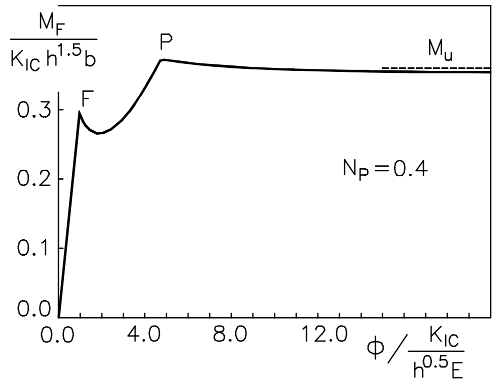

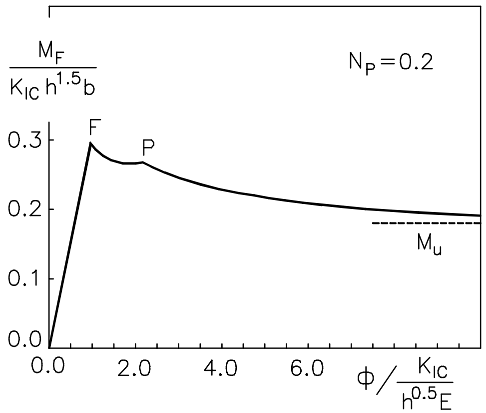

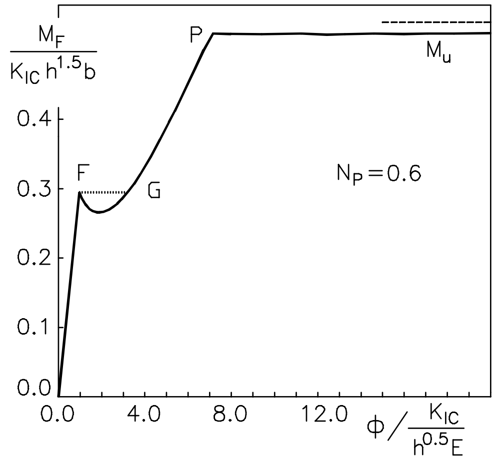

Localized rotation

FLEXURAL RESPONSE OF BRITTLE MATRIX COMPOSITES WITH DISCRETE DUCTILE REINFORCEMENTS

EXPERIMENTS

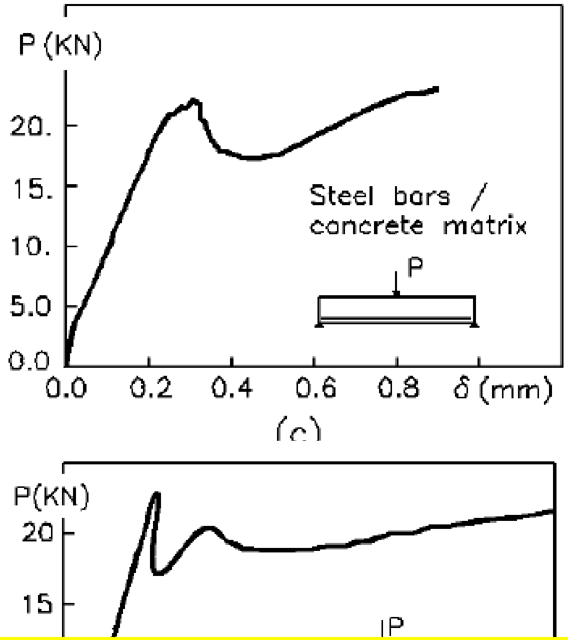

(L
Bosco, Carpinteri & Debernardi, 1990)

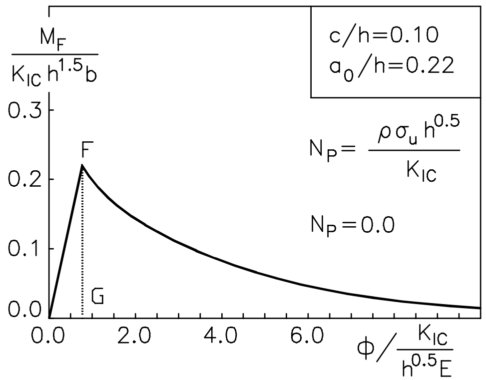

$$N_P = \frac{\rho \sigma_u h^{0.5}}{K_{IC}}$$

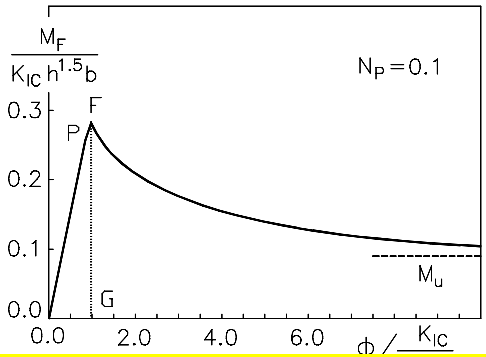

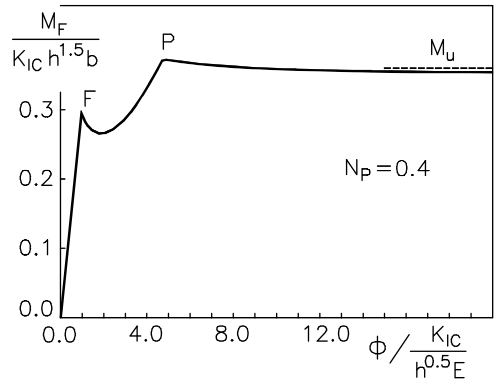

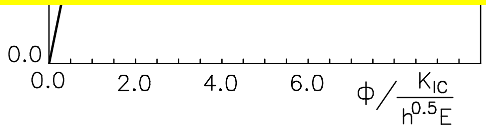

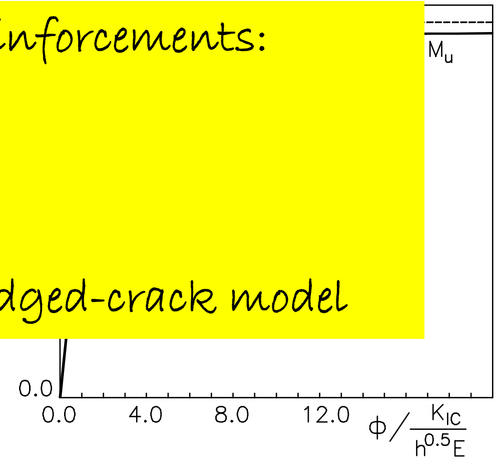

Flexural response of brittle matrix composites with ductile reinforcements:

- controlled by a single brittleness number
- brittle to ductile transition on increasing the beam depth
- local snap-through instabilities can be explained using bridged-crack model

FLEXURAL RESPONSE OF BRITTLE MATRIX COMPOSITES WITH DISCRETE DUCTILE REINFORCEMENTS

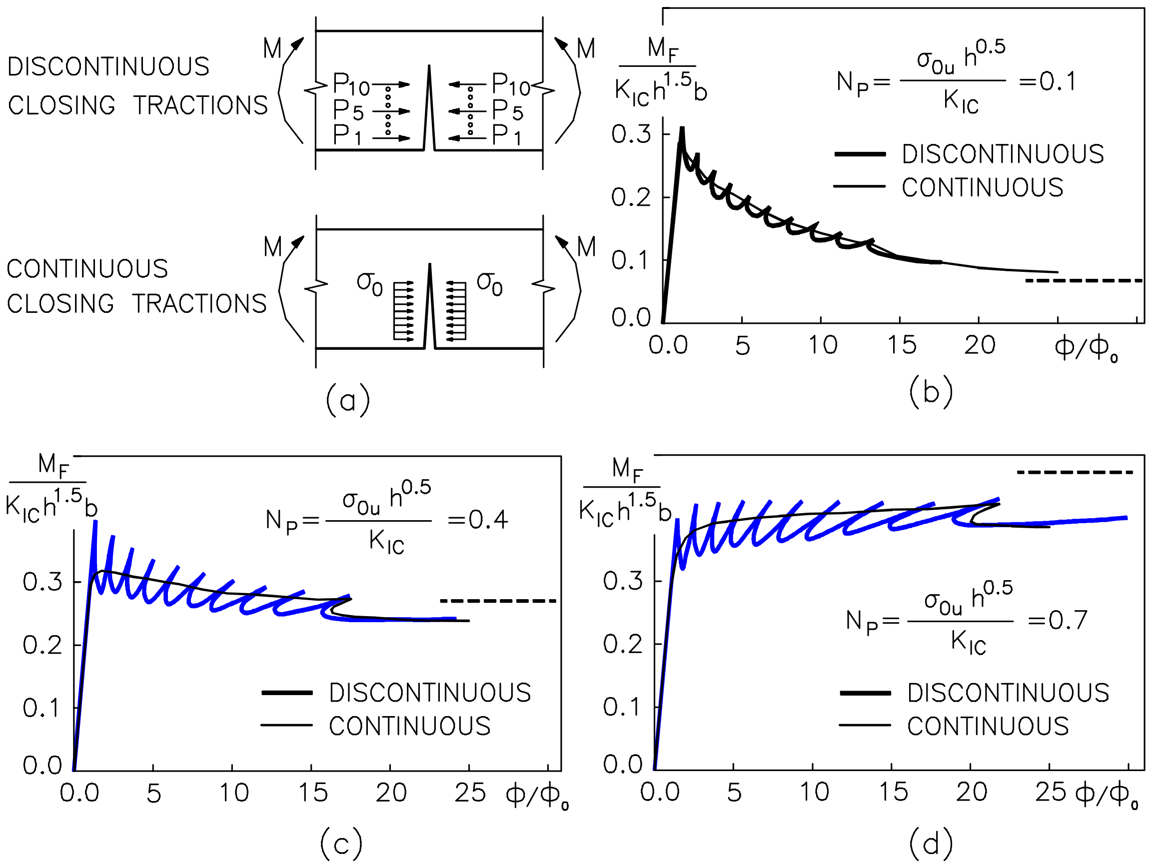

(Carpinteri & Massabò, 1997)

FLEXURAL RESPONSE OF BRITTLE MATRIX COMPOSITES WITH DISCRETE DUCTILE REINFORCEMENTS

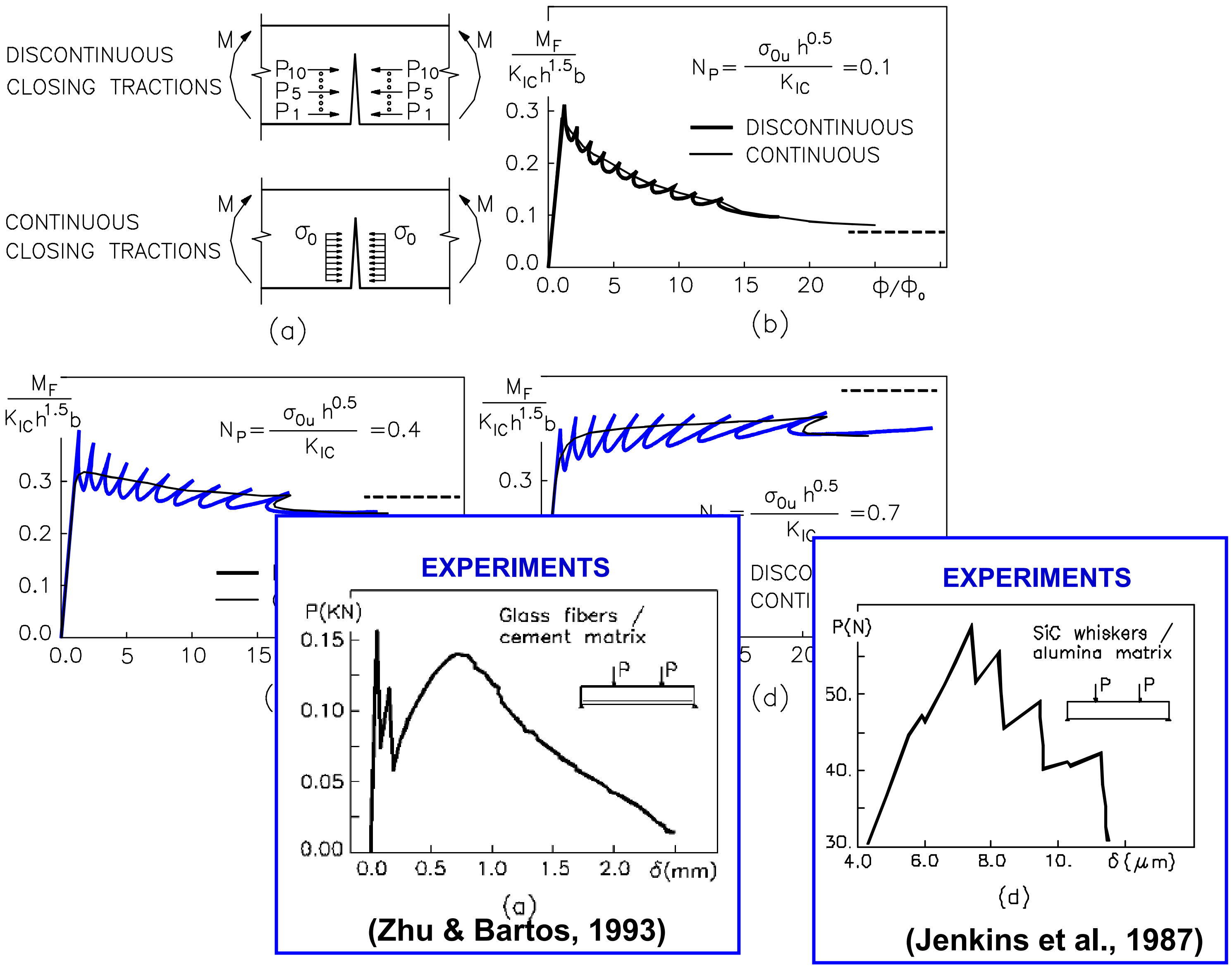

TRANSITIONS IN THE FLEXURAL BEHAVIOR OF FIBER REINFORCED COMPOSITES

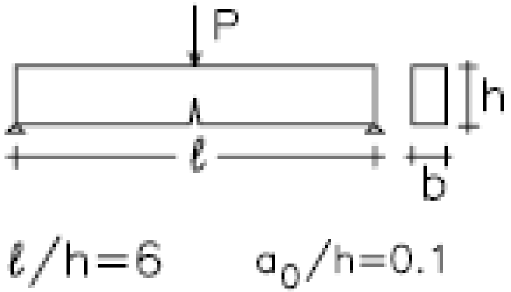

Fiber reinforced brittle matrix composite
(e.g. fiber reinforced high strength concrete; fiber reinforced ceramic)

Bridged-crack model

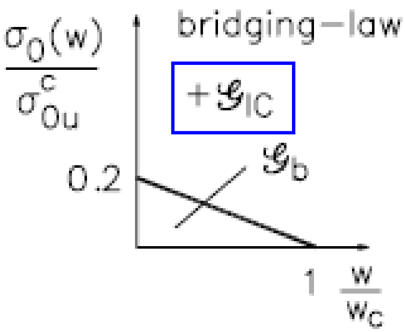

Cohesive-crack model

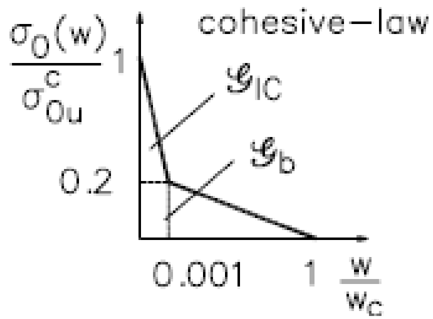

Two dimensionless groups govern mechanical behavior

$$s_E = \frac{\mathcal{G}^c}{\sigma^c_{0u} h} = \frac{\mathcal{G}_b + \mathcal{G}_{IC}}{\sigma^c_{0u} h} \qquad \frac{\mathcal{G}_b}{\mathcal{G}_{IC}} = 250$$

(brittleness number, Carpinteri 1985)

TRANSITIONS IN THE FLEXURAL BEHAVIOR OF FIBER REINFORCED COMPOSITES

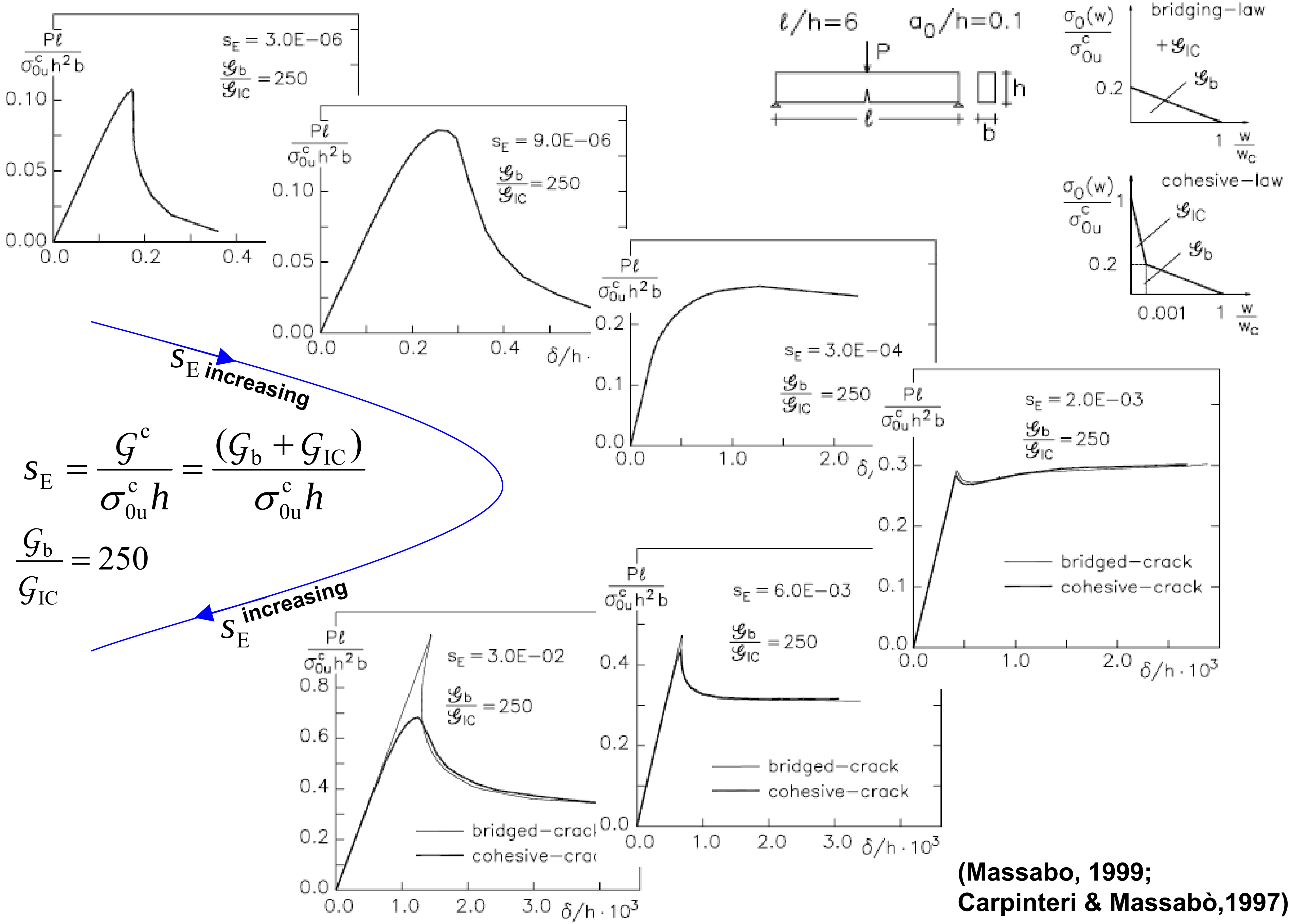

$$s_E = \frac{\mathcal{G}^c}{\sigma_{0u}^c h} = \frac{(\mathcal{G}_b + \mathcal{G}_{IC})}{\sigma_{0u}^c h}$$

$$\frac{\mathcal{G}_b}{\mathcal{G}_{IC}} = 250$$

(Massabo, 1999; Carpinteri & Massabò,1997)

TRANSITIONS IN THE FLEXURAL BEHAVIOR OF FIBER REINFORCED COMPOSITES

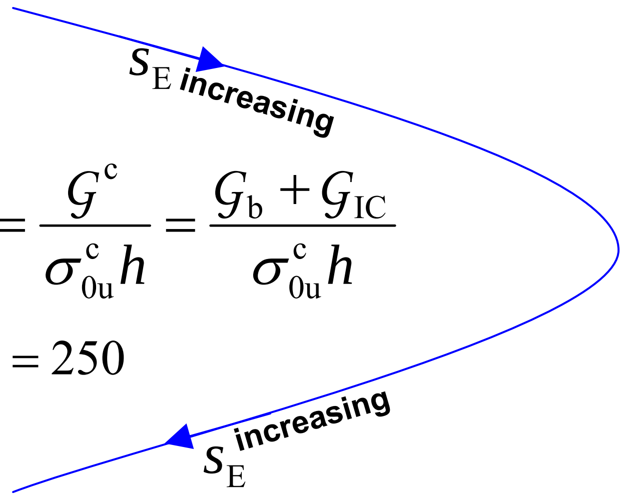

$$s_E = \frac{\mathcal{G}^c}{\sigma^c_{0u} h} = \frac{\mathcal{G}_b + \mathcal{G}_{IC}}{\sigma^c_{0u} h}$$

$$\frac{\mathcal{G}_b}{\mathcal{G}_{IC}} = 250$$

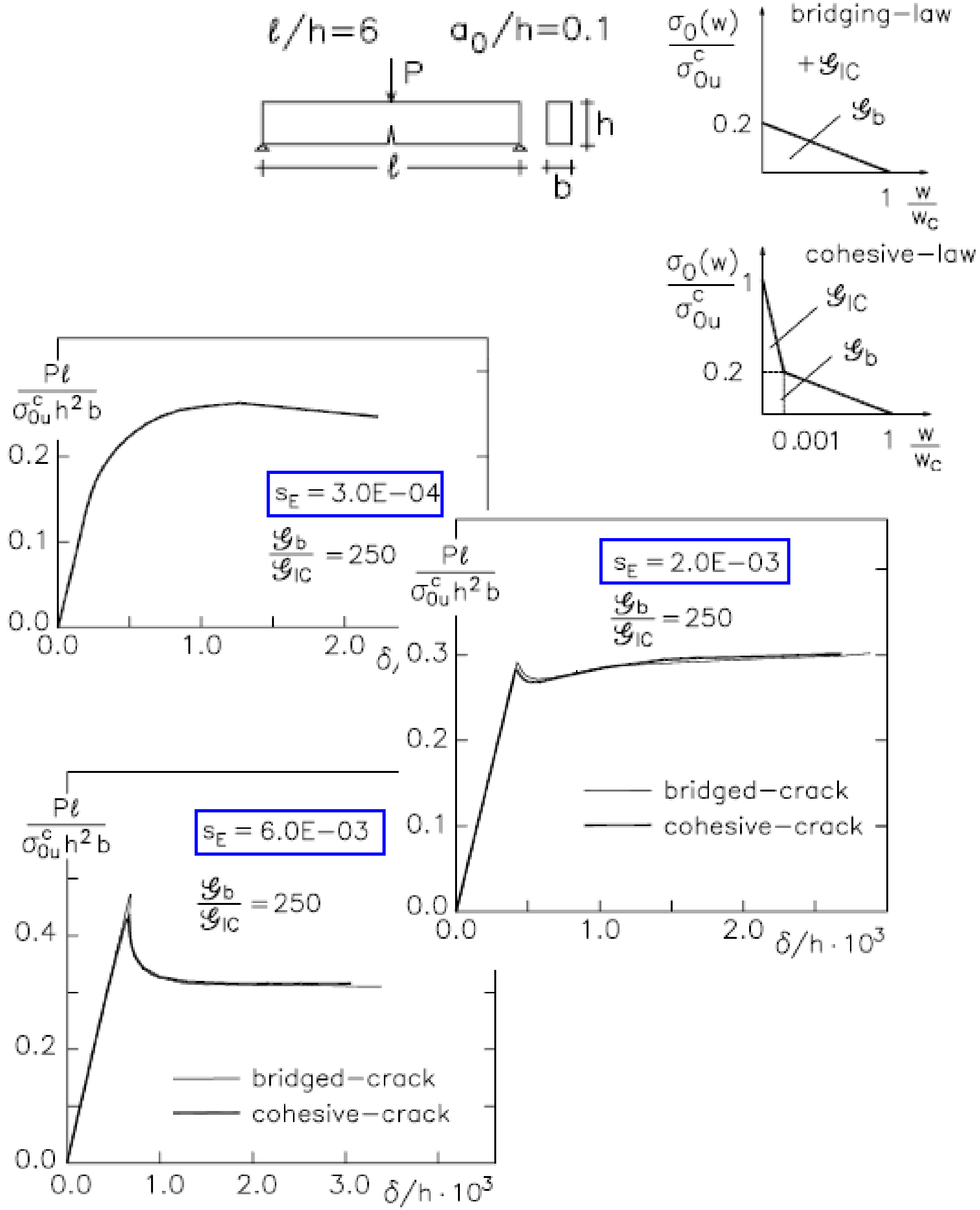

(Massabo, 1999;
Carpinteri & Massabò,1997)

TRANSITIONS IN THE FLEXURAL BEHAVIOR OF FIBER REINFORCED COMPOSITES

EXPERIMENTS

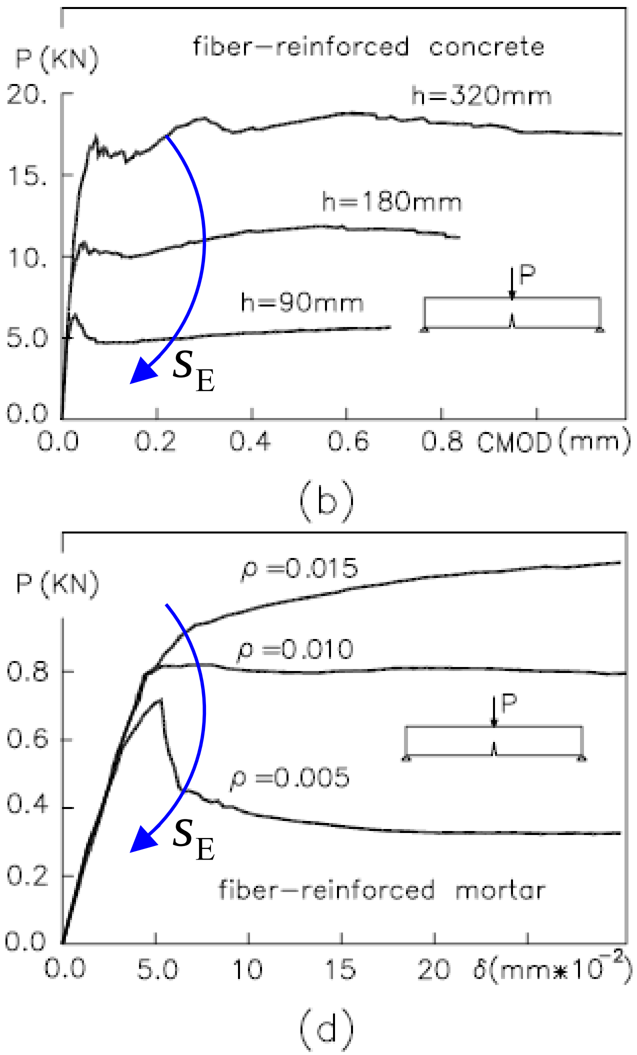

(Jamet, Gettu et al., 1995; Jenq and Shah, 1986)

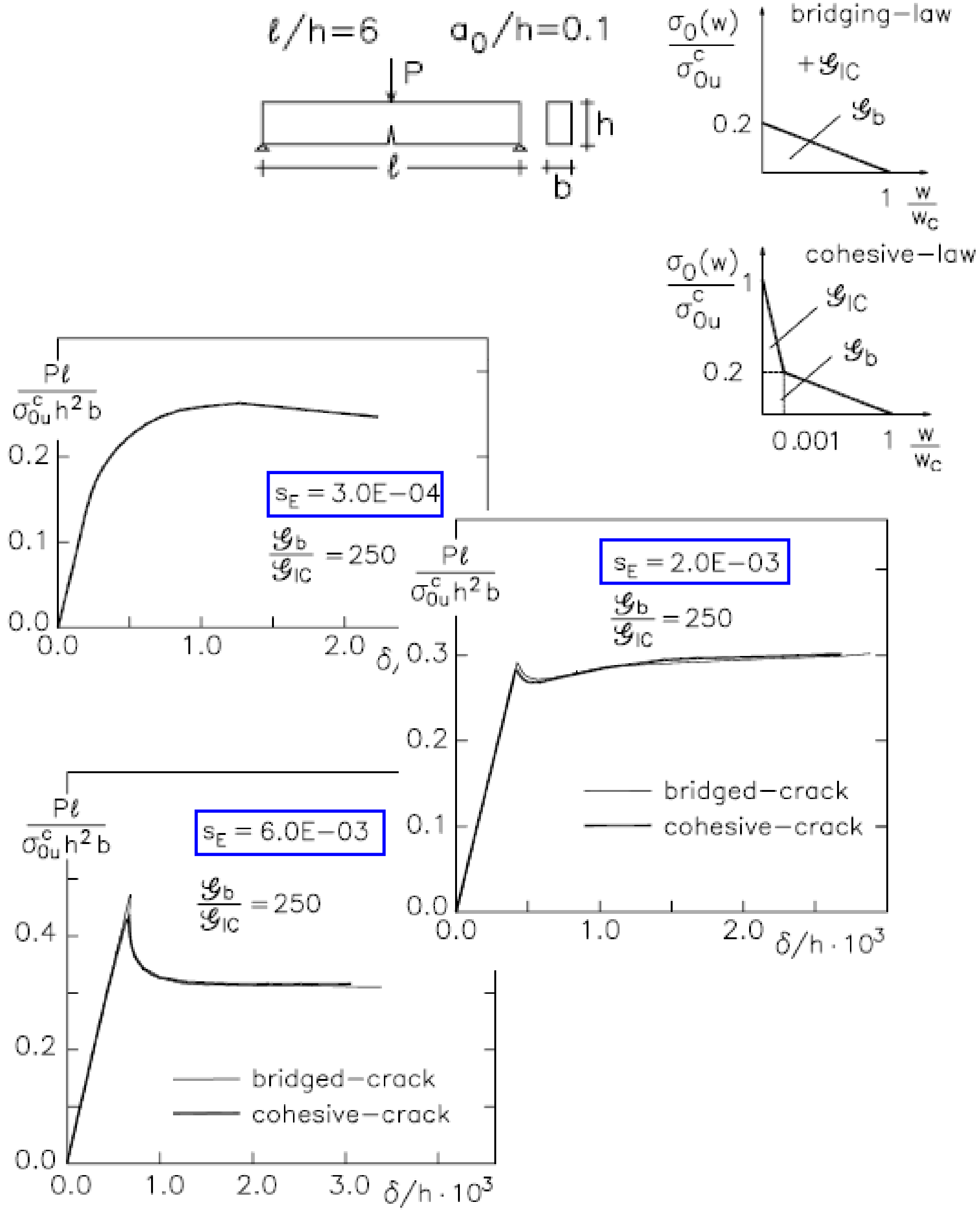

(Massabo, 1999; Carpinteri & Massabò,1997)

TRANSITIONS IN THE FLEXURAL BEHAVIOR OF FIBER REINFORCED COMPOSITES

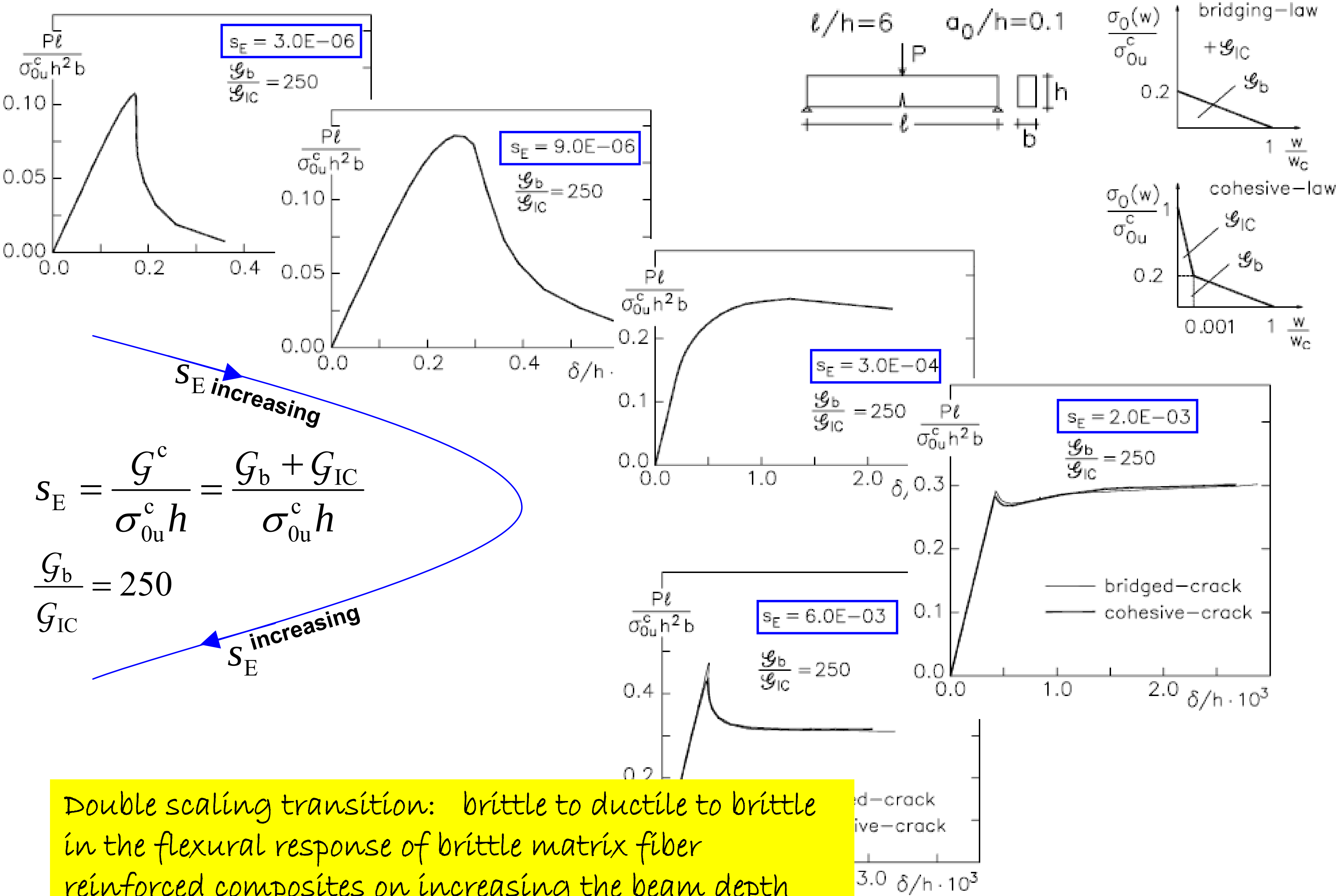

$$s_E = \frac{\mathcal{G}^c}{\sigma^c_{0u} h} = \frac{\mathcal{G}_b + \mathcal{G}_{IC}}{\sigma^c_{0u} h}$$

$$\frac{\mathcal{G}_b}{\mathcal{G}_{IC}} = 250$$

Double scaling transition: brittle to ductile to brittle in the flexural response of brittle matrix fiber reinforced composites on increasing the beam depth

(Massabo, 1999; Carpinteri & Massabò,1997)

TRANSITIONS IN THE FLEXURAL BEHAVIOR OF FIBER REINFORCED COMPOSITES

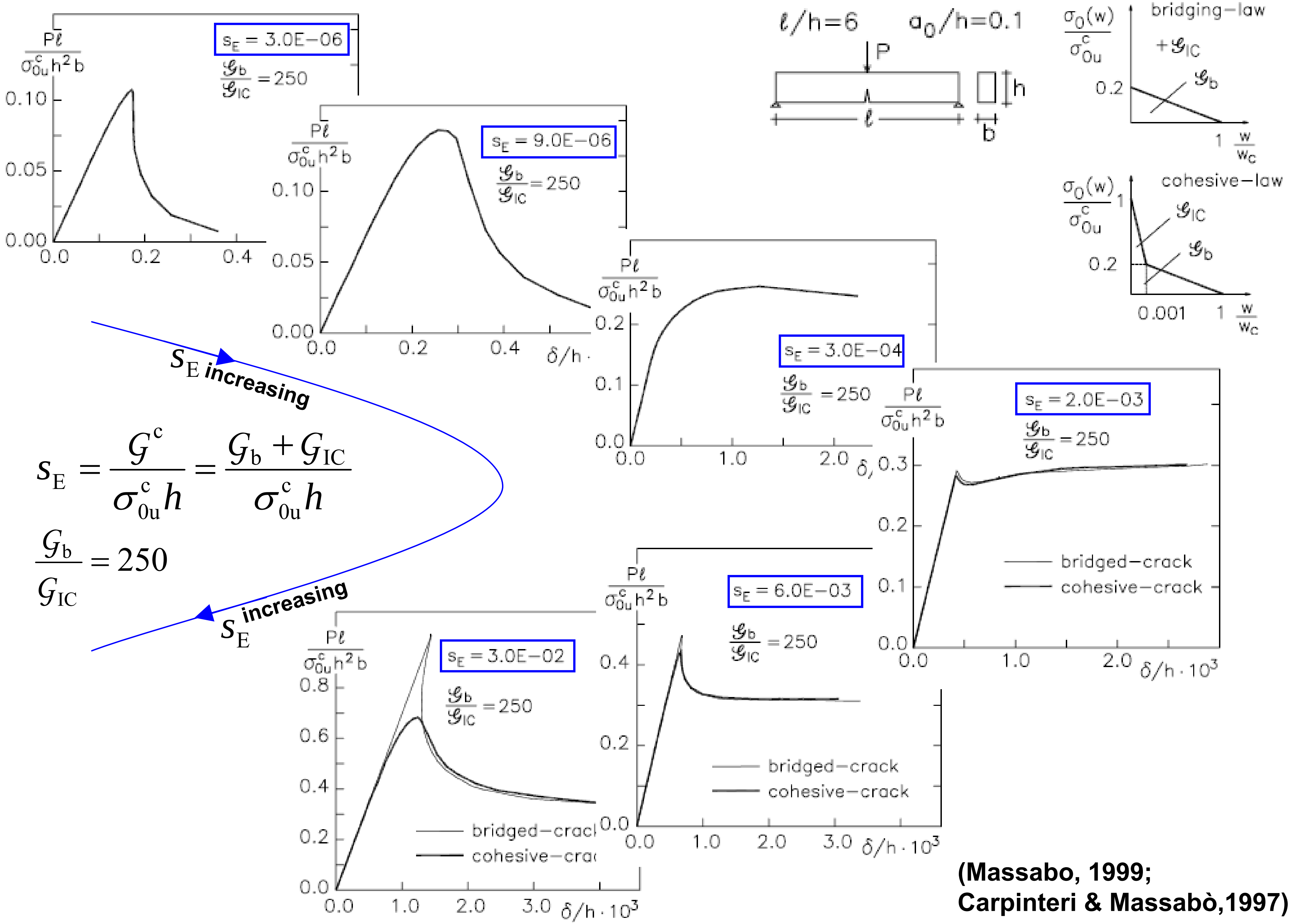

$$s_E = \frac{\mathcal{G}^c}{\sigma_{0u}^c h} = \frac{\mathcal{G}_b + \mathcal{G}_{IC}}{\sigma_{0u}^c h}$$

$$\frac{\mathcal{G}_b}{\mathcal{G}_{IC}} = 250$$

(Massabo, 1999; Carpinteri & Massabò,1997)

TRANSITIONS IN THE FLEXURAL BEHAVIOR OF FIBER REINFORCED COMPOSITES

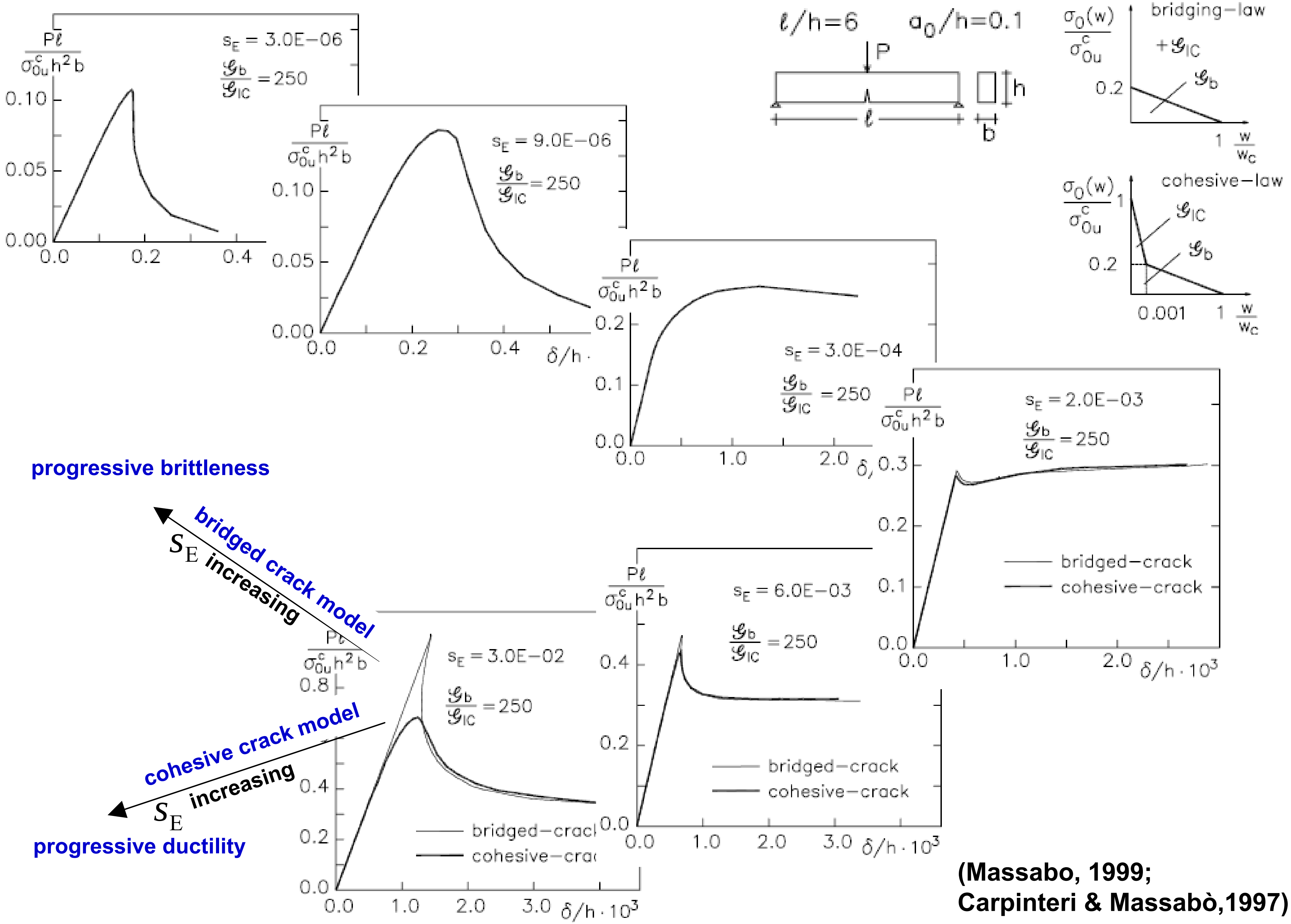

(Massabo, 1999; Carpinteri & Massabò,1997)

TRANSITIONS IN THE FLEXURAL BEHAVIOR OF FIBER REINFORCED COMPOSITES

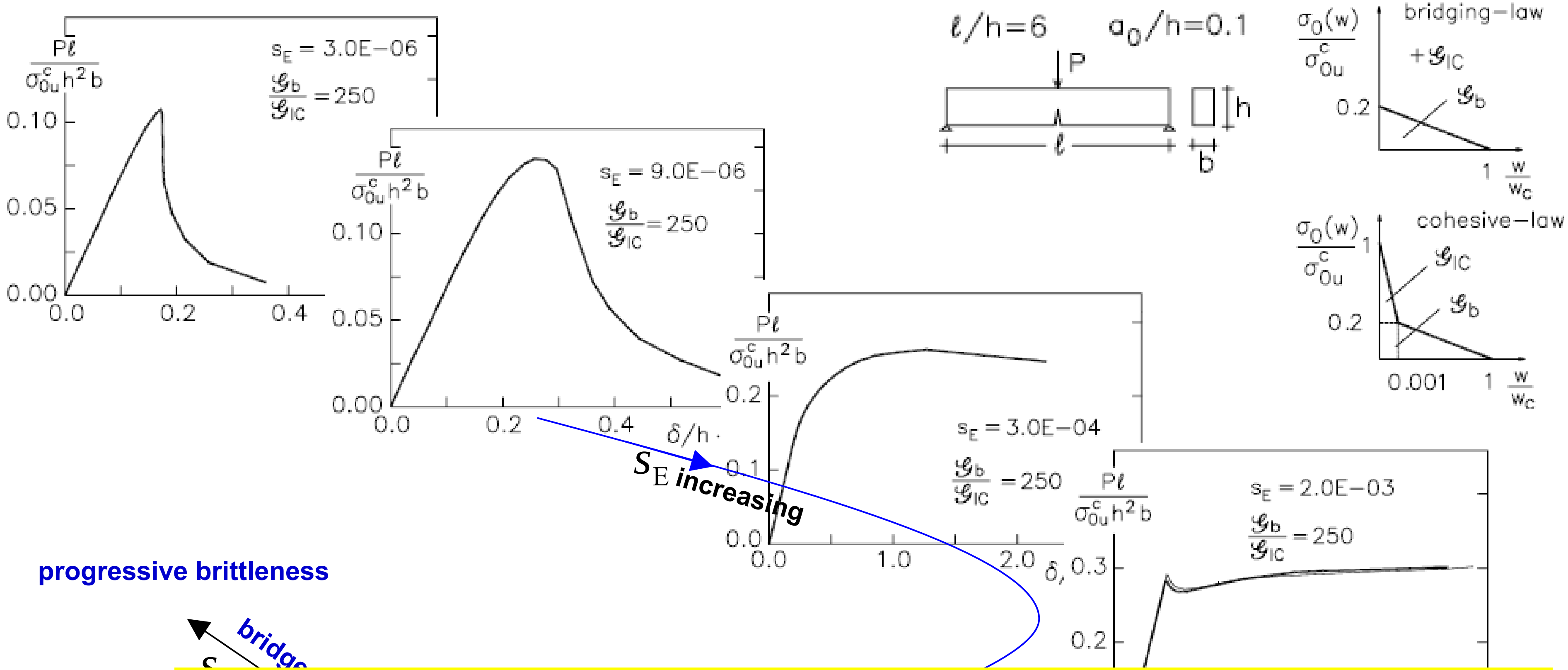

Drawbacks:

- The cohesive crack model is computationally very expensive

- The bridged crack model has limited range of applicability when matrices are not perfectly brittle

- Cohesive crack model must be applied to study crack initiation

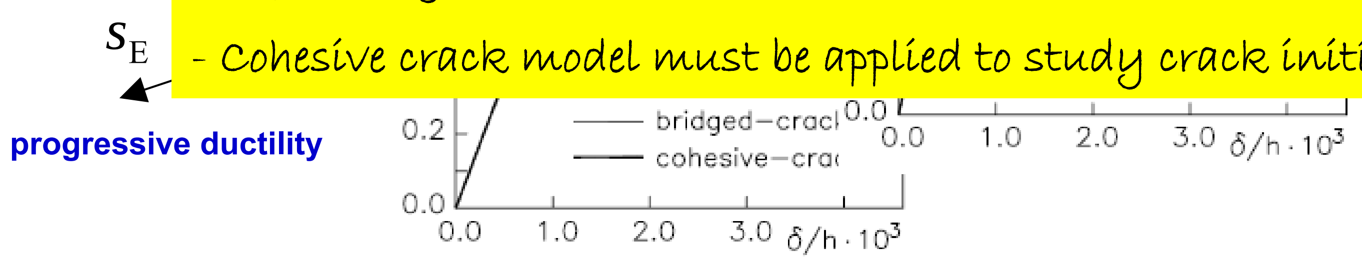

(Massabo, 1999;
Carpinteri & Massabò,1997)

Università degli Studi di Pisa
15 Febbraio 2010

PROBLEMI DI FRATTURA E DANNEGGIAMENTO IN MATERIALI E SISTEMI COMPOSITI

Parte 2:
INTERAZIONE DI MECCANISMI MULTIPLI DI DANNEGGIAMENTO

Roberta Massabò
Università degli Studi di Genova

PEOPLE:

B.N. Cox (Teledyne Scientific, CA, U.S.A.)
A. Cavicchi (post doc, University of Genova, Italy)
M.G. Andrews (former grad. student, Northwestern University, Boeing Co. U.S.A)
F. Campi (grad. student, University of Genova, Italy)

FUNDING:

U.S. Office of Naval Research, N00014-05-1-0098
U.S. Army Research Office, DAAD19-99-C-0042
Italian MIUR

OUTLINE

-Introduction and motivation

- Theoretical models to study the interaction of multiple damage mechanisms in laminates and composite sandwiches;

- Relevant results

MULTIPLE DAMAGE MECHANISMS IN LAMINATES AND SANWICHES

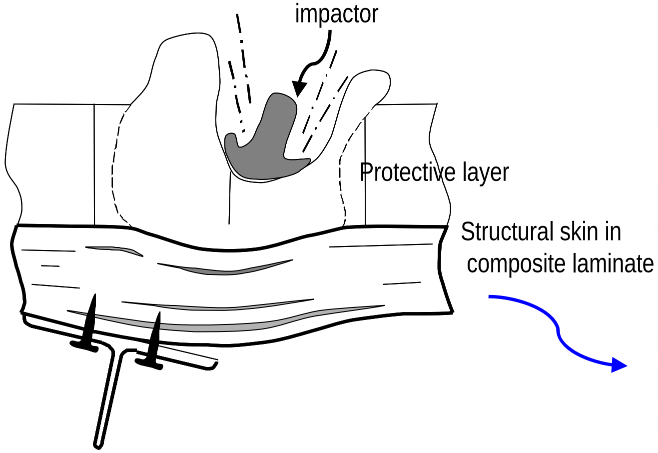

STRUCTURAL COMPOSITE

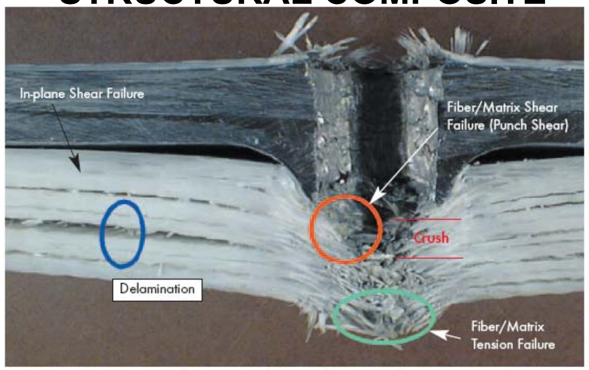

Cheeseman et al., *Amptiac*, (8), 2004.

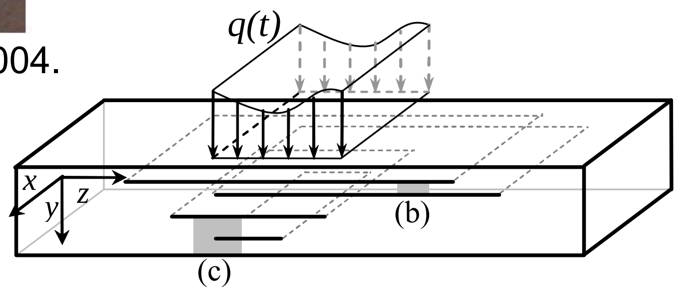

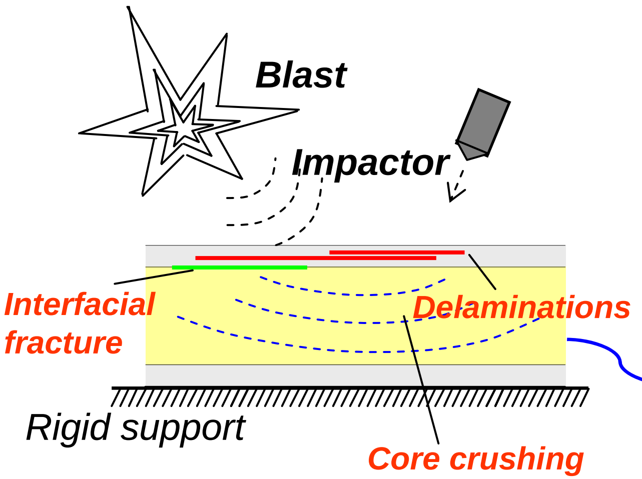

COMPOSITE SANDWICH

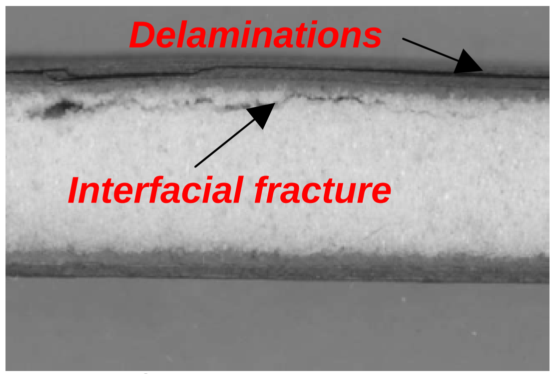

(Kim and Swanson, *Comp. Struct.*, 2001)

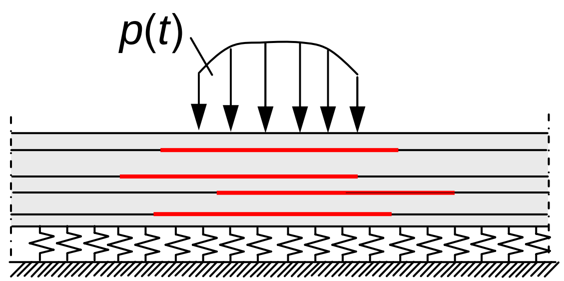

MECHANICAL MODELS
COMPOSITE LAMINATES AND MULTILAYERED SYSTEMS

(a)

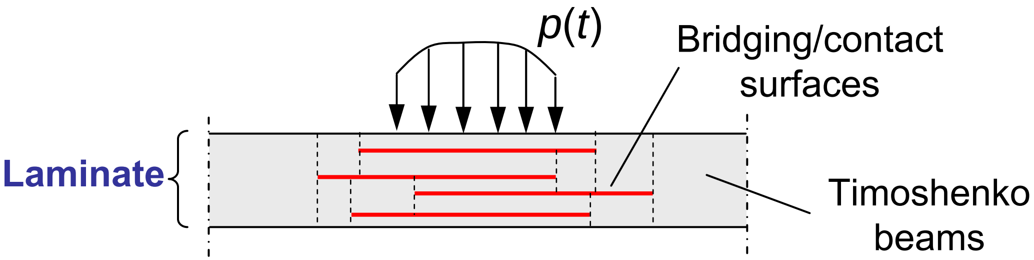

(b)

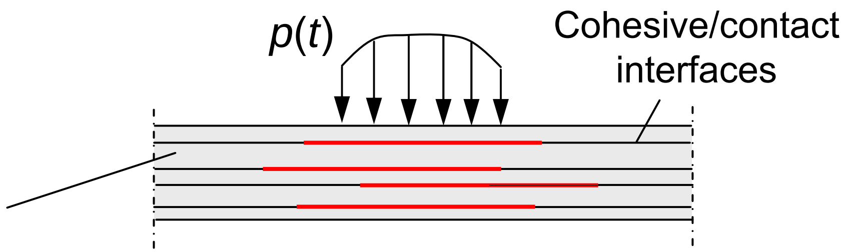

Convenient for homogeneous beams and static loading

Convenient for multilayered beams and dynamic loading

(Andrews, Massabò & Cox, *IJSS*, 2006)

(Andrews & Massabò, *EFM*, 2007)

(Andrews, Massabò, Cavicchi & Cox, *IJSS*, 2009)

(Andrews & Massabò, *Comp. A*, 2008)

MECHANICAL MODELS
FULLY BACKED COMPOSITE SANDWICHES

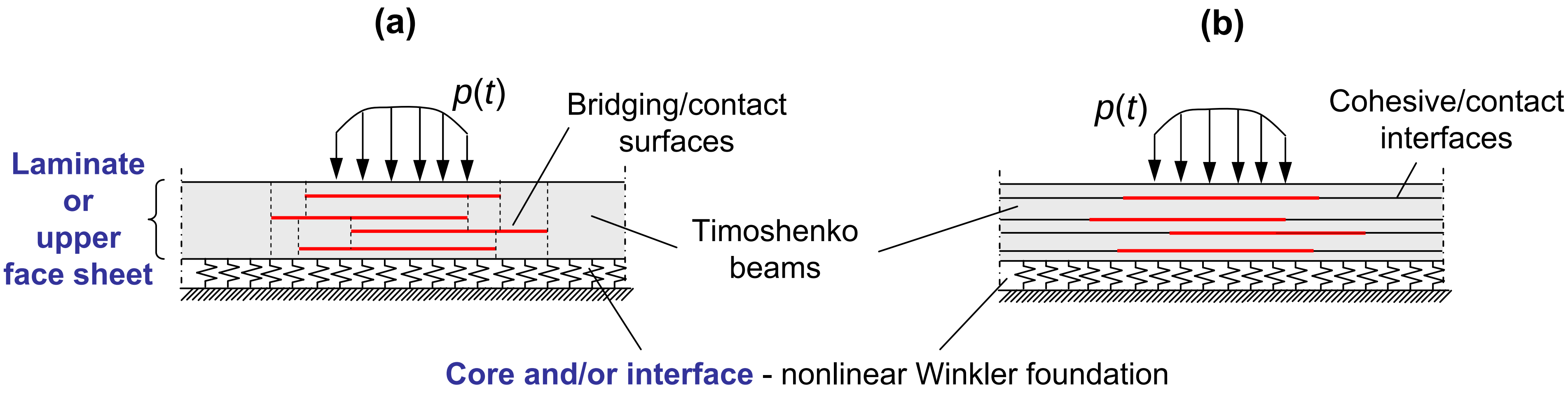

Convent for

Convenient for homogeneous beams and static loading

Convenient for multilayered beams and dynamic loading

(Andrews, Massabò & Cox, *IJSS*, 2006)

(Andrews & Massabò, *EFM*, 2007)

(Cavicchi and Massabò, 2009, proc. ICCM17)

(Andrews, Massabò, Cavicchi & Cox, *IJSS*, 2009)

(Andrews & Massabò, *Comp. A*, 2008)

(Cavicchi and Massabò, 2009, proc. AIMETA)

MECHANICAL MODELS

(a)

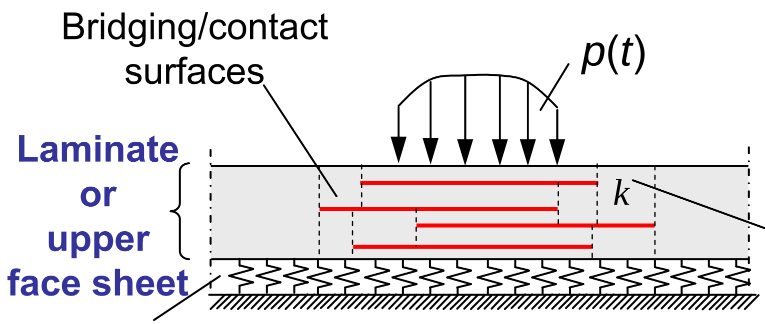

Core/interface – n.l. Winkler foundation

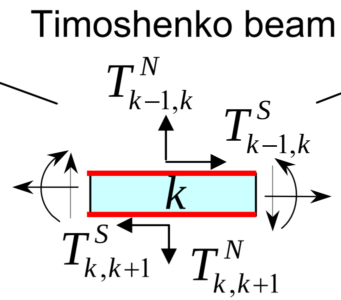

(b)

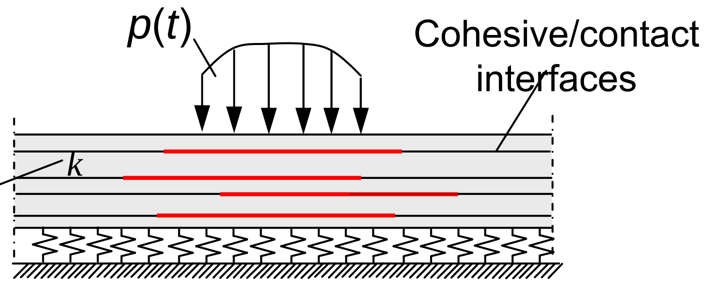

Core/interface – n.l. Winkler foundation

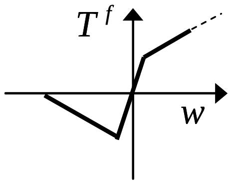

core/interface

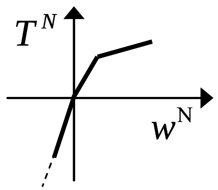

contact/bridging

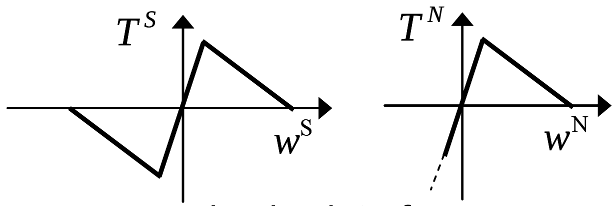

cohesive interfaces

- Homogeneous, orthotropic, linear elastic skin

- Perfectly brittle matrix + crack bridging/contact

- Accurate mode decomposition (Andrews & Massabò, *EFM*, 2007)

- Multi-layered, orthotropic, linear elastic skin

- Cohesive interfaces: perfect adhesion, brittle or cohesive fracture, contact, bridging

MECHANICAL MODELS

(a) | **(b)**

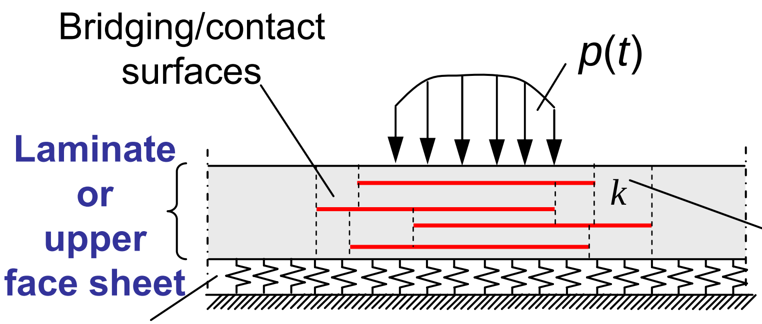

Core/interface – n.l. Winkler foundation

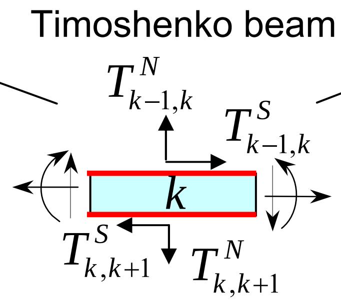

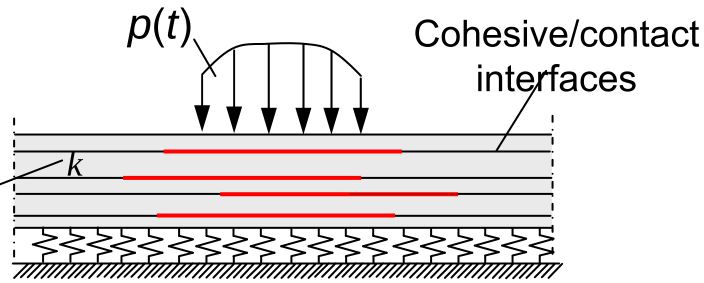

Core/interface – n.l. Winkler foundation

Generalized displacements

$u_k, \mathrm{w}_k, \varphi_k$

Dynamic equilibrium

$$N_k' - T^S_{k,k+1} + T^S_{k-1,k} = \rho_m S_k \ddot{u}_k$$

$$M_k' - V_k - 1/2\, h_k \left(T^S_{k,k+1} + T^S_{k-1,k} \right) = \rho_m I_k \ddot{\varphi}_k$$

$$V_k' + T^N_{k,k+1} - T^N_{k-1,k} = \rho_m S_k \ddot{\mathrm{w}}_k$$

Compatibility

$$\varepsilon_k = u_k'$$

$$\varphi_k = -\mathrm{w}_k' + \gamma_k$$

$$\chi_k = \varphi_k'$$

Constitutive laws

$$N_k = A_k \varepsilon_k$$

$$M_k = D_k \chi_k$$

$$V_k = G_k \gamma_k$$

SOLUTION METHOD

semi-analytic (iterative procedure needed to define contact/bridging regions and plastically admissible fields)

SOLUTION METHOD

numerical: time/space discretization, finite difference solution scheme

INTERACTION EFFECTS – QUASI STATIC LOADING
AMPLIFICATION AND SHIELDING OF FRACTURE PARAMETERS

(Andrews, Massabò and Cox, IJSS, 2006; Andrews and Massabò, Comp. A, 2008)

Energy release rate of upper crack vs. crack length

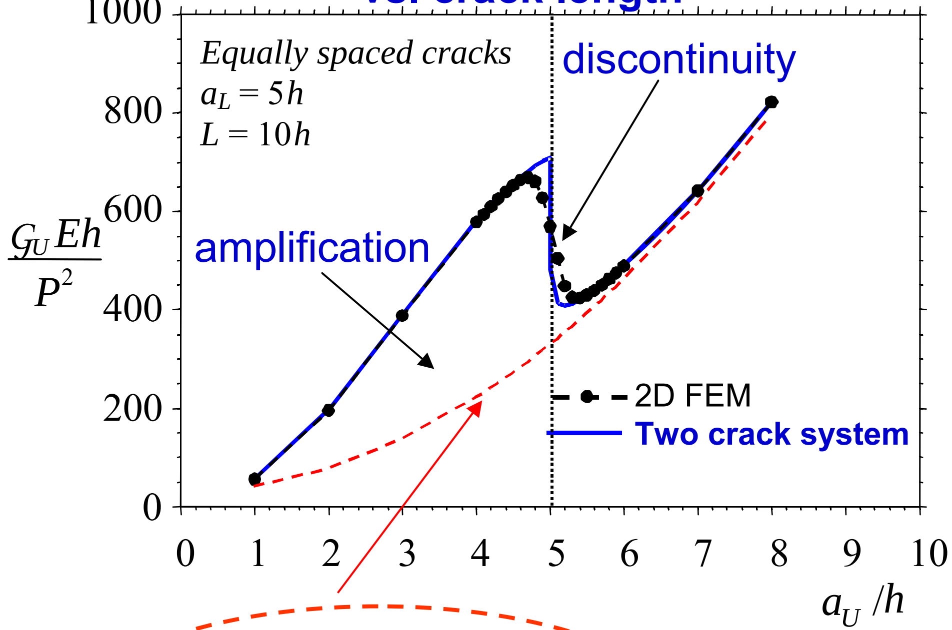

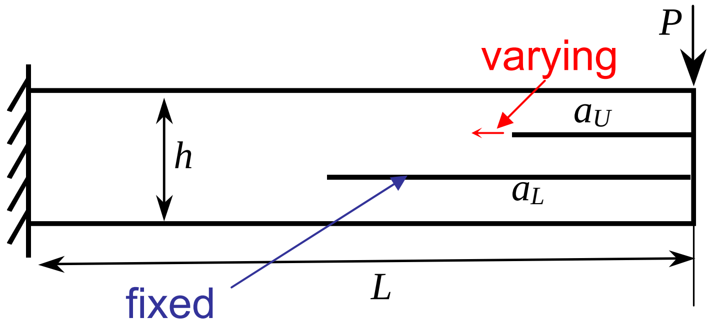

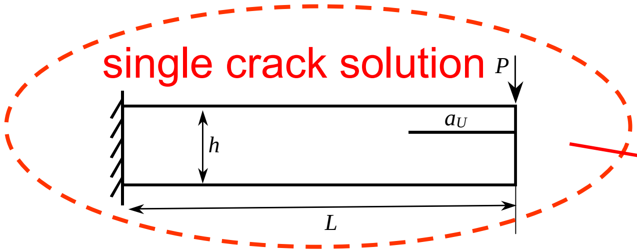

Relative amount of mode II to mode I (lower crack) vs. crack length

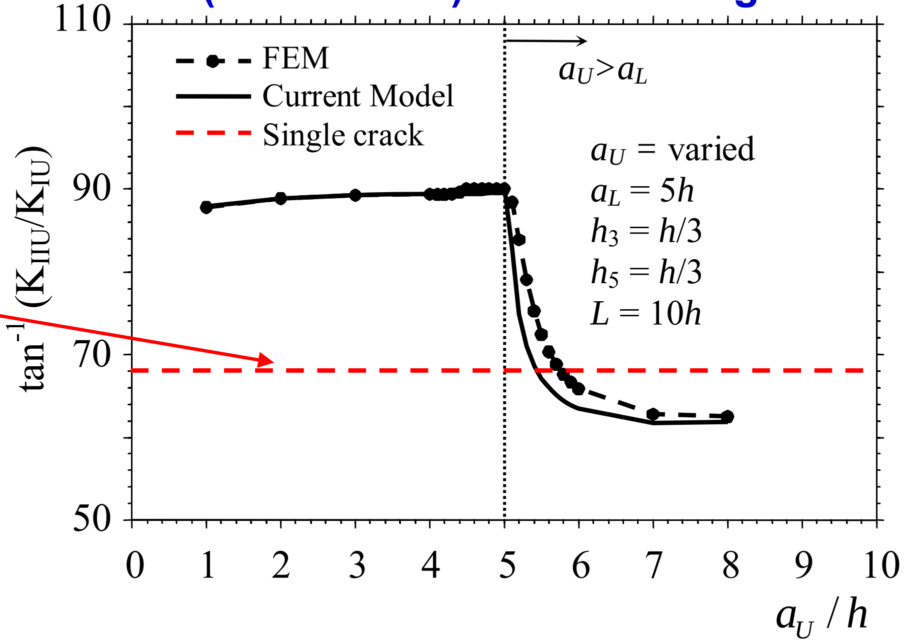

Assumptions:
- **System of two cracks in a cantilever beam**
- **Frictionless contact**
- **Homogeneous, isotropic and perfectly brittle material**

INTERACTION EFFECTS – QUASI STATIC LOADING
AMPLIFICATION AND SHIELDING OF FRACTURE PARAMETERS

(Andrews, Massabò and Cox, IJSS, 2006; Andrews and Massabò, Comp. A, 2008)

Energy release rate of upper crack vs. crack length

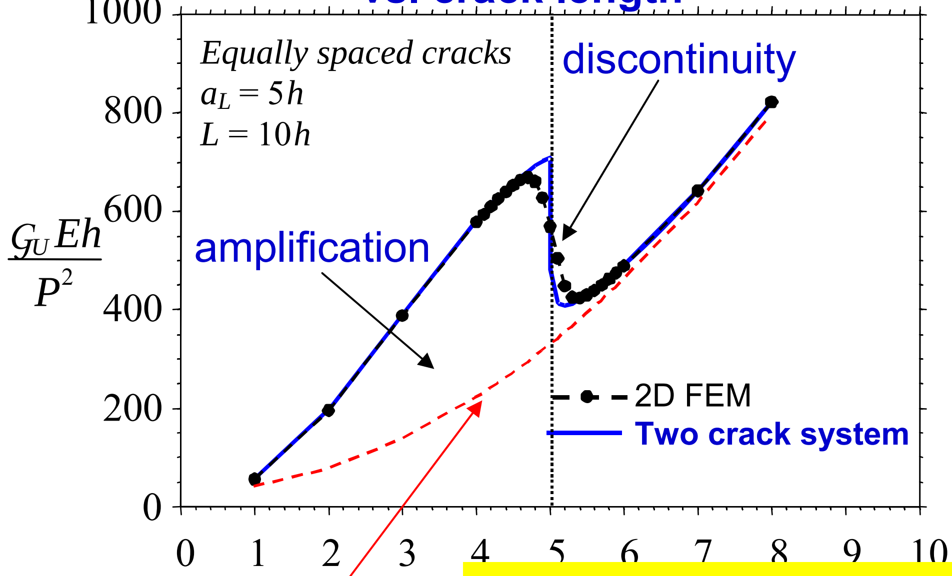

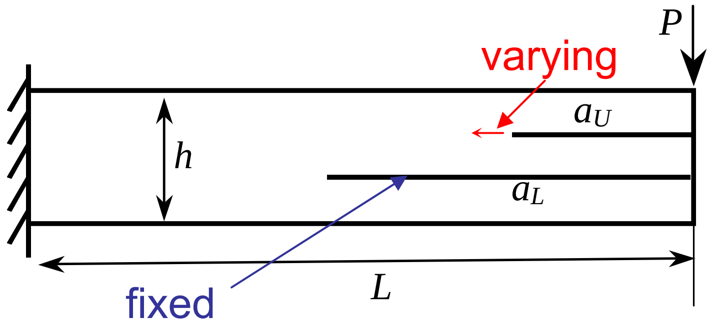

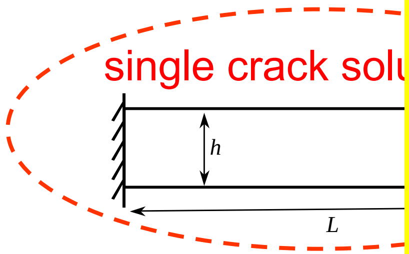

Interaction of multiple delaminations (static loading):
- phenomena of amplification and shielding of energy release rate G
- sudden changes in G when tips are close
- mode ratio variations
- phenomena controlled by through-thickness spacing

→ predictions based on solutions for single delaminations may be unconservative

Assumptions:
- **System of two cracks in a**
- **Frictionless contact**
- **Homogeneous, isotropic and perfectly brittle material**

Relative amount of mode II to mode I (lower crack) vs. crack length

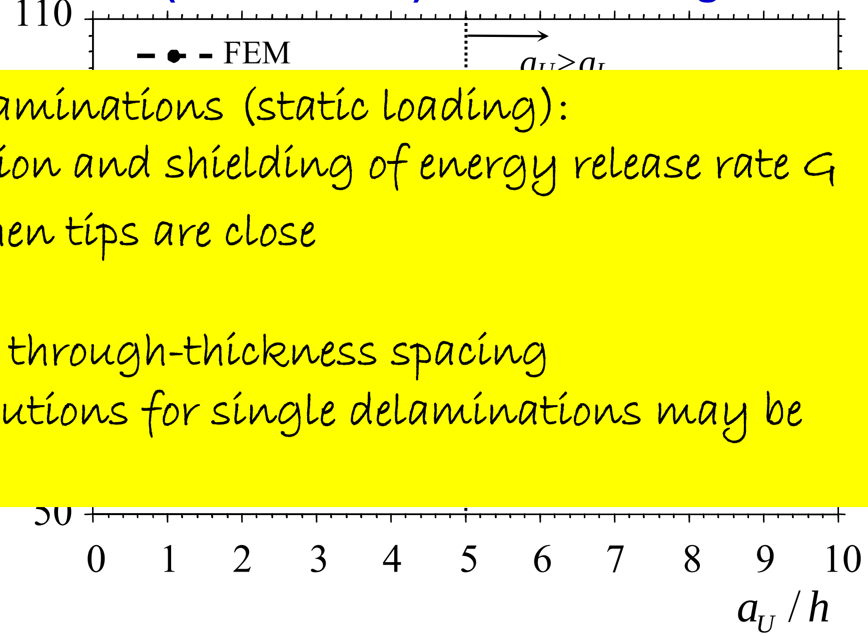

INTERACTION EFFECTS – QUASI STATIC LOADING MACRISTRUCTURAL RESPONSE

(Andrews and Massabò, Comp. A, 2008)

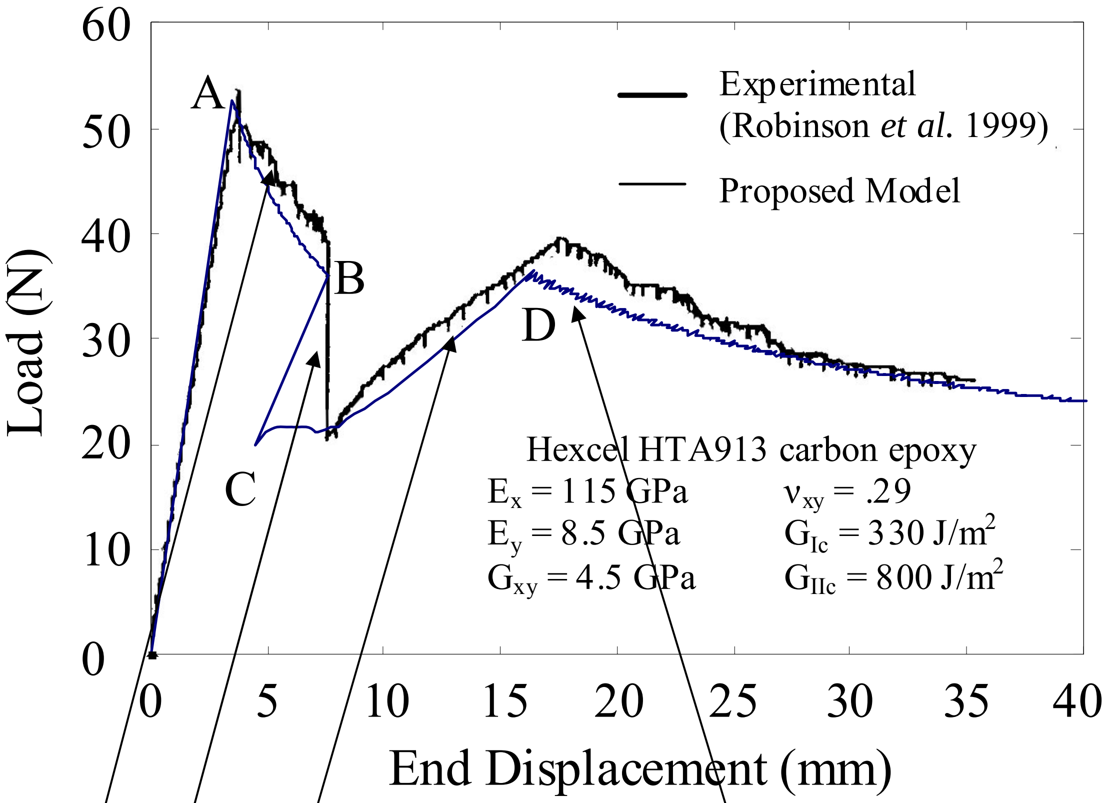

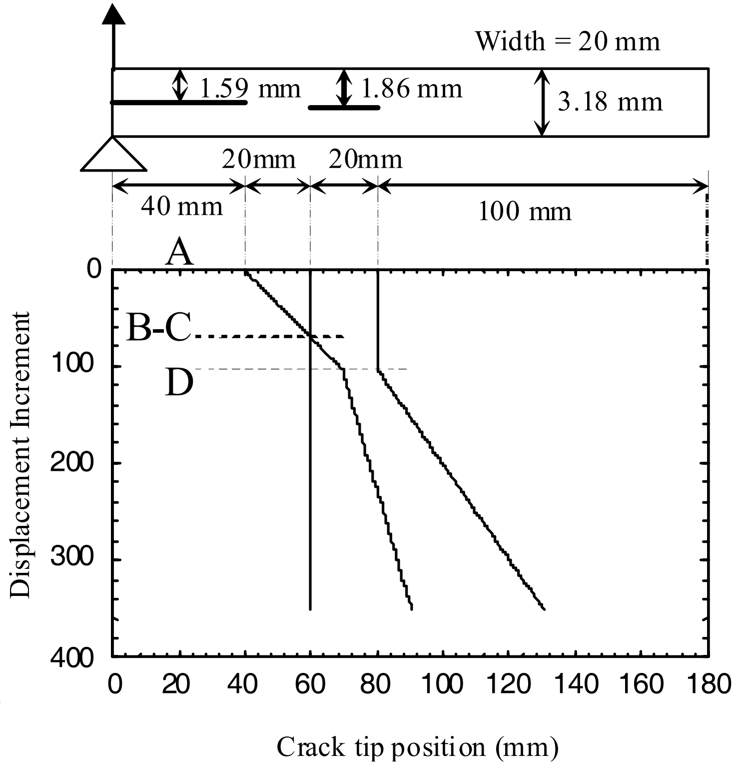

(c)

unstable growth of left crack

amplification

shielding

unstable growth of both cracks

Snap-back and snap-through instabilities due to local amplification and shielding of the crack tip stress fields

Assumptions:
- Frictionless contact
- Homogeneous, orthotropic, perfectly brittle material

INFLUENCE OF CRACK SPACING ON MULTIPLE DELAMINATION

(Andrews, Massabò & Cox, IJSS, 2006)

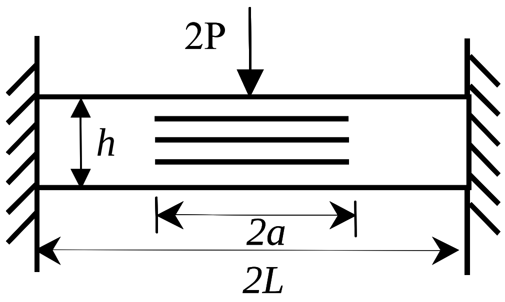

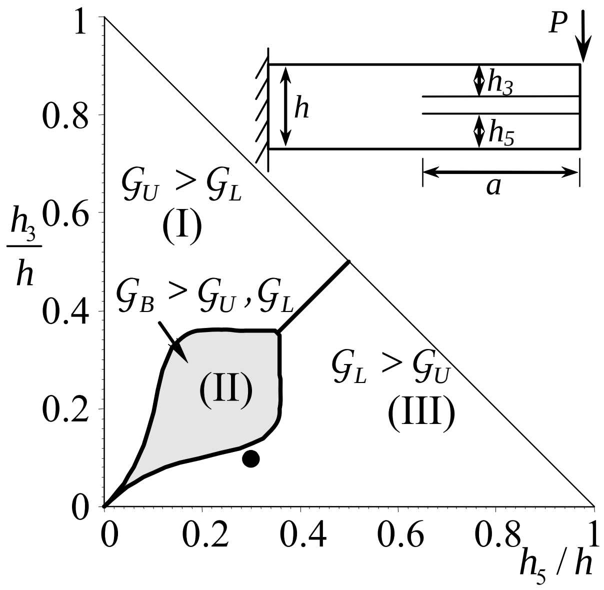

Behavioral maps, depending on crack spacing, define regions characterized by equal length growth

- In grey region equality of length is maintained and is stable with respect to length perturbations

→ Is controlled delamination fracture a feasible tool to improve mechanical performance (e.g. energy absorption)?

Assumptions:
- frictionless contact
- perfectly brittle material

DYNAMIC INTERACTION EFFECTS IN HOMOGENEOUS SYSTEMS
STATIONARY DELAMINATIONS

(Andrews, Massabò, Cavicchi & Cox, IJSS, 2009)

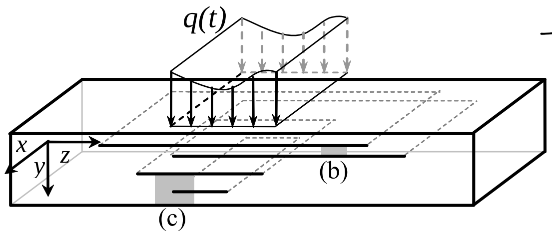

Equally spaced, equal length delaminations

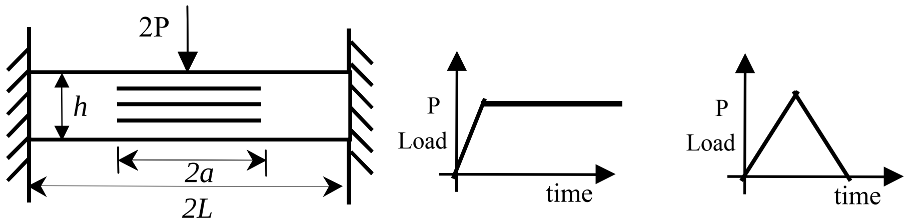

In phase vibrations of delaminated beams

Dynamic and interaction effects uncoupled if loading pulse is long enough

Unequally spaced or unequal length delaminations:

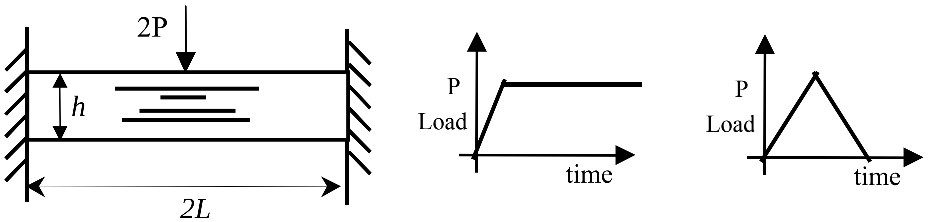

Out of phase vibrations and hammering of delaminated beams after load removal

DYNAMIC INTERACTION EFFECTS - STATIONARY DELAMINATIONS

equally spaced, equal length delaminations, short pulses

Time history of normalized energy release rate in systems with one delamination

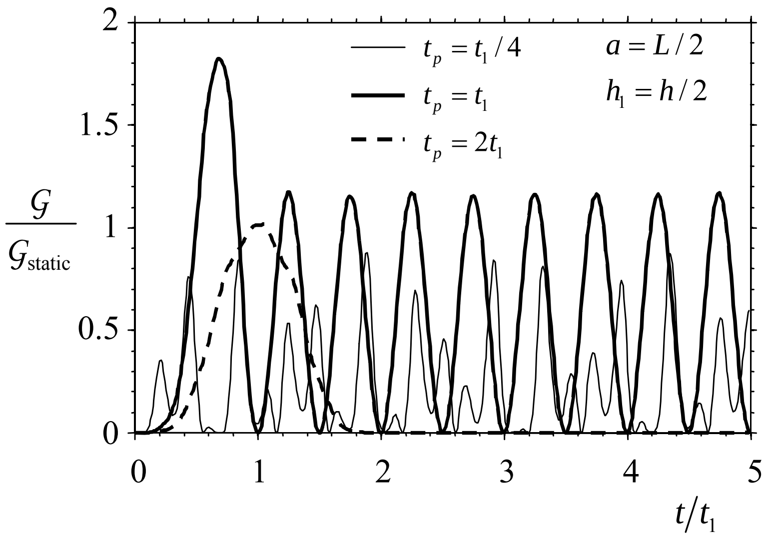

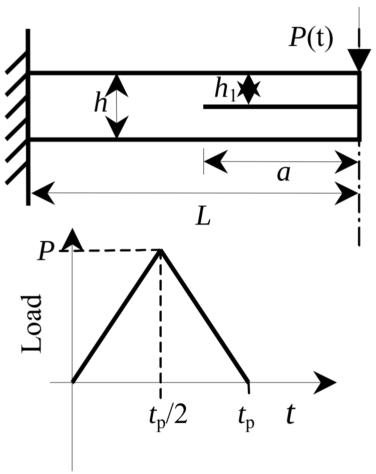

Assumptions:
- One crack in clamped-clamped beam
- Frictionless contact
- Homogeneous, isotropic, perfectly brittle

In phase vibrations of delaminated beams

Dynamic and interaction effects uncoupled if pulse is long enough

DYNAMIC INTERACTION EFFECTS - STATIONARY DELAMINATIONS

unequally spaced, unequal length delaminations, short pulses

Time history of energy release rate components

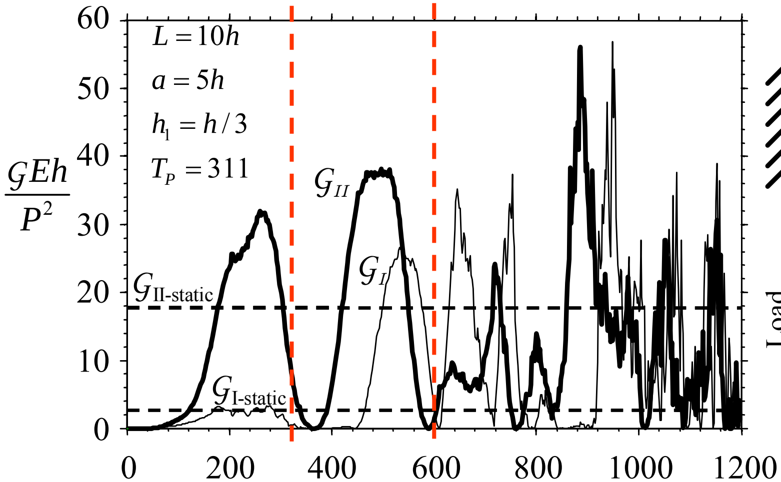

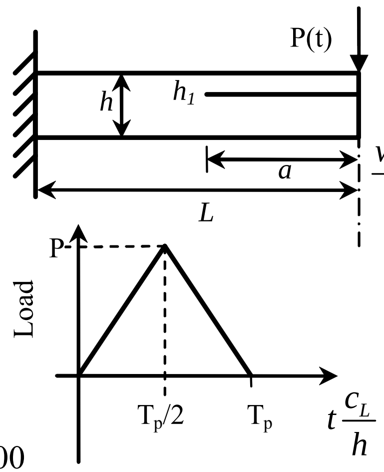

Time history of load point displacements

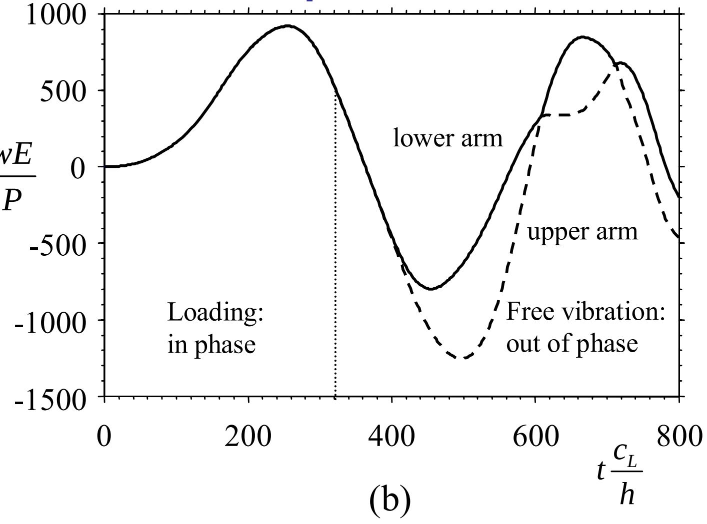

(1) → Forced vibrations

(2) → free vibrations

(3) → hammering

Assumptions:
- One crack in clamped-clamped beam
- Frictionless contact
- Homogeneous, isotropic, perfectly brittle

Out of phase vibrations, amplifications and hammering of delaminated beams after load removal

MULTIPLE DYNAMIC DELAMINATION FRACTURE

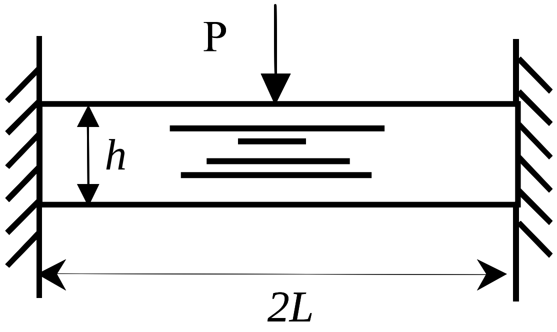

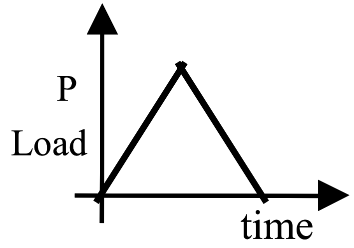

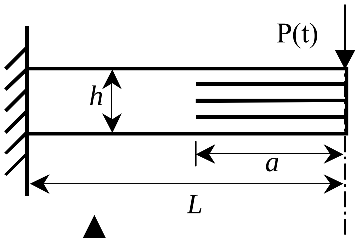

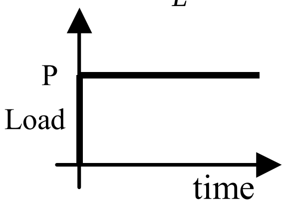

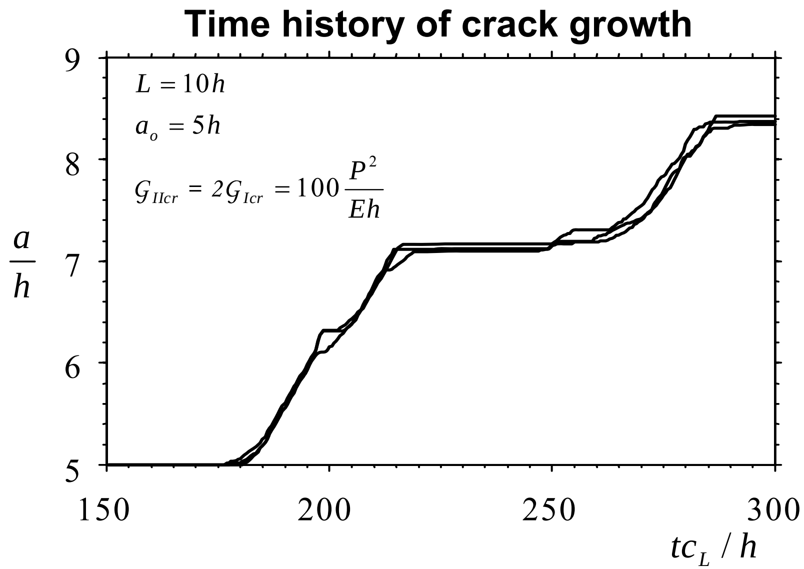

In homogeneous systems under arbitrary dynamic loading conditions:

Equally spaced delaminations propagate to equal length configuration and equality of length is then maintained and stable with respect to length perturbations

Assumptions:
- frictionless contact
- perfectly brittle material

(Andrews, Massabò, Cavicchi & Cox, 2008)

MULTIPLE DYNAMIC DELAMINATION FRACTURE

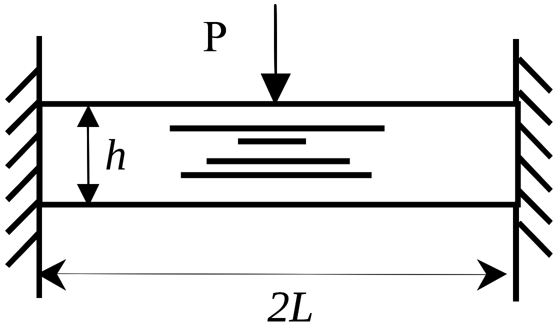

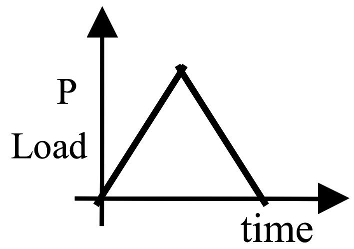

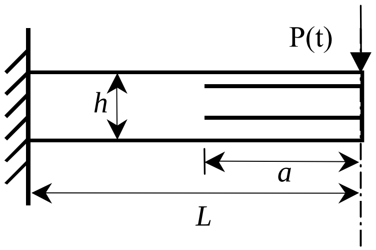

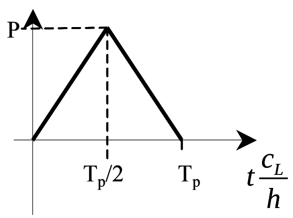

lower loads or higher fracture toughness → **higher loads or lower fracture toughness**

lower speeds … **Higher speeds**

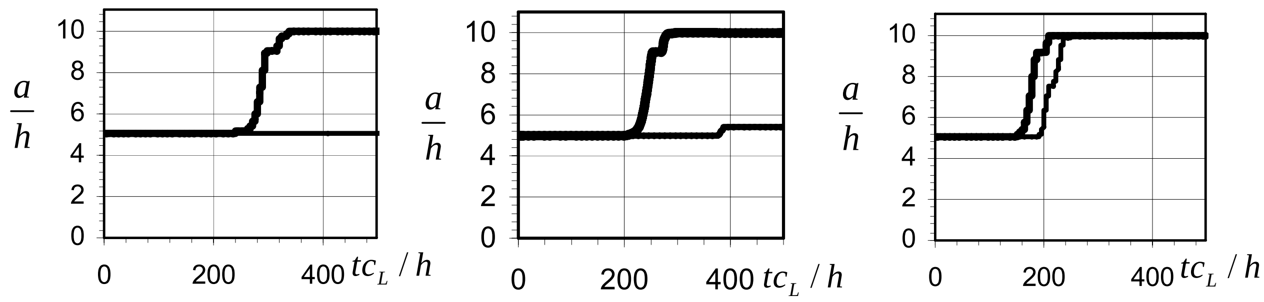

Time history of crack growth

In homogeneous systems under arbitrary dynamic loading conditions:

<u>Unequally spaced delaminations:</u> propagation at higher speed of a single dominant crack can be observed; response controlled by crack spacing

Assumptions:
- frictionless contact
- perfectly brittle material

(Andrews, Massabò, Cavicchi & Cox, 2008)

MULTIPLE DYNAMIC DELAMINATION FRACTURE

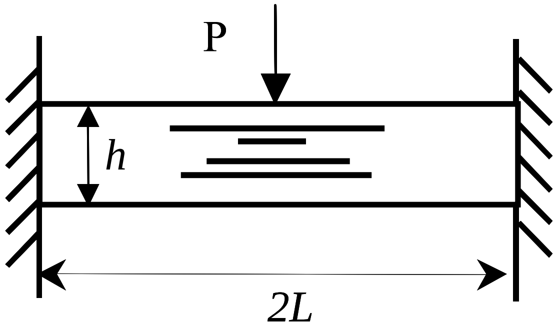

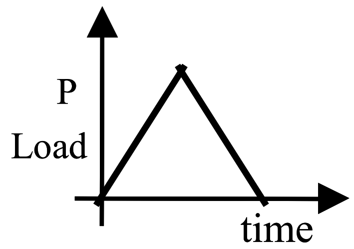

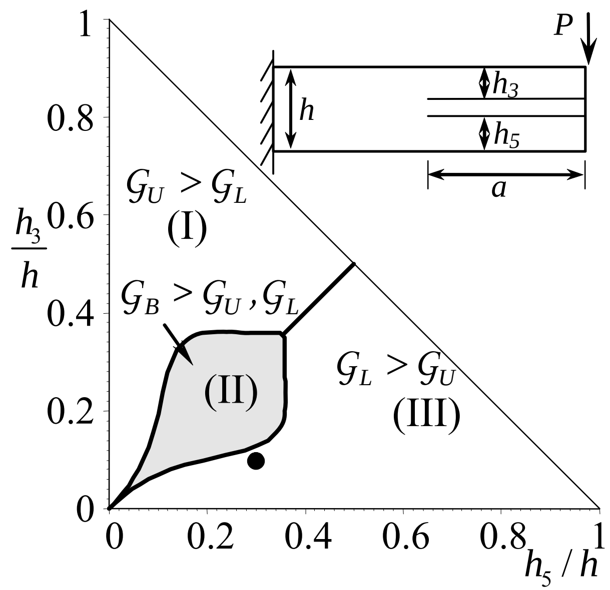

Behavioral maps, depending on crack spacing, define regions characterized by equal length growth

Assumptions:
- frictionless contact
- perfectly brittle material

(Andrews, Massabò & Cox, 2006)

CONTROLLED DELAMINATION FRACTURE TO IMPROVE MECHANICAL PERFORMANCE AGAINST DYNAMIC LOADINGS

Displacement controlled dynamic growth with fixed initial strain energy $\mathcal{L}$

(a)

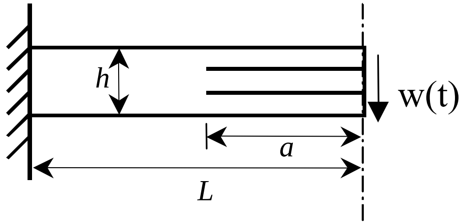

equally spaced cracks

(b)

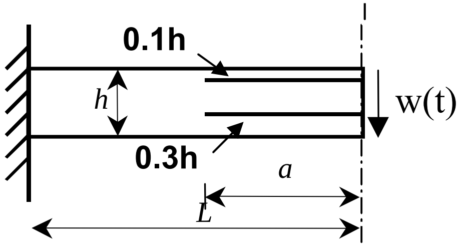

unequally spaced cracks

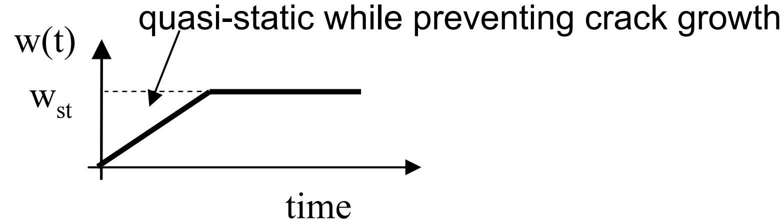

Assumptions:

$\mathcal{G}_{cr} h / \mathcal{L}$ leading to small / moderate crack speeds

Frictionless contact

Homogeneous, isotropic, perfectly brittle material

CONTROLLED DELAMINATION FRACTURE TO IMPROVE MECHANICAL PERFORMANCE AGAINST DYNAMIC LOADINGS

Displacement controlled dynamic growth with fixed initial strain energy $\mathcal{L}$

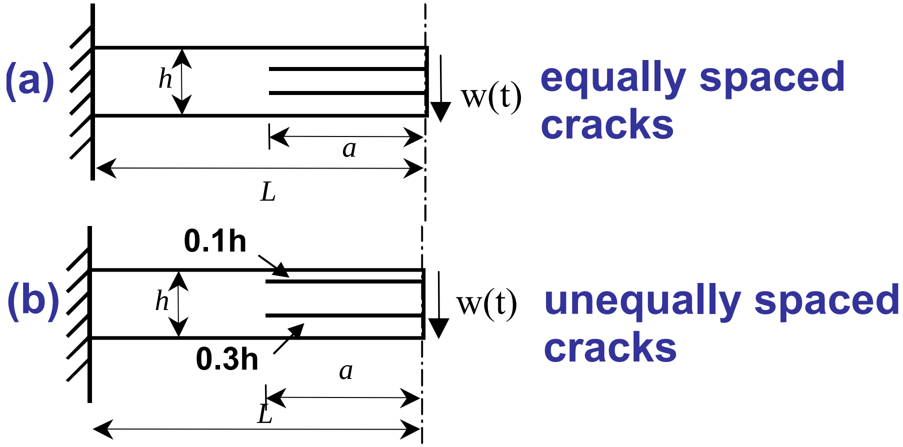

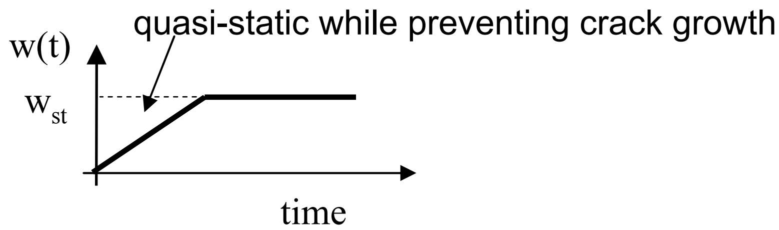

Assumptions:

$\mathcal{G}_{cr} h / \mathcal{L}$ leading to small / moderate crack speeds

Frictionless contact

Homogeneous, isotropic, perfectly brittle material

Time history of crack growth

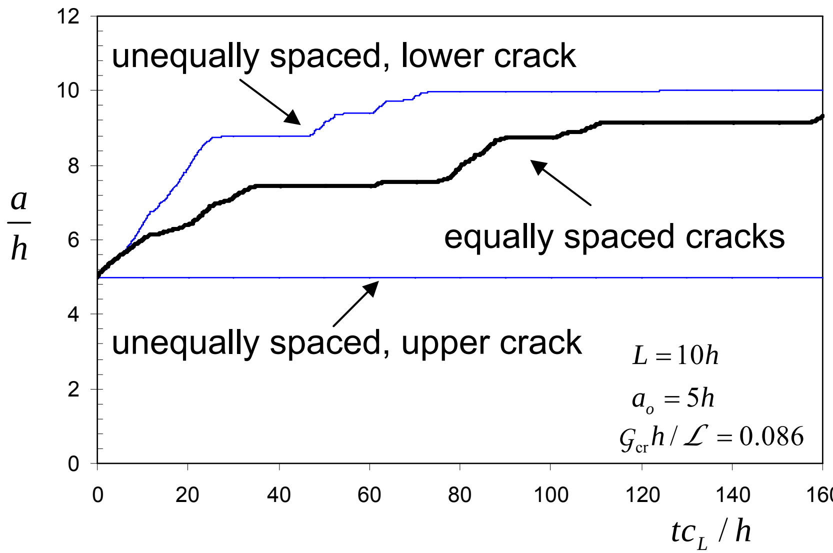

Time history of expended energy

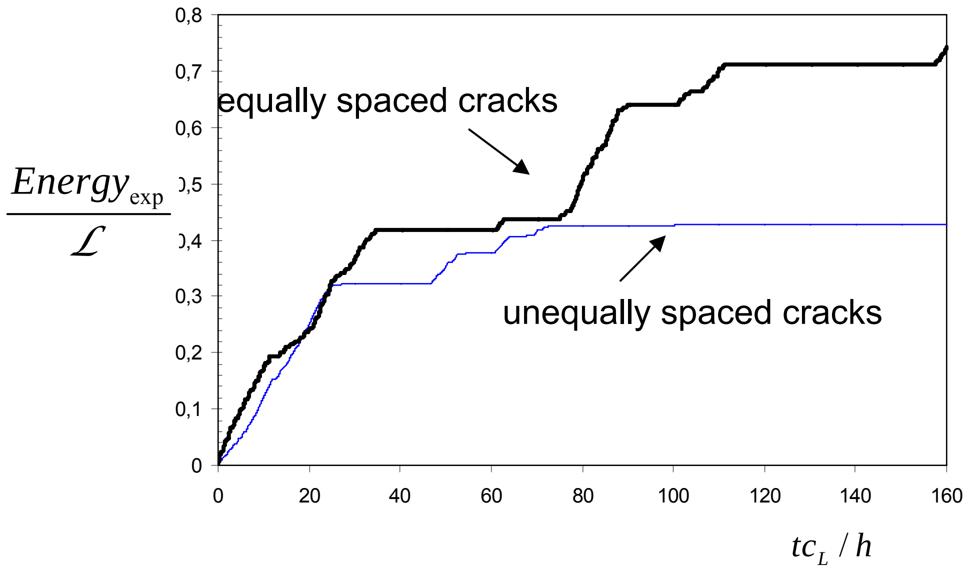

CONTROLLED DELAMINATION FRACTURE TO IMPROVE MECHANICAL PERFORMANCE AGAINST DYNAMIC LOADINGS

Displacement controlled dynamic growth with fixed initial strain energy $\mathcal{L}$

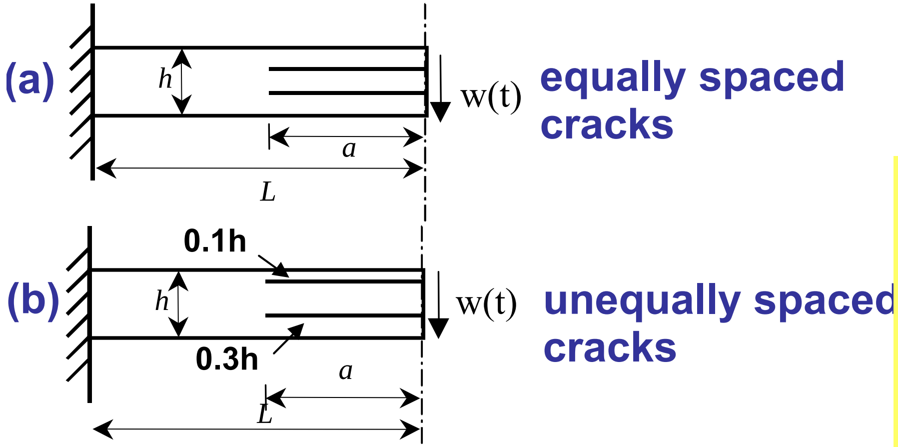

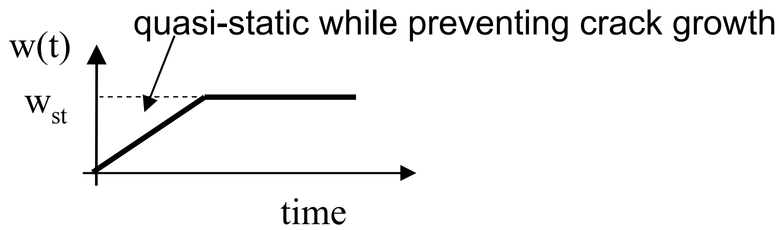

Energy absorption through multiple delamination fracture in laminated plates can be optimized via a material design that favour crack formation along predefined planes

eds

Time history of crack growth

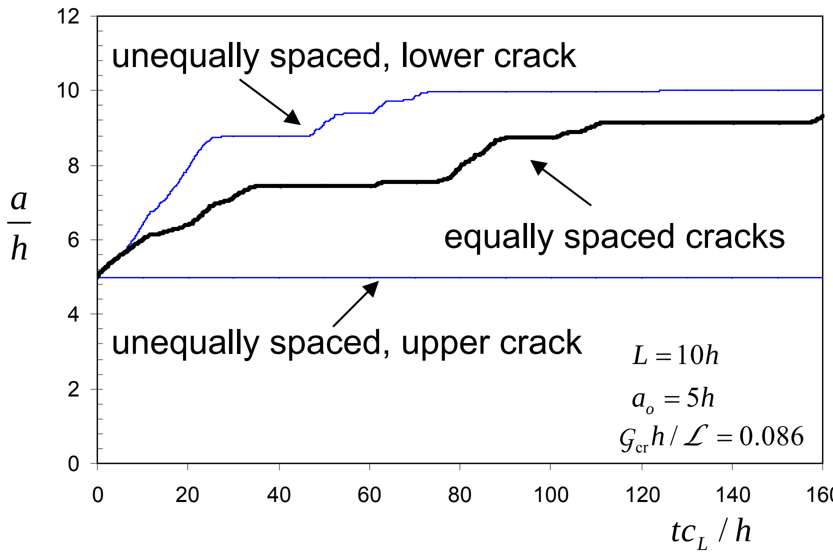

Time history of expended energy

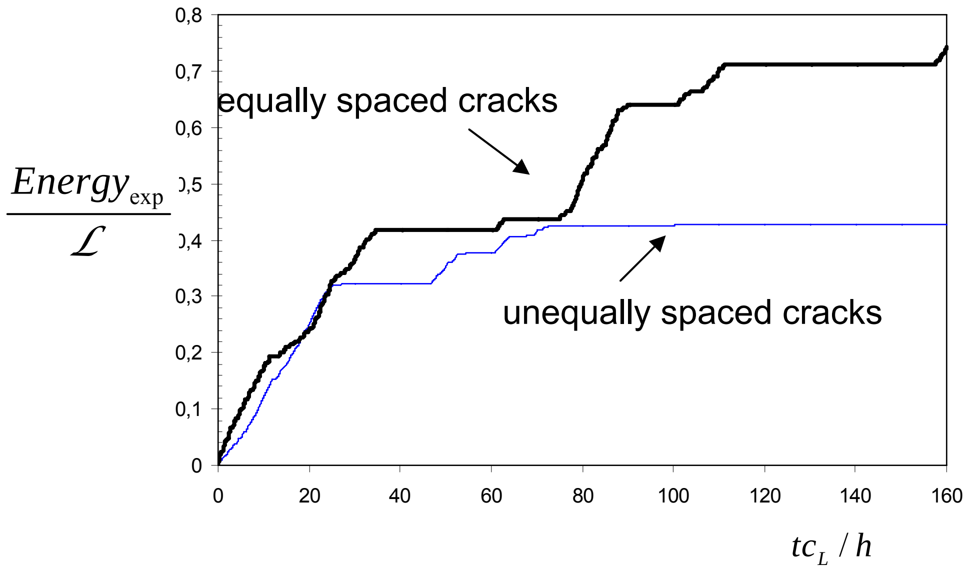

INFLUENCE OF CRACK BRIDGING MECHANISMS
STATIONARY DELAMINATIONS

Linear proportional bridging

$$k^N, k^S = 0.01E/h$$

(values for a typical stitched laminate)

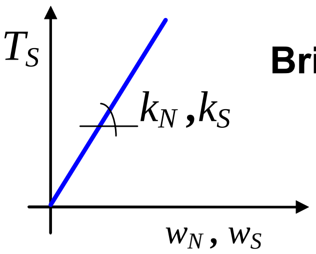

Bridging tractions

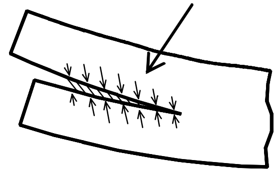

Time history of energy release rate components

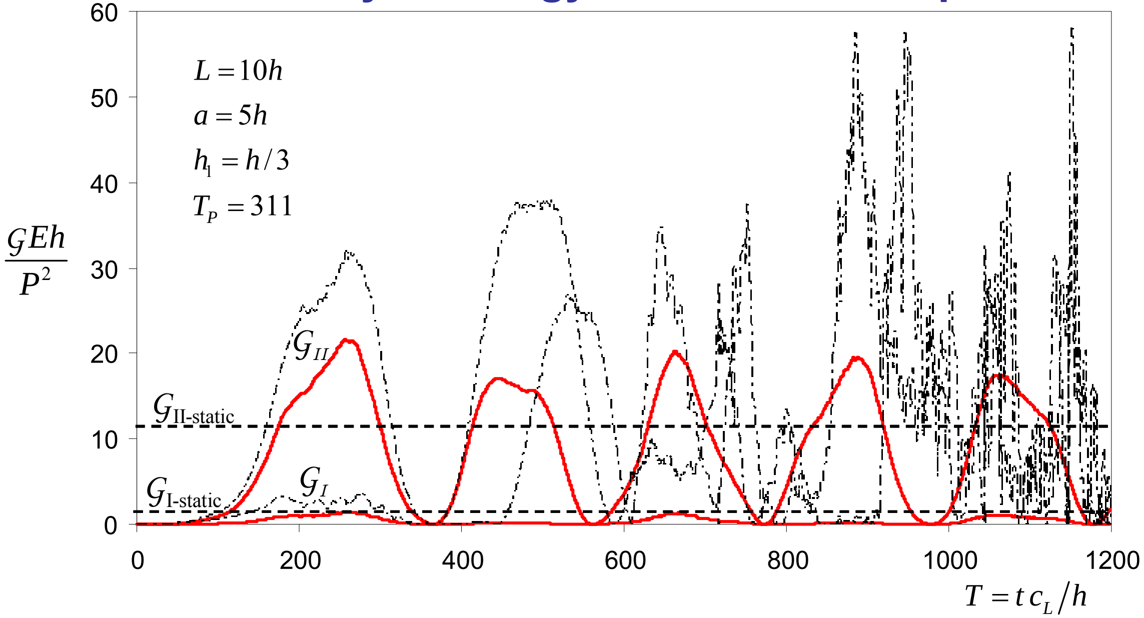

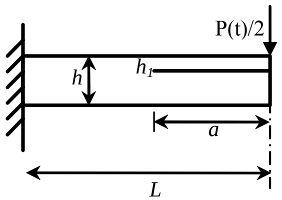

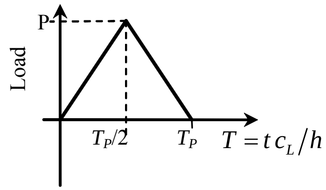

Bridging mechanisms:

- shield crack tip field from applied loading
- Problem becomes mode II
- stabilize free vibration phase

ENERGY ABSORPTION THROUGH MULTIPLE DELAMINATION
INFLUENCE OF CRACK BRIDGING MECHANISMS

Displacement controlled dynamic growth with fixed initial strain energy $\mathcal{L}$

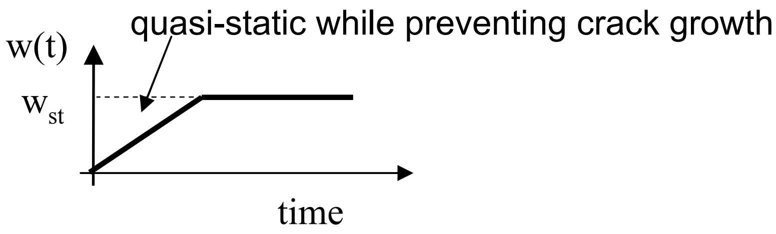

Results for: $\mathcal{G}_{cr} h / \mathcal{L} = 0.086$ **leading to small / moderate crack speeds**

(a)

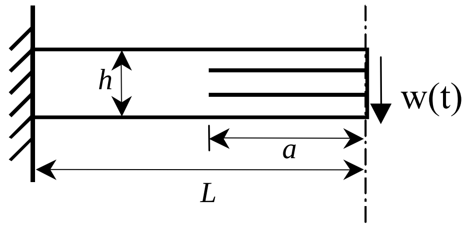

Equally spaced cracks

(b)

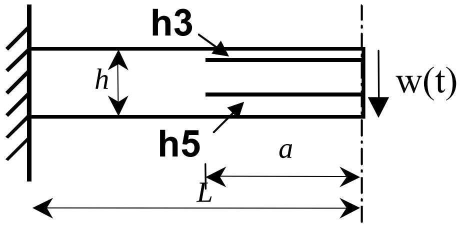

unequally spaced cracks, h3=0.1h, h5=0.3h

Time history of crack growth

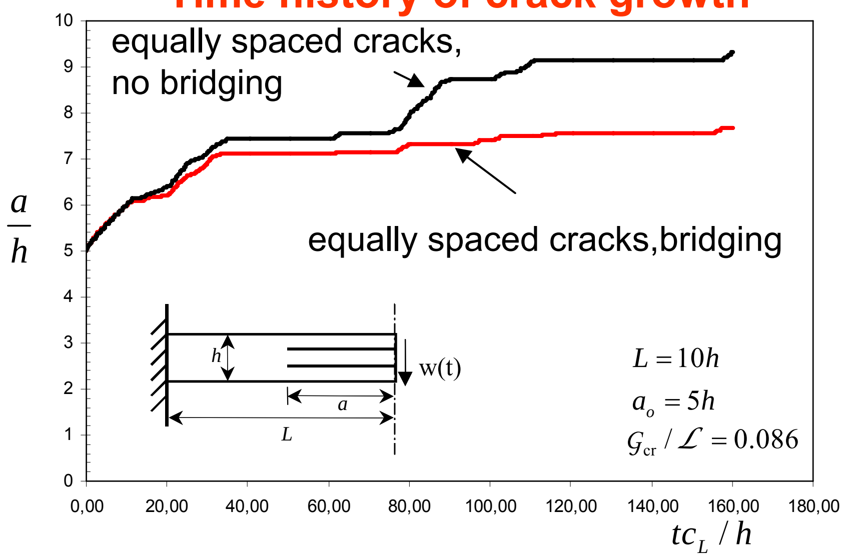

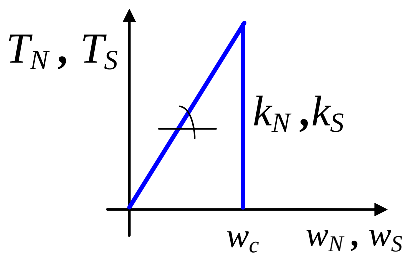

Bridging tractions

$$k^N, k^S = 0.01 E / h$$

$$w_c = 0.1 h$$

(values for a typical stitched laminate)

ENERGY ABSORPTION THROUGH MULTIPLE DELAMINATION
INFLUENCE OF CRACK BRIDGING MECHANISMS

Displacement controlled dynamic growth with fixed initial strain energy $\mathcal{L}$

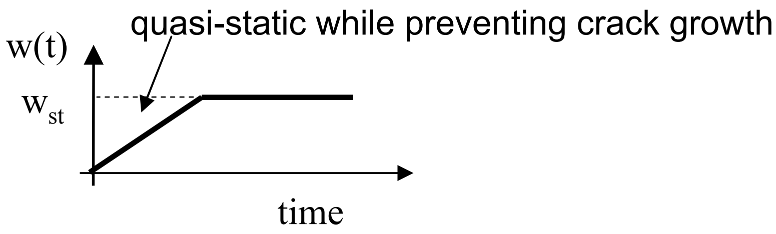

Results for: $\mathcal{G}_{cr} h / \mathcal{L} = 0.086$ leading to small / moderate crack speeds

(a)

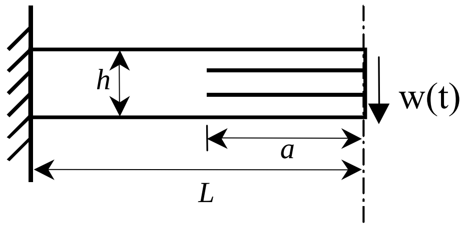

Equally spaced cracks

(b)

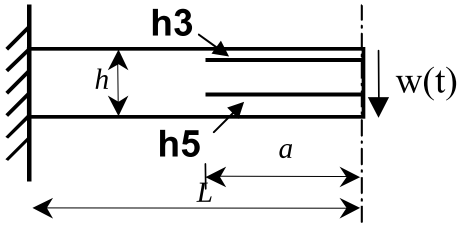

unequally spaced cracks, h3=0.1h, h5=0.3h

Time history of crack growth

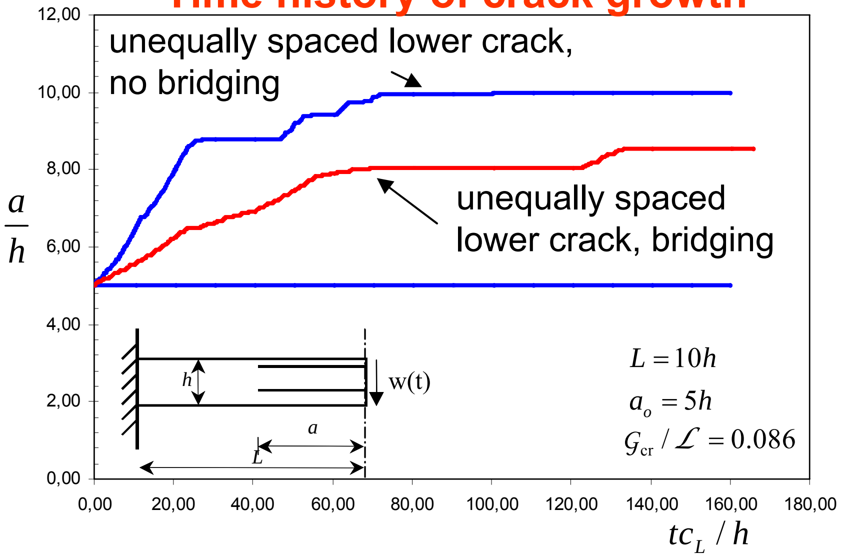

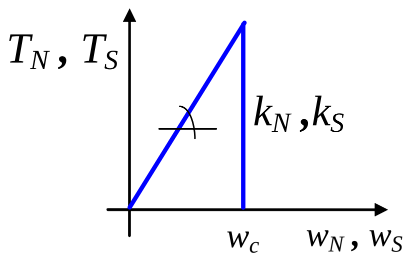

Bridging tractions

$$k^N, k^S = 0.01E/h$$

$$w_c = 0.1h$$

(values for a typical stitched laminate)

ENERGY ABSORPTION THROUGH MULTIPLE DELAMINATION
INFLUENCE OF CRACK BRIDGING MECHANISMS

Displacement controlled dynamic growth with fixed initial strain energy $\mathcal{L}$

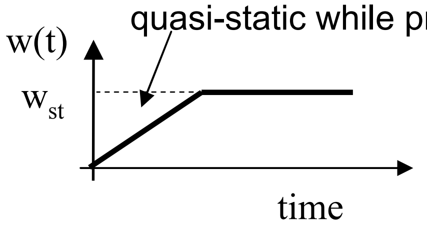

Results for: $\mathcal{G}_{cr} h / \mathcal{L} = 0.086$ **leading to small / moderate crack speeds**

Bridging mechanisms in the regime of low to moderate crack speeds:

- reduce crack speed
- may lead to crack arrest
- minimize differences in the response of systems with equally and unequally spaced cracks

Time history of crack growth

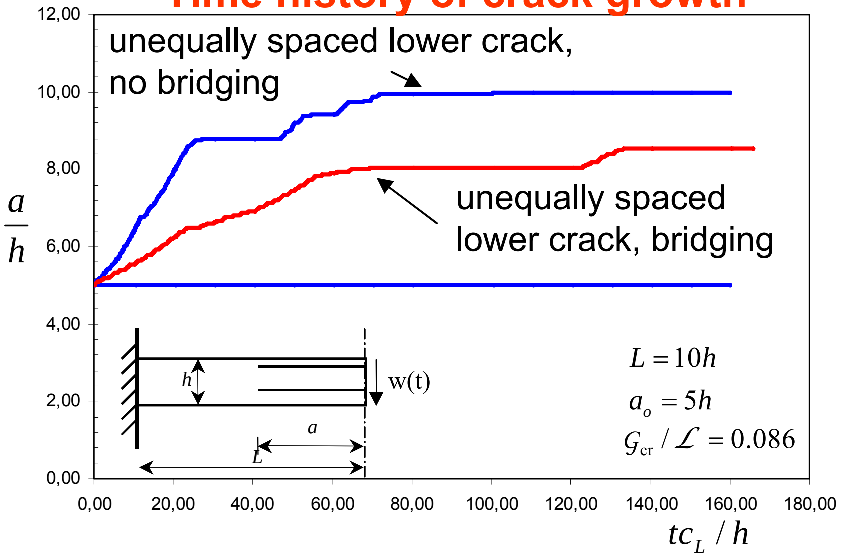

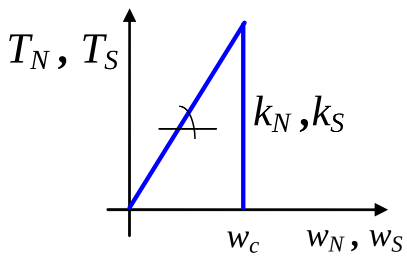

Bridging tractions

$$k^N, k^S = 0.01E/h$$

$$w_c = 0.1h$$

(values for a typical stitched laminate)

INTERACTION EFFECTS IN SANDWICH BEAMS
SHIELDING OF FRACTURE PARAMETERS AND ENERGY BARRIERS
(quasi static loading, elastic foundation)

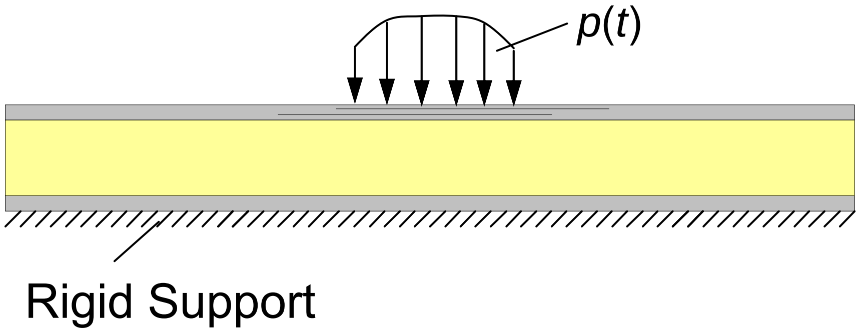

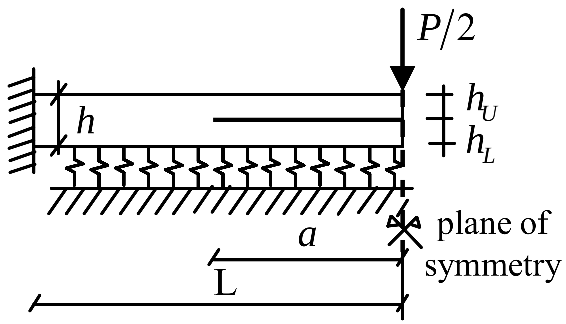

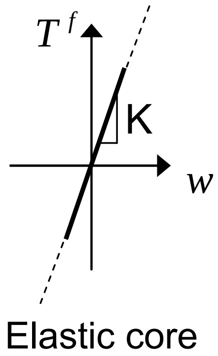

$L/h = 10$

$h_U/h = 0.5$

Perfect core/skin interface

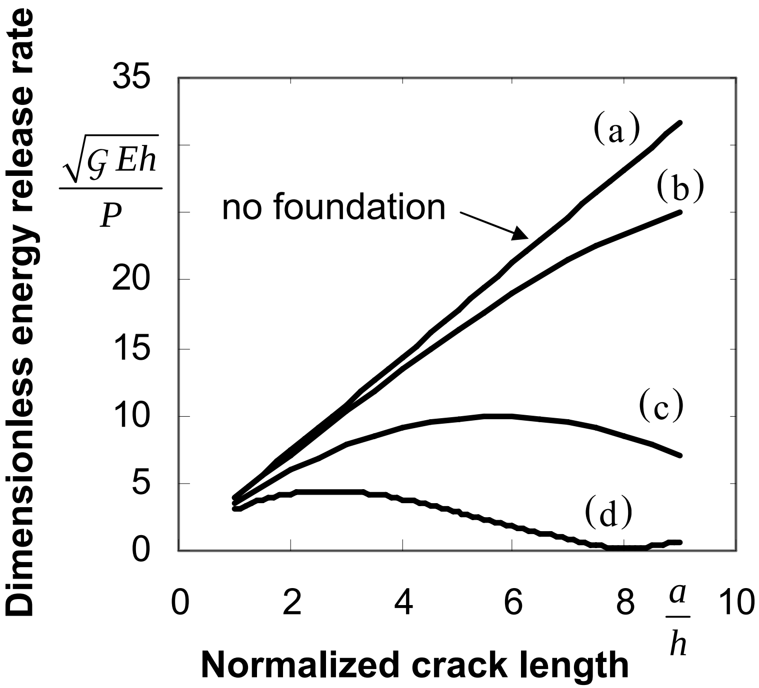

(a) $\frac{hK}{E} = 0$

(b) $\frac{hK}{E} = 10^{-4}$

(c) $\frac{hK}{E} = 10^{-3}$

(d) $\frac{hK}{E} = 10^{-2}$

- Face-core interactions shield crack tips from applied loads
- Transition in energy release rate on increasing the core-skin stiffness ratio
- Minimum in G defines energy barrier to crack propagation

INTERACTION EFFECTS IN SANDWICH BEAMS
SHIELDING OF FRACTURE PARAMETERS AND ENERGY BARRIERS
(quasi static loading, elastic foundation)

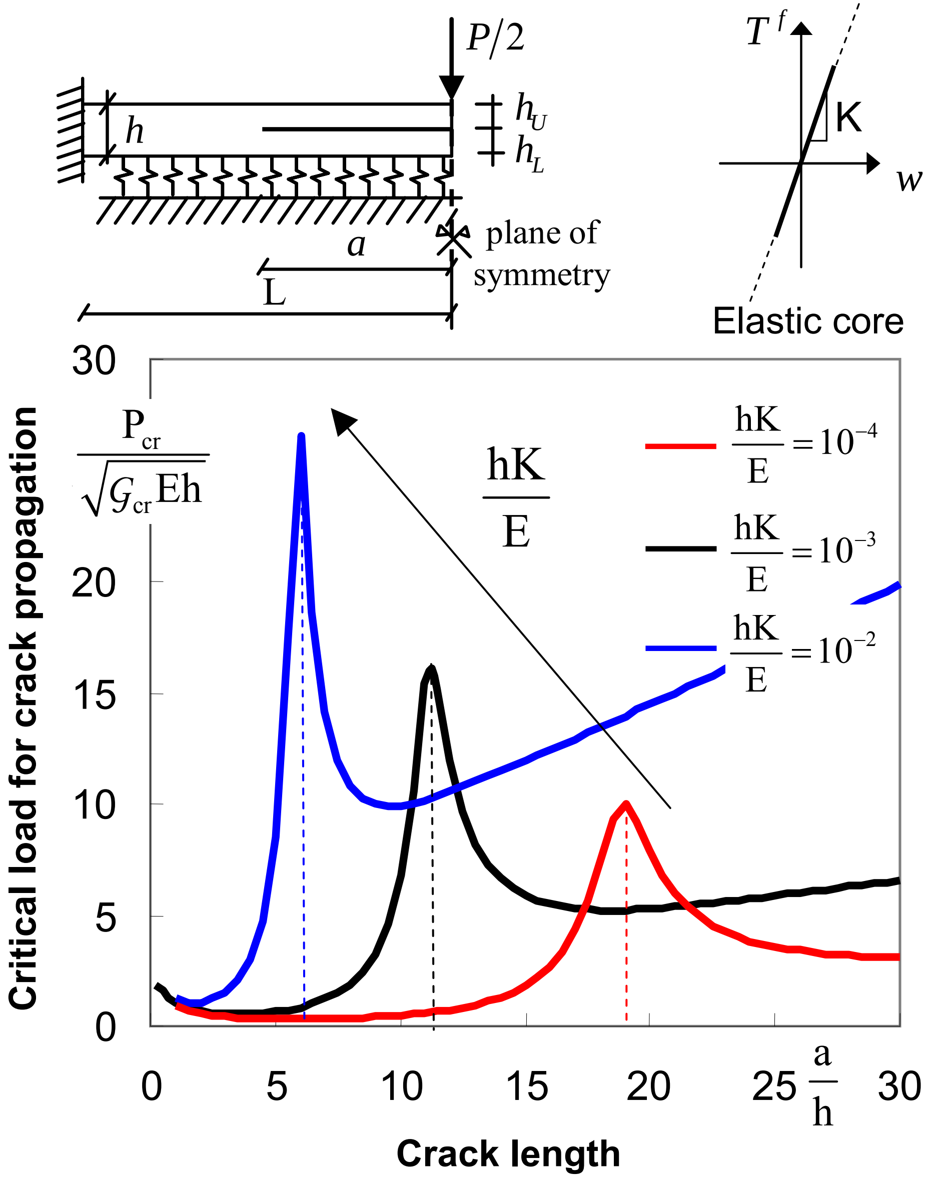

$L/h = 100$ Brittle skin, $\mathcal{G}_{cr}$

$h_U/h = 0.5$ Perfect core/skin interface

$\mathcal{G} = \mathcal{G}_{cr}$ (crack growth criterion)

-Energy barrier for a characteristic length of the crack depending on the core-skin stiffness ratio

INTERACTION EFFECTS IN SANDWICH BEAMS
SHIELDING OF FRACTURE PARAMETERS AND ENERGY BARRIERS
(quasi static loading, elastic foundation)

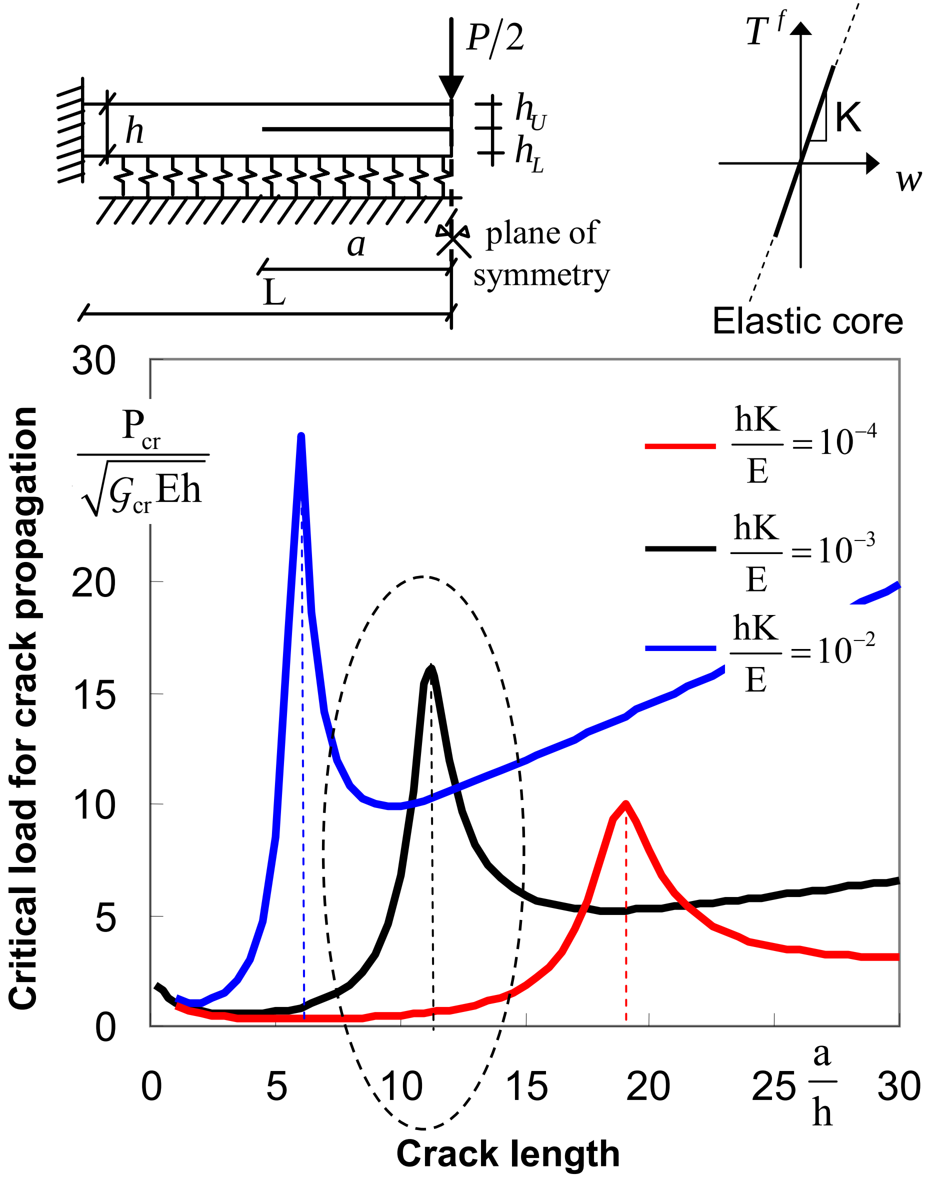

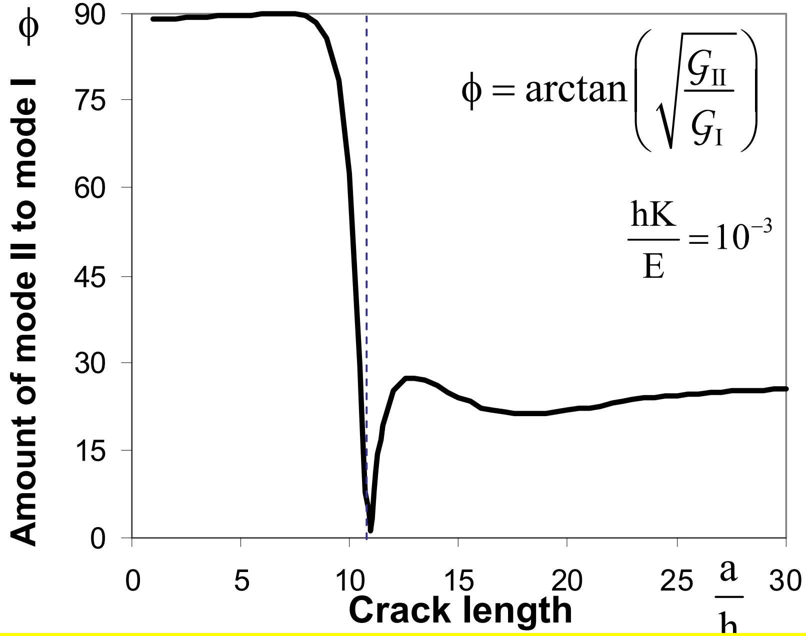

-Energy barrier for a characteristic length of the crack depending on the core-skin stiffness ratio

- Sudden transition from mode II to mixed mode fracture at the barrier

INFLUENCE OF CORE PLASTICITY ON FRACTURE PARAMETERS AND MECHANICAL RESPONSE

(static loading, elastic-plastic foundation)

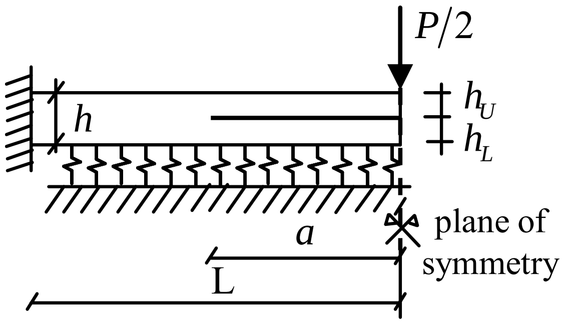

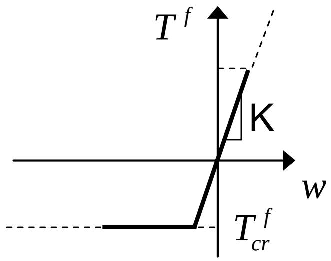

Elastic-plastic core

$L/h = 100$ $\quad \frac{T^f_{cr}}{E} = 10^{-3}$ $\quad \frac{hK}{E} = 10^{-3}$

$h_U/h = 0.5$

Perfect core/skin interface

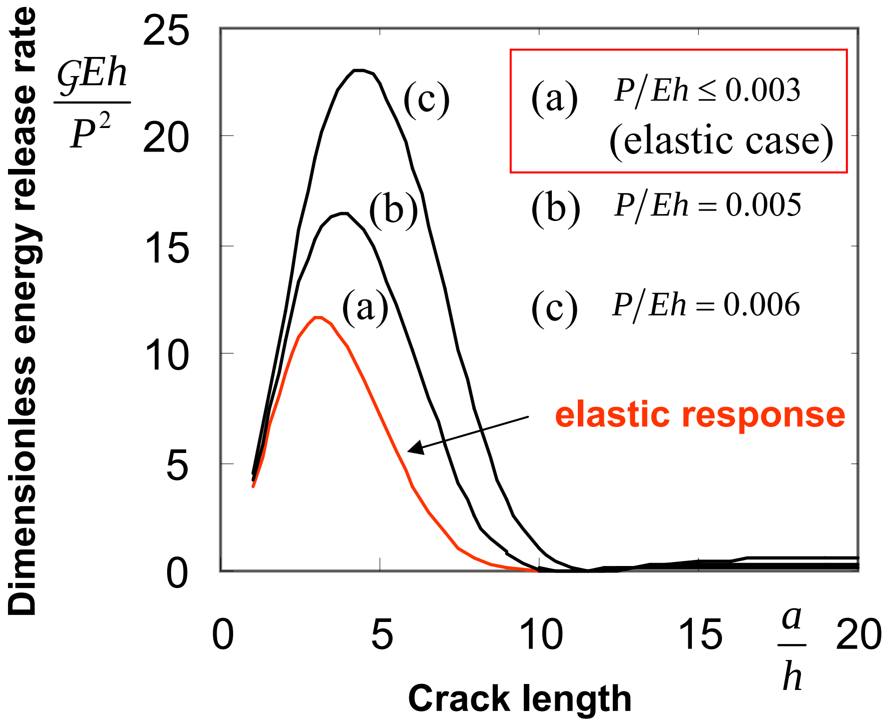

- Plasticity of the core reduces elastic shielding and modifies dependence of energy release rate on applied load

INFLUENCE OF CORE PLASTICITY ON FRACTURE PARAMETERS AND MECHANICAL RESPONSE

(static loading, elastic-plastic foundation)

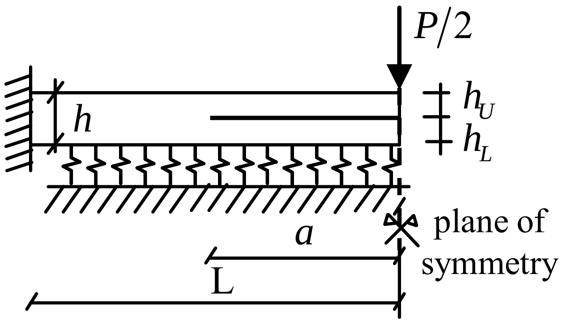

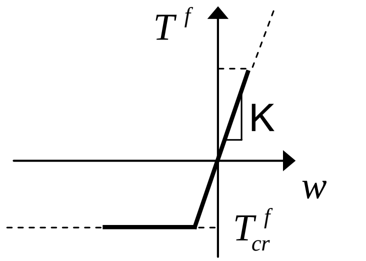

Elastic-plastic core

$L/h = 100$ $\mathcal{G} = \mathcal{G}_{cr}$ (crack growth criterion)

$h_U/h = 0.5$ $\dfrac{\mathcal{G}_{cr}}{Eh} = 10^{-5}$ $\dfrac{hK}{E} = 10^{-3}$

Perfect core/skin interface

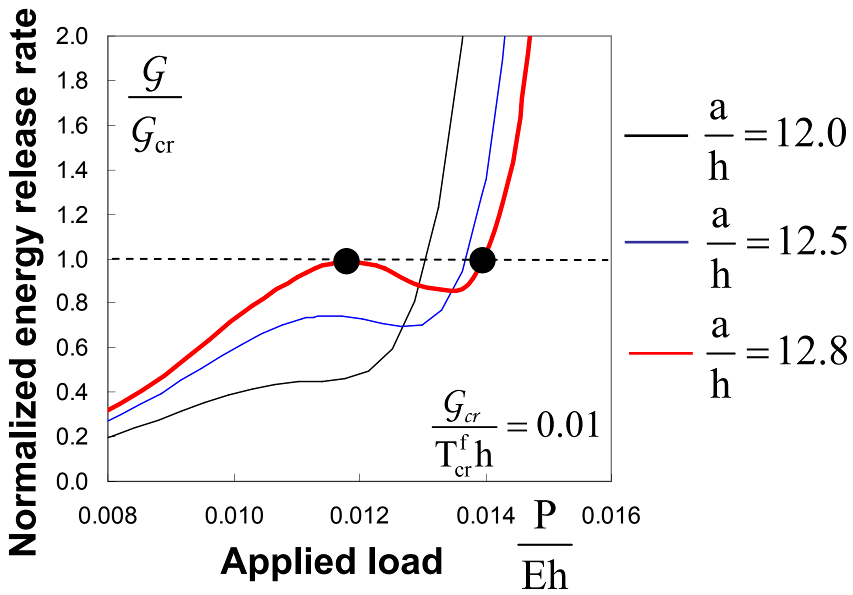

- The problem solution is not unique

- The response depends on the loading and propagation histories

INFLUENCE OF CORE PLASTICITY ON FRACTURE PARAMETERS AND MECHANICAL RESPONSE

(static loading, elastic-plastic foundation)

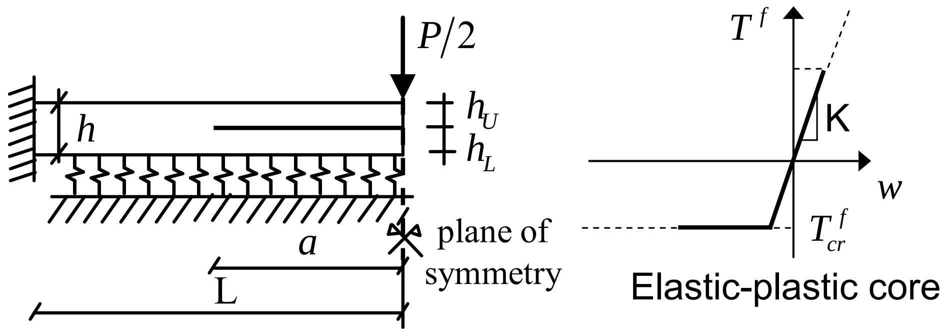

$L/h = 100$ $\mathcal{G} = \mathcal{G}_{cr}$ (crack growth criterion)

$h_U/h = 0.5$ $\frac{\mathcal{G}_{cr}}{Eh} = 10^{-5}$ $\frac{hK}{E} = 10^{-3}$

Perfect core/skin interface

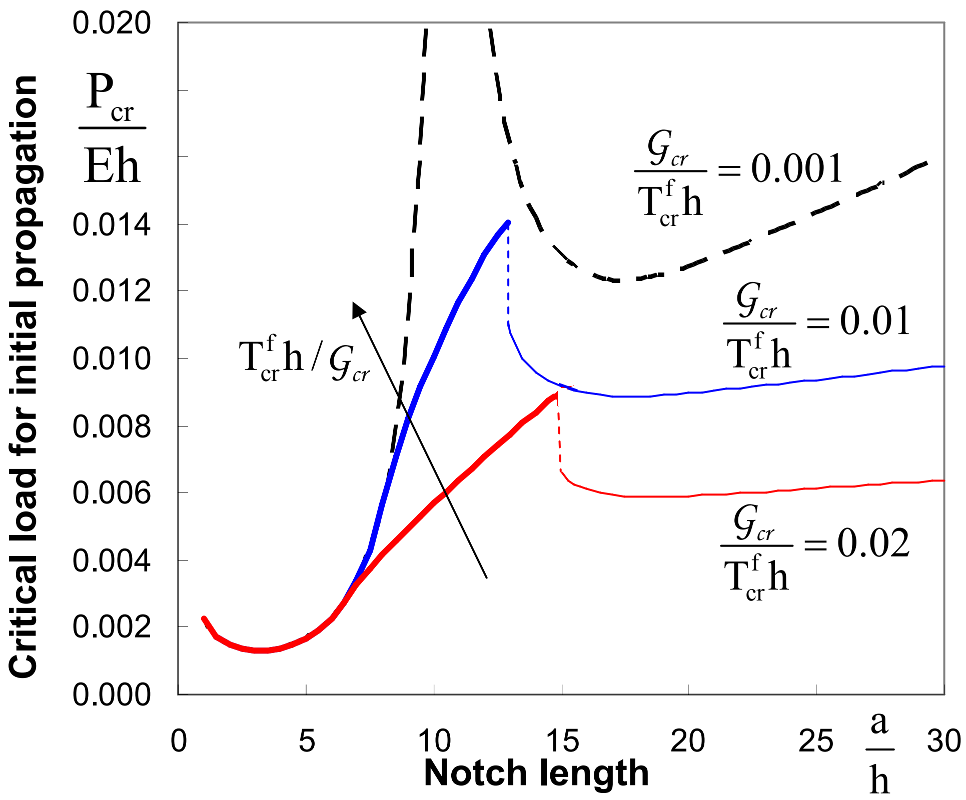

- The problem solution is not unique
- The response depends on the loading and propagation histories

MULTIPLE DYNAMIC DELAMINATION FRACTURE OF THE SKIN

(dynamic loading, elastic foundation)

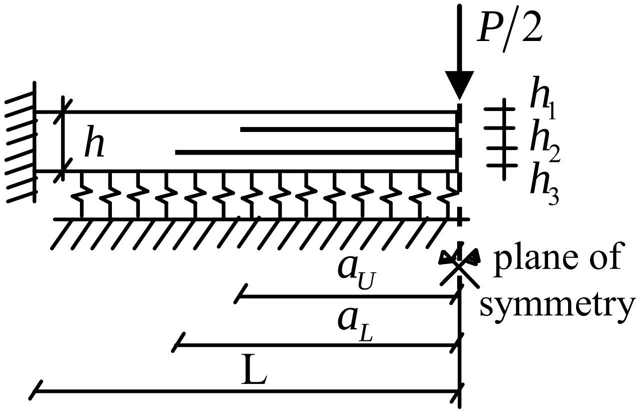

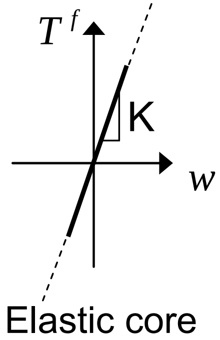

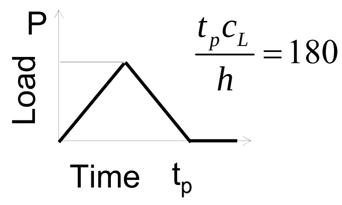

$L/h = 10$

$h_U/h = 1/3 \qquad h_L/h = 1/3$

$\dfrac{P_{max}}{\sqrt{\mathcal{G}_{cr}\, Eh}} = 1 \qquad \dfrac{hK}{E} = 10^{-3}$

$\mathcal{G} \geq \mathcal{G}_{cr}$ (crack growth criterion)

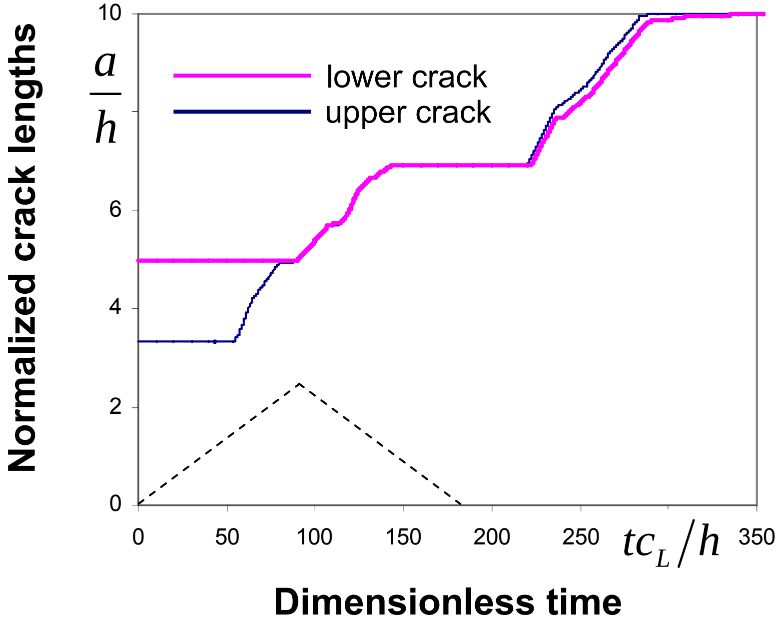

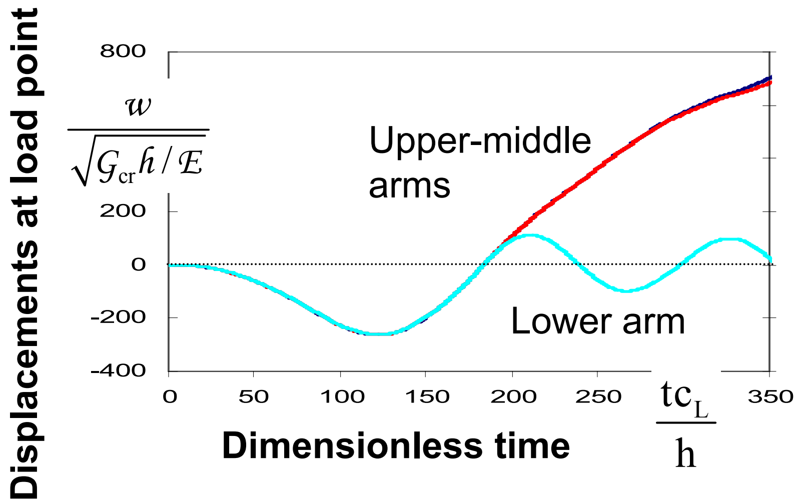

MULTIPLE DYNAMIC DELAMINATION FRACTURE OF THE SKIN

(dynamic loading, elastic foundation)

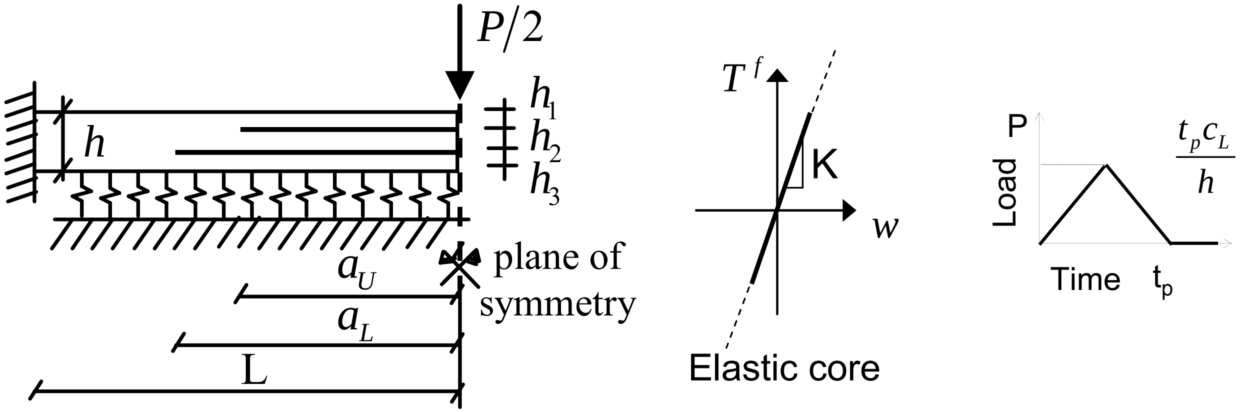

$\frac{t_p c_L}{h} = 180$

$L/h = 10$

$h_U/h = 1/3 \quad h_L/h = 1/3$

$\frac{P_{max}}{\sqrt{\mathcal{G}_{cr} Eh}} = 1 \quad \frac{hK}{E} = 10^{-3}$

$\mathcal{G} \geq \mathcal{G}_{cr}$ (crack growth criterion)

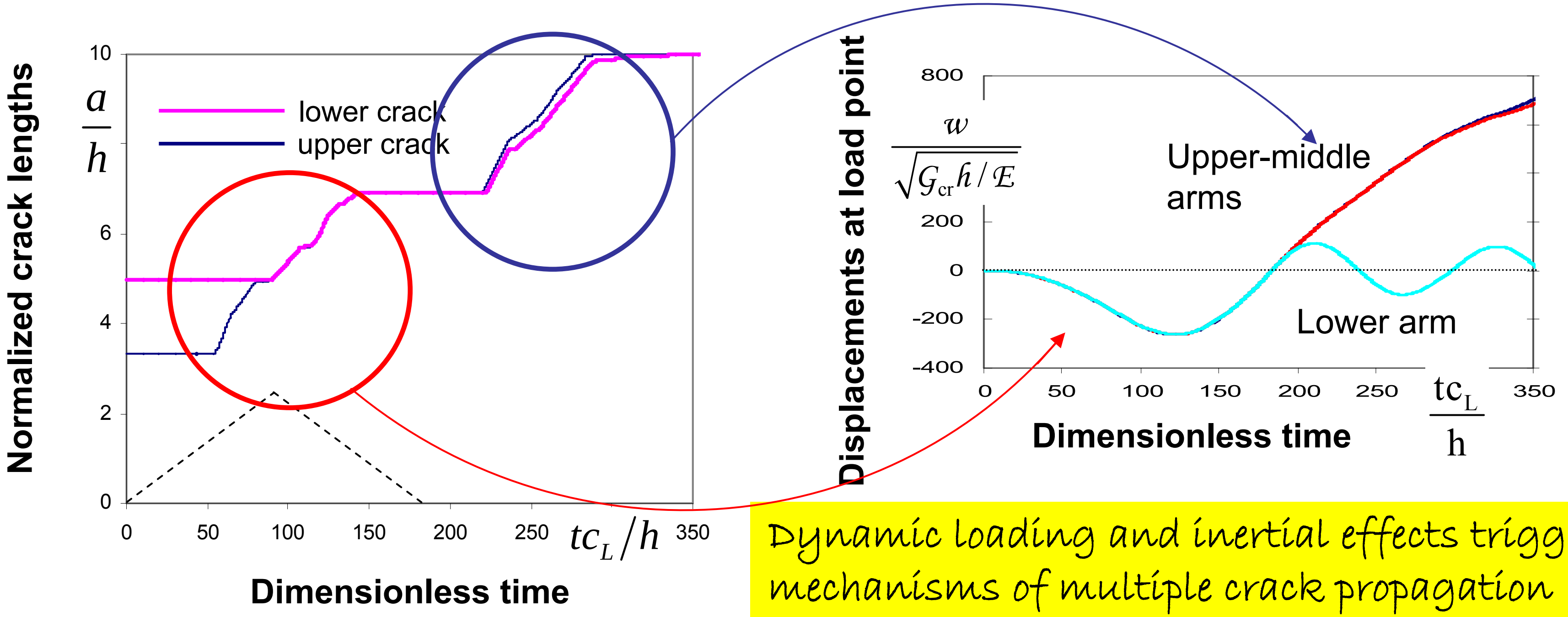

Dynamic loading and inertial effects trigger mechanisms of multiple crack propagation that are absent in quasi-static cases

CONCLUSIONS

- Static and dynamic interaction effects of multiple damage mechanisms in composite laminates, multilayered systems and composite sandwiches have been investigated

- Interaction effects on fracture parameters include: amplification and shielding of the energy release rate of one crack due to the presence of other cracks, modification of mode ratios, crack shielding and energy barriers due to the presence of elastic cores

- Interaction effects on macrostructural response include: snap-back and snap-through instabilities, hyper-strength, crack pull along

- Controlled delamination fracture can be a viable tool to improve damage/impact tolerance and energy absorption

- Crack bridging mechanisms stabilize the response of multiply delaminated beams in the free vibration phase after the removal of the load; they reduce crack speed and may lead to crack arrest

- Plasticity of the core reduces shielding of the fracture parameters; the problem solution becomes non unique and the response dependent on loading and propagation history; work is in progress ….